European Journal of Environmental and Safety Sciences 2014 2(2): 23-27
ISSN 1339-472X European Science and Research Institute (Original Research Paper)

The rate of oxygen consumption from a cone calorimeter as an original criterion of evaluation of the fire risk for the Resin Kit polymers

Jozef Rychlý[a] · Martina Hudáková[b] · Lyda Rychlá[a] · Katarína Csomorová[a]

[a]*Polymer Institute, Slovak Academy of Sciences, Dúbravská cesta 9, 84541 Bratislava, Slovakia*
[b]*Fire Research Institute, Ministry of Interior of the Slovak Republic, Rožňavská 11, 83104 Bratislava, Slovakia*

ABSTRACT

The results obtained from cone calorimetry burning of 50 polymers at 35 kW m^{-2} that were supplied in the form of plates by the Resin Kit Company (Woonsocket, RI) are presented. For thermally thin polymer samples in the form of plates a special rectangular holder (of the surface 83 cm^2) was used made from stainless steel (9.1x9.1x0.3) cm. The evaluation of cone calorimetry records for non-standard sample sizes was based on the oxygen consumption from which the heat release rate is subsequently derived by means of the surface of burned sample. Thermogravimetry (TG) measurements were performed using a Mettler Toledo TGA/SDTA 851e instrument in a nitrogen flow (30 ml min^{-1}) using a heating rate of 5 °C min^{-1} in a temperature range from room temperature up to 550 °C. The results were complemented by the tendency of respective polymers to ignition and the relation of time to ignition with non-isothermal thermogravimetry runs in nitrogen has been searched for.

Keywords: Burning of polymers • Cone calorimeter • Oxygen consumption • Non-isothermal thermogravimetry

1. Introduction

In the literature a lot of data on the combustion of various polymers (industrially produced or newly synthesized) has been published in an attempt to show how the respective modification upgraded the flame performance of a given polymer. Cone calorimeter based on oxygen consumption has been used in the most cases and flammability parameters have been assessed [1-8]. Heat release rate vs. time is usually the first graph that may be encountered in the most of such assessments. To obtain the reliable data the standard set up of instrument involving (10x10) cm at least 1 cm thick sample is needed. Recalculation of oxygen consumption to kW m^{-2} of heat release rate takes into account the empirical knowledge that 1 g of oxygen consumed during burning leads to the release of 13.1 kJ of heat and calibration of the instrument taking into account the surface of the sample above which is the flame sitting.

The present paper submits results obtained on cone calorimetry burning of some polymers selected from the Resin Kit Company (Woonsocket, RI). The samples were supplied in the form of plates 2 mm thick and as such they have nonstandard dimensions. The cuts from these plates having the surface 36 cm^2 were used. The polymers were characterized by specific gravity, tensile strength, Izod impact, Rockwell hardness, deflection temperature, mold shrinkage and weight/cubic inch, but did not provide information about the presence or identity of additives. The resin kit polymers involve polystyrene and its copolymers, ABS copolymers, acrylics, polyamides, polyesters, cellulose derivatives, polyolefins and their copolymers, flame retarded samples and samples filled with inorganic additives, polysulphones, polycarbonates, polyphenylene sulfides, etc. (See the Table 1).

The attention has been focused on the relation of the heat release rate data and rate of oxygen consumption in the non-standard cases [4] where the surface of measured samples has been changed due to the sample melting during combustion. The evaluation of cone calorimetry records of heat release rate and oxygen consumption vs. time during burning at the cone radianccy 35 kW m^{-2} were complemented by the tendency of respective polymers to ignition and its relation with non-isothermal thermogravimetry runs in nitrogen has been searched for.

Jozef Rychlý (corresponding author)
Polymer Institute, Slovak Academy of Sciences, Dúbravská cesta 9, 84541 Bratislava, Slovakia
e-mail: jozef.rychly@savba.sk

Table 1 The Resin Kit polymers

Sample No. *TOC*[a]	Polymer	Sample No.	Polymer	Sample No.	Polymer
1 ***1.93***	Polystyrene (general purpose)	**18** ***1.41***	Thermoplastic polyester (PETG)	**35** ***2.05***	Synthetic elastomer (Styrene block copolymer)
2 ***2.06***	Polystyrene (medium impact)	**19** ***1.31***	Polyphenylene oxide (PPO)	**36** ***1.90***	Polypropylene (glass filled)
3 ***2.02***	Polystyrene (High impact)	**20** ***1.20***	Polycarbonate	**37** ***1.23***	Urethane elastomer, thermoplastic (TPU)
4 ***1.68***	Styrene Acrylonitrile (SAN)	**21** ***1.04***	Polysulfone	**38** ***2.42***	Polypropylene (Flame retardant)
5 ***1.94***	Acrylonitrile-butadiene-styrene (ABS)-Transparent	**22** ***2.08***	Polybutylene	**39** ***1.62***	Polyester elastomer
6 ***1.88***	Acrylonitrile-butadiene-styrene (ABS)-medium impact	**23** ***2.80***	Ionomer	**40** **1.03**	Acrylonitrile butadiene styrene (ABS) flame retardant
7 ***1.96***	Acrylonitrile-butadiene-styrene (ABS)-high impact	**24** ***3.08***	Polyethylene (low density)	**41** ***2.92***	Polyallomer
8 ***2.06***	Styrene butadiene block copolymer	**25** ***3.04***	Polyethylene (High density)	**42** ***2.15***	Styrene terpolymer
9 ***1.51***	Acrylic	**26** ***2.93***	Polypropylene (Copolymer)	**43** ***3.03***	Polymethyl pentene
10 ***1.88***	Modified acrylic	**27** ***2.93***	Polypropylene (Homopolymer)	**44** ***1.73***	Polypropylene (Talc reinforced)
11 ***1.45***	Cellulose acetate	**28** ***2.66***	Polypropylene (Baryum sulfate reinforced)	**45** ***1.76***	Polypropylene (Calcium carbonate reinforced)
12 ***1.46***	Cellulose acetate butyrate	**29** ***1.08***	Polyvinyl chloride (PVC flexible)	**46** ***1.80***	Polypropylene (Mica reinforced)
13 ***1.46***	Cellulose acetate propionate	**30** ***0.79***	Polyvinyl chloride (PVC rigid)	**47** ***1.33***	Nylon 66 (33% of glass)
14 ***1.48***	Nylon (transparent)	**31** ***0.96***	Acetal resin (homopolymer)	**48** ***2.58***	Thermoplastic rubber (TPV)
15 ***2.05***	Nylon type 66	**32** ***1.01***	Acetal resin (copolymer)	**49** ***3.00***	Polyethylene (medium density)
16 ***2.11***	Nylon type 6	**33** ***0.41***	Polyphenylene sulfide (PPS)	**50** ***1.90***	Acrylonitrile butadiene styrene (ABS) nylon alloy
17 ***1.45***	Thermoplastic polyester (PBT)	**34** **2.77**	EVA copolymer		

[a] *stands for TOC, total oxygen consumption/g of polymer sample*

2. Material and methods

The list of the polymers is given in the Table 1. Polymers that were graphically presented are in the red. In the Table 1 there is the total oxygen consumed related to 1 g of burned polymer.

Dual cone calorimeter was the product of Fire testing technology, England. For thermally thin polymer samples in the form of plates a special rectangular holder (of the surface 83 cm^2) was used made from stainless steel (9.1x9.1x0.3) cm. The holder was placed into the sample holder supplied by cone calorimeter producer. The bottom of the holder was isolated from the main holder by 5 mm thick layer of kaowool. The centre of the samples was situated 6 cm from the lowest part of the cone heater.

The heat release rate was calibrated by burning methane. The reproducibility of burning experiments as it concerns the ignition time, heat release rate, mass loss and total smoke production under conditions of piloted ignition was good provided that the holders with sample were initially thermostated to the room temperature.

The cone radiancy 35 kW m^{-2} which corresponds to a certain cone temperature (770 ^oC) was set according to the calibration diagram for a distance of the sample from the cone edge 6 cm.

Thermogravimetry (TG) measurements were performed using a Mettler Toledo TGA/SDTA 851e instrument in a nitrogen flow (30 ml min^{-1}) using a heating rate of 5 °C min^{-1} in a temperature range from room temperature up to 550 °C. Indium and aluminium were used for temperature calibration. The amount of samples applied was around 3 mg.

3. Results and discussion

Fig.1 shows the oxygen consumption during burning of several polymers in cone calorimeter. These curves are original records from the instrument and the data such as heat release rate (HRR), total heat release (THR) are derived from it via the surface of the burning polymer. The surface of the burning polymer is the parameter inserted by the cone calorimeter operator and therefore to obtain reliable heat release rate data it must be kept constant during all experiment. This is also the reason why the calorimeter producer strictly requires using the standard sizes of samples (surface 100 cm^2). The shape of heat release rate curve is formally identical with the rate of oxygen consumption (Fig. 2) and is related to it through the calibration constant. Some discrepancies may be however observed when correlating e.g. the total heat release (THR) with total oxygen consumed (TOC) (Fig. 3). In the case of polymers as polypropylene (sample 27) that melts after ignition and spreads over the sample holder the declination from the straight line was observed. In the red color, there are depicted the samples that melted when the melt was evidently spread along the sample holder. Straight line corresponds to the samples which surface did not change during the burning. Recalculation from the slope gives the initial surface 28 cm^2 that is 80 % of the real surface of the samples that were initially put to the holder (36 cm^2). The interesting fact seen from the Fig. 1 is the steady but slight increase of the amount of oxygen consumed after the flame extinction that may be ascribed to the subsequent oxidation of the carbon residue being formed from polymer degradation (Fig. 1).

From this aspect, the amount of oxygen consumed related to 1 g of polymer burned (Table 1) appears to be more reliable criterion of rating of flammability of polymers having non standard sizes.

The release of volatiles during programmed heating for some samples from the Resin Kit may be exemplified in the Fig. 4. The selection of polymers shown was done so that we can easily come to the conclusion that the ignitability of the polymer is related to the facility of polymer decomposition. Time to ignition in a cone calorimeter moves from the very low value for plasticized PVC (23 s) to the thermally stable polymers such as polyphenylene sulphide, polysulfone and polycarbonate (100-300 s). Thermal stability of polymethyl methacrylate (PMMA), polystyrene, polypropylene and polyethylene follow this tendency even more perfectly, namely (40, 65, 69 and 81) s, respectively. However, when plotting time to ignition from cone calorimeter vs. temperature of the maximum rate of volatiles release from thermogravimetry for all polymers from the Resin Kit examined we see that the correlation is rather poor and that the general relation, namely that the higher temperature of the volatiles release means the higher time to ignition is not valid unambiguously (Fig. 5).

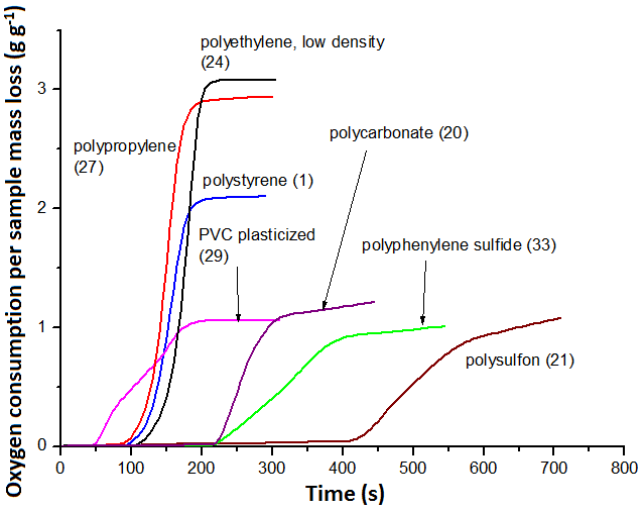

Figure 1 The cone calorimetry runs of oxygen consumption per gram of polymer sample during the burning of polymers (the cone radiancy 35 kW m^{-2})

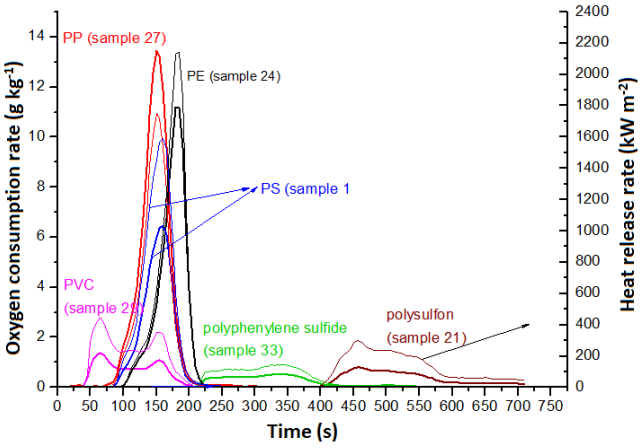

Figure 2 The comparison of the lines of oxygen consumption rate and heat release rate for burning of the selected group of polymers from the Table 1 (weaker lines are related to the heat release rate; cone radiancy 35 kW m^{-2})

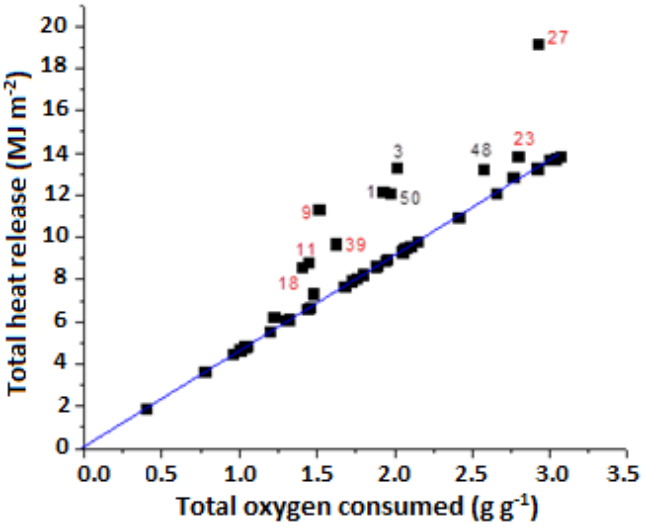

Figure 3 The correlation between total heat released and total oxygen consumed for cone calorimeter measurements of resin kit polymers

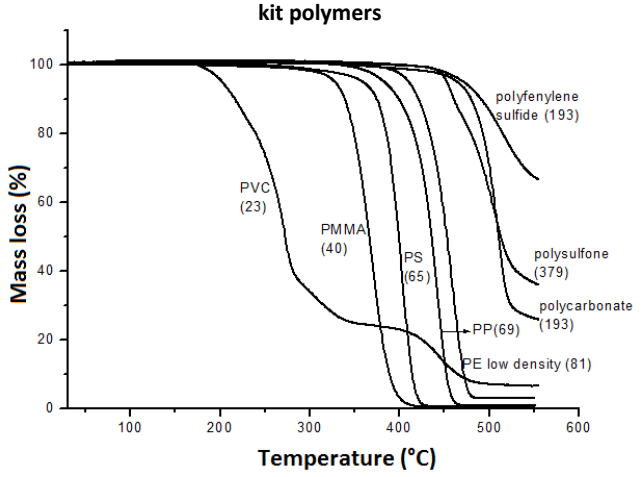

Figure 4 Example of TG records for polymers No. 29, 9, 1, 27, 24, 20, 21 and 33 from the Resin Kit (the rate of sample heating 5 °C min^{-1}, nitrogen atmosphere, the numbers in brackets denote the time to ignition (s) in cone calorimeter at the cone radiancy 35 kW m^{-2})

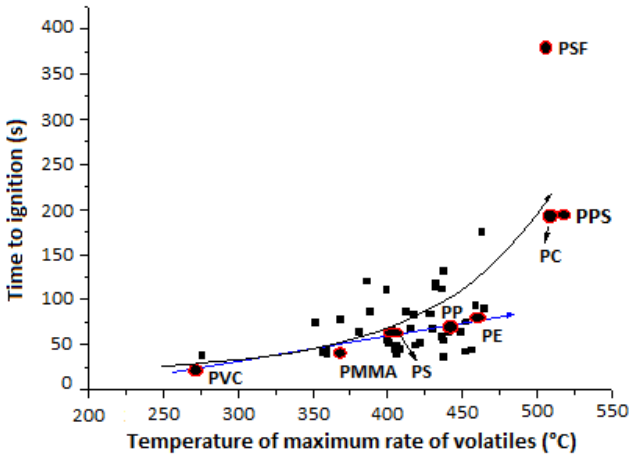

Figure 5 Correlation of the time to ignition from cone calorimeter with the temperature of the maximum rate of volatiles released from thermogravimetry

4. Conclusion

1. From the correlation between total heat released and total oxygen consumed it follows that initial surface of burning sample inserted into the instrument by operator is the important parameter affecting the resulting heat release rate release. It was deduced that the surface holding the flame is 80 %, approximately, of this initial value.
2. In the case of samples with non-standard sizes, the total oxygen consumed or the rate of oxygen consumption is more reliable parameter of flammability than the total heat released and heat release rate data.
3. Time to ignition does not correlate well with thermal stability of polymers as determined by non-isothermal thermogravimetry. From the Fig. 4 and 5, however, is seen that there may be found groups of polymers for which the idea of good correlation may be adopted.

Acknowledgements

This publication is the result of the project implementation: Centre for materials, layers and systems for applications and chemical processes under extreme conditions. Part II supported by the Research & Development Operational Programme funded by the ERDF.

References

[1] Babrauskas V, Peacock RD. Heat release rate: the single most important variable in fire hazard. *Fire Saf J* 1992;18(3):255-72.

[2] Huggett C. Estimation of rate of heat release by means of oxygen consumption measurements. *Fire Mater* 1980;4(2):61-5.

[3] International Organization for Standardization. ISO 5660-1:2002. Reaction-to-fire tests: Heat release, smoke production and mass loss rate. Part 1: Heat release rate (cone calorimeter method). Geneva: ISO; 2002.

[4] Lindholm J, Brink A, Hupa M. The influence of decreased sample size on cone calorimeter results. *Fire Mater* 2012;36(1):63-73.

[5] Rychlý J, Rychlá L, Csomorová K. Characterisation of materials burning by a cone calorimeter: 1 pure polymers. *J Mater Sci Eng A* 2012;2(2):174-82.

[6] Shi L, Chew MYL. Fire behaviors of polymers under autoignition conditions in a cone calorimeter. *Fire Saf J* 2013;61(1):243-253.

[7] Reisen F, Bhujel M, Leonard L. Particle and volatile organic emissions from the combustion of a range of building and furnishing materials using a cone calorimeter. *Fire Saf J* 2014;69(1):76-88.

[8] Ezinwa JU, Robson LD, Torvi DA. Evaluating models for predicting full-scale fire behaviour of polyurethane foam using cone calorimeter data. *Fire Technol* 2014;50(3):693-719.

European Journal of Environmental and Safety Sciences 2014 2(2): 28-36
ISSN 1339-472X European Science and Research Institute (Original Research Paper)

Short-term change in the thermal conductivity of a loam soil after a forest fire

Carles M. Rubio[a,b]

[a]*Department of Nanotechnology, Materials and Processes, Advanced Technology Centre Ascamm Foundation, 08290 Cerdanyola del Valles, Spain*
[b]*GRAM, Department of Physical Geography, University of Barcelona, 08001 Barcelona, Spain*

ABSTRACT

The purpose of this work is to explore the variability in the soil thermal conductivity of burnt soil and assess the effects of the ashes on the heat transfer when they were incorporated into the soil matrix. A set of 42 soil samples from the Montgrí massif experimental plot between the surface and 5 cm depth was collected before and after the soil was burnt. A thermal characterization of the soil was carried out and for that, the dry out curves were constructed. These presented the relationship between water content and thermal conductivity for both types of soil samples, burnt and non-burnt soil. The results show that soil is more conductive to the heat pulse transfer before the soil was burnt (0.378 W m^{-1} C^{-1}) than after the soil was exposed to the fire (0.337 W m^{-1} C^{-1}). Therefore, within a range of moisture scenarios, the values of thermal conductivity decreased after soil was burnt. An experimental concern was based on observing the soil thermal behavior when ash collected after fire was incorporated into the burnt soil matrix. In this case, soil thermal and soil hydrodynamic behavior were different according to the type of ash. Soil mixed with white ash showed higher thermal conductivity than soil mixed with black ash. To sum up, the soil thermal conductivity decreased when soil was burnt. However, soil thermal conductivity was different differences depending on the type of ash incorporated into the matrix. White ash transferred the heat pulse better than black ash.

Keywords: Ash · Forest fire · Thermal properties · Water content

1. Introduction

Forest fires are part of the Earth's ecosystems and they determine the vegetation characteristics, the soil properties and the hydrological behavior. Fires are an important agent in Boreal, Temperate, Tropical and Mediterranean ecosystems, where are especially recurrent during summertime [1-2]. Ash is one of the several components affecting soil behaviour after forest fires [3], but little is known about the impact of ash on soil thermal properties.

Fire has shaped global ecosystems for over 350 million years and has been a driving force for the evolution and spread of new plants and biomes [4]. The impact of fire on soils may vary between extremely beneficial or extremely harmful, able to cause irreversible degradation processes. Low-intensity and short-in-time fires do not cause significant impacts in soils. In contrast, irreversible damages may occur after high-intensity fires, when heat penetrates deeply into the soil and the heat pulse is maintained for a long time [5-6]. Some researchers have studied the variation in the chemical [7] and physical properties [8] soils after fire, although some aspects are not yet fully explained or have not been considered in the literature. Some of these are soil properties governing the heat flow transport inside the soil matrix, which are especially affected by three important physical and chemical variables: compaction, moisture content and mineralogy.

Intensity of impacts may vary depending on the severity of soil heating during a wildfire. In some cases, burning induces the formation of a water-repellent surface or subsurface soil layer, the destruction of most of the organic material in the upper few centimeters of soil decrease ag-

Carles M. Rubio (corresponding author)
Department of Nanotechnology, Materials and Processes, Advanced Technology Centre Ascamm Foundation, 08290 Cerdanyola del Valles, Spain
GRAM, Department of Physical Geography, University of Barcelona, 08001 Barcelona, Spain
e-mail: crubio@ascamm.com

gregate stability [9-10], changes in soil pH and soil chemistry, differences in soil water content, increase bulk density and reduce soil porosity [11-12]. Hence, when biomass burns on or above soil surface, the heat pulse penetrates into the soil body causing damages to roots and changes to microbial populations [13-14].

Prescribed burning is a useful tool to maintain the shrublands, especially in Mediterranean area. When properly applied, prescribed fire largely consumes litter and soil organic matter and, depending upon the completeness of combustion [15], this can be a major mechanism for nitrogen loss [16-18]. After prescribed fire, some nutrients are concentrated in the ash [19]. Some authors have defined ash as the waste of residues resulting from burning [20-22]. However, this explanation is rather focused on industrial burnings. Other authors have defined ash as the particulate residue remaining or deposited on the ground that consists of mineral materials and charred organic components [3].

Ash is composed of carbonates, silicates, apathite, oxides, hydroxides, sulphates and chlorine [23], and may include elements which may show a certain degree of toxicity [24-25]. Also, the chemical and physical properties of ash were studied by Ulery et al. [26], Goforth et al. [27], Smith and Hudak [28] and Úbeda et al. [29] in order to improve the current methodology to estimate and evaluate ash properties using updated and new techniques [23, 29].

Few research works have been conducted on the impact of ash on soil physical properties. Currently, it is known that an ash layer on the soil could increase the water retention on the soil surface, and therefore decrease runoff [30-33]. Some authors have observed that fine ash particles can collapse soil pores [33] and seal the soil surface [34-35]. According to Bodí et al. [36] several types of ash may be generated for burning different vegetal species. After low-severity combustion, ash produced is usually darker, more coarsely textured and less permeable than ash produced after severe combustion. Dark ash from low-severity burning may induce or enhance soil water repellency, so contributing to increased runoff rates and sediment yields [3].

Changes in soil thermal conductivity (λ) after burning are less obvious [13]. These changes are related with fire impacts on soil structure. Soil thermal conductivity is strongly determined by soil structure [37], and soil composition [38-39]. Usually, changes in aggregation occur in most soils after partial or complete combustion of soil organic matter.

Consequently, the purpose of this research is to explore the variability of soil thermal conductivity in a fire-affected Mediterranean loam soil. In order to achieve this goal, the following objectives were considered: (i) to study the relationship between soil thermal conductivity and water content, (ii) to evaluate the influence of different amounts of ash on soil thermal conductivity, and (iii) to determine the impact of ash incorporated into the soil matrix on soil thermal conductivity under different conditions of moisture content.

2. Material and methods

2.1. Study area

The study area is located in the north-eastern corner of the Iberian Peninsula in the coastal mountains of Catalonia (Figure 1). Vegetation is typically Mediterranean, composed by pine plantations (*Pinus halepensis*) with shrubland of kermes oak (*Quercus coccifera*), rockrose (*Cistus albidus*), rosemary (*Rosmarinus officinalis*) and mastic (*Pistacea lentiscus*). At the time of the fire, the air temperature was 12.5 ºC with air relative moisture at about 60%. Two sets of 42 soil samples (0-5 cm depth) were collected before and just after the fire using a homogeneous grid (geographical coordinates 42º5’13’’N 3º10’33’’E).

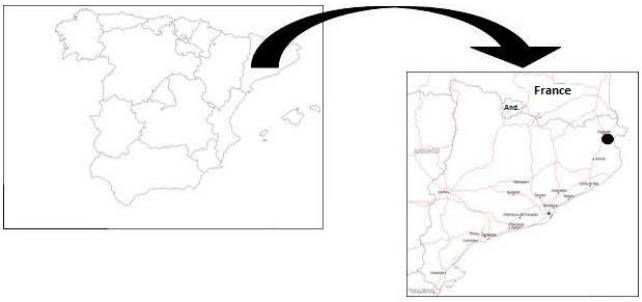

Figure 1 Location of the study site (the black point indicates the sampling area)

2.2. Laboratory analysis

The soil surface temperature was measured in every sampling spot with an infrared thermometer after burning. In order to characterize the soil, chemical and physical variables were analyzed. Particle-size distribution was determined using the wet sieve method for the particles between 50 μm and 2000 μm, and a dispersion laser beam device (Malvern Mastersizer/E) for particles smaller than 50 μm. Bulk density and porosity were determined using undisturbed sample volumes (around 100 cm^3 per collected sample) [40]. Calcium carbonate content was determined using a Bernard calcimeter [41]. Hygroscopic water content was determined by weight differences after drying the samples at 105 ºC for 24 hours. The pH and electrical conductivity were analyzed using an extract of distilled water (w:v, 1:2.5 ratio), and measured with a pH-meter and conductivity meter [42]. The organic matter content was determined according to the sulfochromic oxidation and titration method [43].

In order to determine the variability of the soil thermal conductivity (λ), composed samples were prepared using the 42 samples of each scenario (i.e. before and after the area was burnt). In order to study the relationship between thermal conductivity and water content $\theta(\lambda)$, different dry-out curves were calculated [44-45]. The dry-out curves were constructed by wetting up air dry samples with distilled water. Thus, 6 different moisture points on the dry-out curve were obtained. Soil and water were homogenized and packed into a soil column device up to reach the bulk density determined in the laboratory bulk density test such as it is described above. Soil columns were covered and insulated in a thermal chamber until steady-state conditions were reached, i.e. constant weight and temperature. The water content was calculated by drying the sample in the oven and observing, after 24 hours, the loss of weight. The thermal conductivity as a function of water content was measured with the methodology developed according to the analysis described by Rubio [46]. A SH-1 dual needle thermal sensor combined with KD2-Pro (Decagon Devices, Inc.) reader-logger allowed to obtain reliable and accurate soil thermal conductivity values.

An experimental design with ashes was performed using soil column devices, as well. To carry out the ongoing research, several volumes of two types of ashes (white and black) were used. White and black ash samples were collected from some burnt patches into the experimental plot. The colour of ashes indicates differences in the temperature reached on the soil surface and also indicates differences in the physical and chemical composition of ashes [47-48]. Ash samples were mixed with burnt soil to get samples (10, 20, 30, 40, 50, 60, 70, 80 and 90) % ash/soil ratios in volume. Mixed samples were air-dried during until constant weight and soil thermal conductivity was determined.

2.3. Statistical analysis

To evaluate whether the dataset follows a normal distribution, i.e. the parametric or non-parametric distribution of the dataset, a frequency histogram was constructed. The normal distribution of data was rejected by visual examination of histograms. So, non-parametric tests were used to study differences between mean values (Mann-Whitney U-test) and possible correlations (Spearman's rank correlation coefficient). The SPSS software pack was used for computations [49]. The Mann-Whitney U-test is a non-parametric statistical hypothesis test used when assessing whether their population mean ranks differ. In this work, the test was used as an alternative to the paired Student's t-test because the samples did not follow a normal distribution.

To observe the statistical dependence between two groups of samples, burnt soil and non-burnt soil, the Spearman's rank correlation coefficient was calculated. The coefficient assesses how well the relationship between two variables can be described using a monotonic function. Spearman's coefficient is appropriate for both continuous and discrete variables with a significance level of $P < 0.05$.

Also, we used the Wilcoxon Signed-Rank Test to asses if the thermal properties differences between black and white ashes were significant when these were incorporated at the sample soil sample. The Wilcoxon test is a non-parametric statistical hypothesis test used when assessing whether their population mean ranks differ. In this work, the test was used as an alternative to the paired Student's t-test because the samples did not follow a normal distribution.

Eventually, we used two objective quantities to express the differences in terms of thermal conductivity between non-burnt soil and burnt soil, as well as to quantify the differences when 90 % of ash (black or white ash) was incorporated into non-burnt soil matrix, as the alternative way to investigate how much alter the soil thermal properties when the ash is incorporated in the soil. The mean error (ME) quantifies the systematic bias between burnt soil and non-burnt soil thermal conductivities. The root mean square error (RMSE) determines the deviation in the comparison from the measurement.

$$\mathrm{ME} = \frac{1}{n}\sum_{i=1}^{n}(\theta_{\mathrm{i}} - \hat{\theta}_{\mathrm{i}}) \quad (1)$$

$$\mathrm{RMSE} = \sqrt{\frac{1}{n}\sum_{i=1}^{n}(\theta_{\mathrm{i}} - \hat{\theta}_{\mathrm{i}})^2} \quad (2)$$

where θi and θi denote respectively measured non-burnt soil and determined burnt soil values of thermal conductivity at any specified water content ω. Then n is the number of samples or different measures for which the ME and RMSE were calculated.

3. Results and discussion

3.1. Characterization of soil physical and chemical properties

According to the USDA textural classification [50], soil texture is loam. The values of chemical and physical properties before and after fire are as follows: sand particle size increased (from 39.3 % to 41.7 %) and the silt particle size decreased (from 35.1 % to 32.4 %). Mean bulk density was around 1.1 g cm^{-3}, and mean total organic carbon content was about 11.2 % and 10.9 %. Mean electric conductivity increased, showing values from 126 μs cm^{-1} before burnt up to 199 μs cm^{-1} at 25 ºC after burnt. On the other hand, the values of the variables pH, mean calcium carbonate con-

tent, and mean hygroscopic water content are similar for the samples between not burnt and burnt soil.

3.2. Characterization of soil thermal conductivity measurements

The Mann-Whitney U-test has shown a Z value about -1.849, then solving for the Z value in the normal distribution table confirms that the soils differ around 6.5 % for 30 degrees of freedom, for $p \leq 0.05$. Therefore, the test is not allowed to accept the null hypothesis, hence the two soils (burnt and non-burnt) that presented slight differences between them, and on the whole of the dry-out curve. On the other hand, Spearman's coefficient has shown an r of 0.98 significant at a $p \leq 0.01$.

Table 1 shows differences between both soil thermal conductivities for a burnt and non-burnt soil. At any water content, thermal conductivity from burnt soil was lower than thermal conductivity from non-burnt soil, with differences between (0.03 and 0.06) W m^{-1} C^{-1}.

On the other hand, steady-state conditions are reached for water contents above 0.10 g_{H2O} g_{soil}^{-1}. The critical point in the burnt soil was stronger, presenting a critical reaction approximately at 0.08 g_{H2O} g_{soil}^{-1}; whereas, the non-burnt samples showed a critical point around 0.06 g_{H2O} g_{soil}^{-1} (Table 1).

Table 1 Relationship between thermal conductivity and water content, for a loam soil before and after prescribed fire (WC = water content (g_{H2O} g_{soil}^{-1}); λ = thermal conductivity (W m^{-1} C^{-1}) and Std = standard deviation)

	Burnt Soil			Non-Burnt Soil		
	WC	λ	Std	WC	λ	Std
Air dry	0.03	0.16	0.001	0.03	0.19	0.001
Moisture-1	0.07	0.18	0.002	0.05	0.24	0.001
Moisture-2	0.08	0.21	0.002	0.07	0.25	0.001
Moisture-3	0.11	0.26	0.003	0.10	0.29	0.006
Moisture-4	0.14	0.31	0.002	0.13	0.35	0.007
Saturation	0.58	0.90	0.004	0.56	0.95	0.004

Differences between both samples maybe due to organic matter content, as the thermal conductivity of organic mater is lower than that of the mineral matter [44-45] .

Temperature monitoring indicated that, during the experiment, mean temperature was around 21.5 ºC in non-burnt soil samples. In contrast, mean temperature of the burnt soil samples during the experiment was around 18.5 ºC. These differences may indicate certain variations in the thermal conductivity, especially when soil was close to saturation. Hence, Figure 2 shows divergences on soil thermal conductivity values for the whole dry-out curve. In non-saturated soils, high temperatures may cause water evaporation under certain conditions. This fact should be explained in terms of the temperature dependence of liquid flow in porous media, owing to the results from the temperature effects on water viscosity and volumetric moisture content, through the hydraulic conductivity gradient and consequently the heat transfer. On the other hand, in the saturated zone of the curve, viscosity effects are the only cause for the variations in thermal conductivity (and also liquid velocities) as influenced by temperature [51]. Thus, in more humid regions of the curve, conductive heat transfer and liquid water transport usually are the primary modes of transport related to the transient mechanism of thermal energy and moisture flow. When the heat pulse is transferred in drier regions of the curve, conductive heat transfer and vapour water transport are the dominant processes of thermal energy transport [52].

3.3. Determination of the effect of ashes on soil thermal properties

Eventually, a new experiment with ash was carried out. After the prescribed fire several quantities of ash were collected, and used in percentage of weight to mix with non-burnt soil matrix. The ashes were sampled from different patches from the burnt soil surface. Black ash was found where the temperature measured with the infrared thermometer was around 150 ºC. If the temperature reaches more than 400 ºC combustion of organic carbon begins to produce white ash. In our plot, the temperature on the soil surface, measured just after prescribed fire with the same infrared thermometer reached the 600 ºC.

The first step of this research work was to observe the relationship between bulk density and porosity using burnt soil and different types of ash (black and white ash). This relationship is shown in Figure 2, where the linear relation between both variables showed well-compacted soil samples. The porosity pattern decreased in proportion to the increase in the bulk density. In both cases, two well-defined groups of burnt soil samples were determined in terms of type of ash, which shown the Spearman's coefficient r 0.97 significant for $p \leq 0.01$.

The soil repacked with black ash had lower bulk density values than soil mixed with white ash, which had a lower porosity. Massman et al. [53] observed differences in the bulk density values of two soils (from 0 to 5 cm depth) after being burnt. This fact provides evidence of the incorporation of a certain quantity of ash into a few top centimeters of the soil surface [48], [54]. The incorporation of ash provides a lower bulk density in the upper soil layer [53]. White ash shows lower specific weight than black ash [29] and less particle size, as well. Nonetheless, some studies

about forest fire such as Certini [55] and Badía and Martí [56] document that the bulk density of soil increases significantly as a result of forest fire. This fact is because of the collapse of aggregates and clogging of voids by the ash and dispersed clay minerals, due the high presence of extractable sodium and potassium in ash solution that increase clay dispersion [57-59] cited in Pereira et al. [60]. As a consequence, soil porosity and permeability decreases [55].

Figure 3a presents data on thermal conductivity for different percentages of black and white ash, which were mixed with burnt soil. The measurements in the test were always carried out using burnt dry soil samples. The soils mixed with white ash (dotted line) had a higher thermal conductivity than black ash (continuous line). These differences might be attributed to the large organic carbon content of black ash, which was not completely consumed during the prescribed fire [61]. Thus, soil organic matter contributed to decrease soil thermal conductivity. In terms of particle size, black ash is coarser than white ash [3] increasing the porosity. Consequently, a higher void in the soil matrix will decrease the heat transfer. When organic matter content increases, soil shows a poorer soil heat pulse transfer [62]. On the other hand, higher bulk density of the white ash compared to black ash increased the target bulk density, and contributed to improve soil thermal conductivity, except in the measurement with 90 % by volume of ash (Figure 3a), where the soil thermal conductivity drastically decreased for both types of samples. Eventually, a Wilcoxon signed rank test has shown a Z value about -2.386 with asympthotic significance value of 0.017 for $p < 0.05$. Therefore, the test rejects the null hypothesis; hence the two soils samples with several percentages of ash (black and white) have presented slight differences between them.

The relationship between thermal conductivity as a function of water content is shown in Figure 3b. The test was performed using the soil samples with 90 % volume of ash, for both black and the white ash. Soil thermal conductivity, as a function of water content, was determined between water content at air-dry soil and the theoretical point at field capacity. For the new observation points, the quantity of water added to the soil samples was the same as for the dry out curves shown in Figure 2. Nevertheless the soil samples mixed with ash (Figure 3b) demonstrated substantially different water dynamics. Soil mixed with black ash increased its water retention content close to saturation (from 0.585 $g_{H2O}\ g_{soil}^{-1}$ to 0.745 $g_{H2O}\ g_{soil}^{-1}$), yet its thermal conductivity value decreased (from 0.900 W m^{-1} C^{-1} to 0.705 W m^{-1} C^{-1}), if the values are compared against soil lambda values before to mix with ash. The soil mixed with white ash had a lower value of thermal conductivity (0.848 W m^{-1} C^{-1}), meanwhile the water content at saturation was slightly lower (0.445 $g_{H2O}\ g_{soil}^{-1}$).

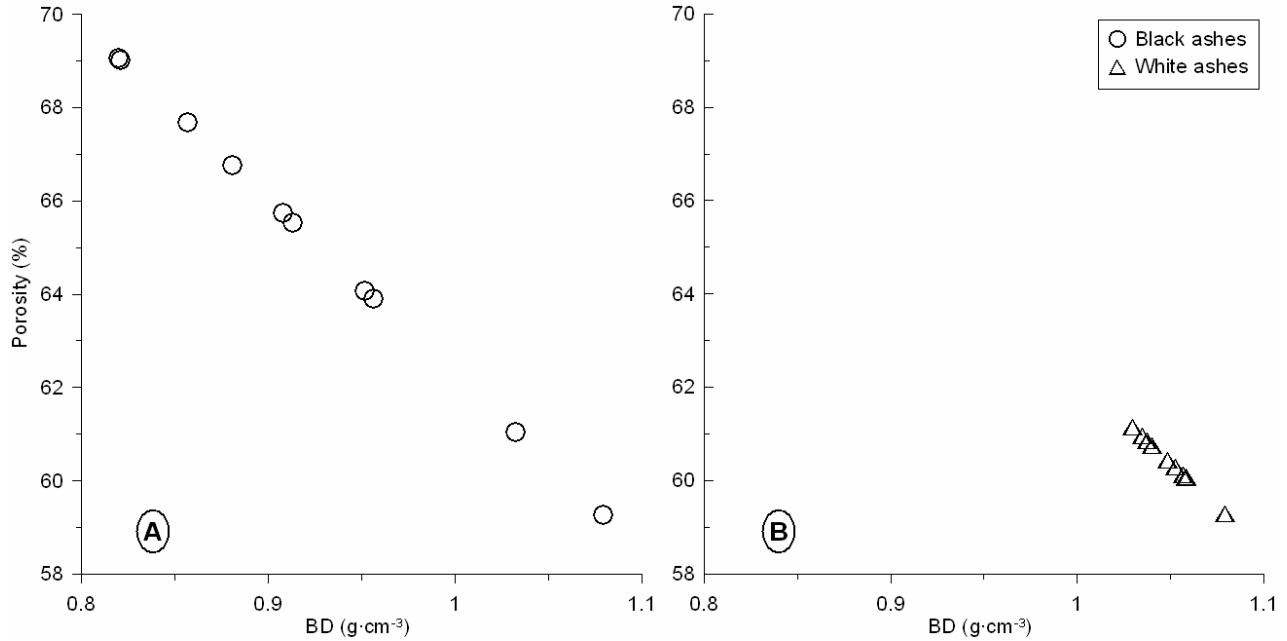

Figure 2 Relationship between soil bulk density (BD) and total soil porosity (effect for a burnt loam soil mixed with black ash and white ash) [44]

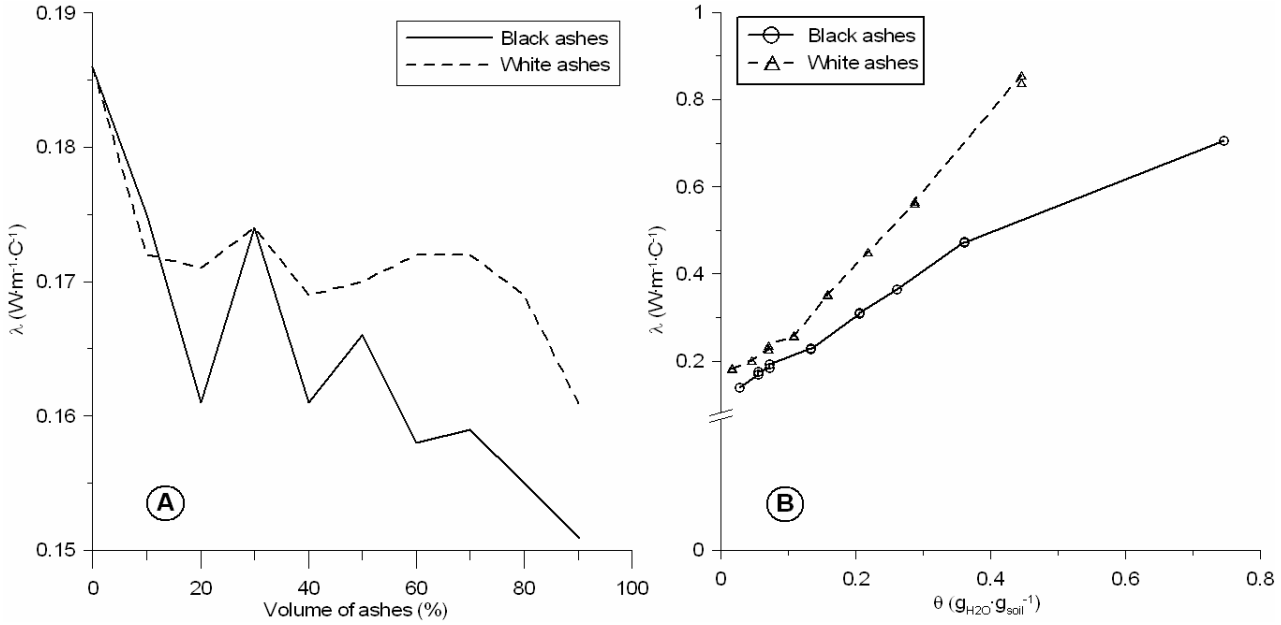

Figure 3 Effect of the ash on soil physical properties. A) Relationship between thermal conductivity (λ) and volume of ash; B) Relationship between thermal conductivity (λ) and gravimetric water content (θ), being the soil matrix mixed with 90 % of white ash and 90% of black ash. [44]

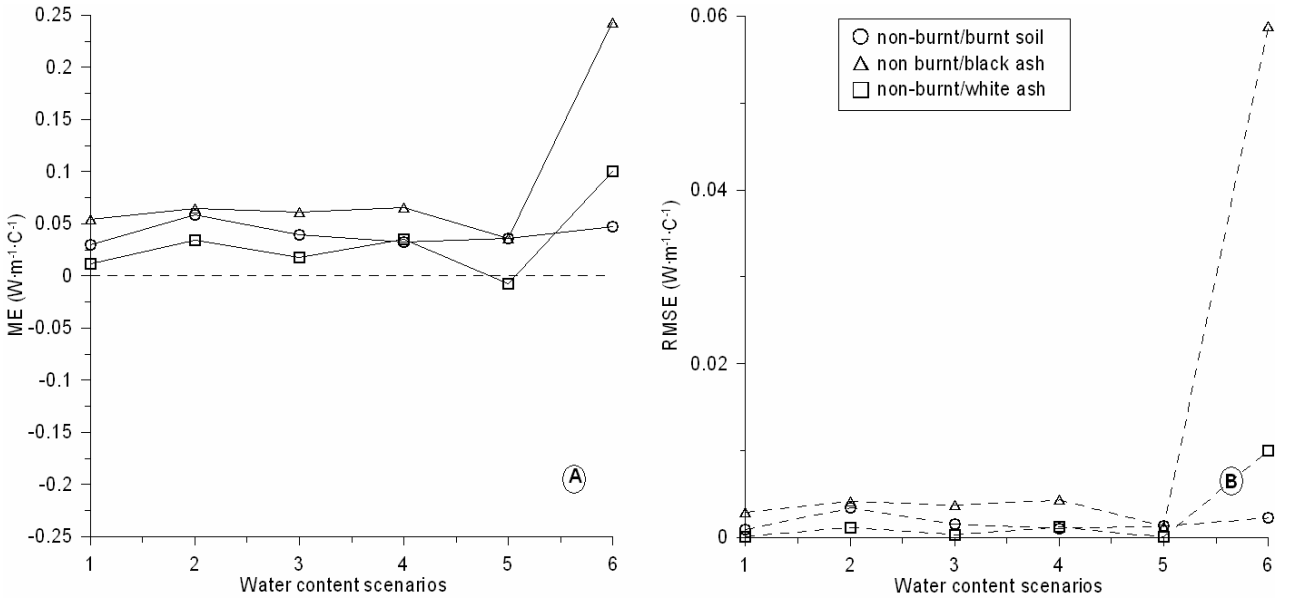

Figure 4 Mean error (ME, graph A) and root mean square error (RMSE, graph B) of the soil thermal conductivity curve and the three conditions analyzed: burnt soil, burnt soil with 90 % black ash, and burnt soil with 90 % white ash

Figure 3b shows clear differences between white and black ash when these were incorporated into the soil matrix. In this case, the Wilcoxon signed rank test has eventually shown a *Z* value about -2.524 with asymptotic significance value of 0.012 for $p < 0.05$. Therefore, the test either is allowed to accept the null hypothesis, hence the two soils samples presented significant differences as well. Over the entire two mean dry-out curves, differences were larger at values closer to saturation. An acceptable explanation could be as follows: (i) soil mixed with white ashes had a finer particle size distribution, which increased the water film around the particles because of the larger area. Moreover, the white ash increased the bulk density and as a result the air within the soil pores was reduced. Therefore, a rather high compaction of black ash involved a better heat flux transfer. It had high influence due to water film around the ash [63] because of the contact resistivity among particles that was reduced as well as the volume of air; (ii) the black ash particle size was larger than the white ash particle size. Also, the organic carbon content increased in the soil ma-

trix. The combination of both features produced a low thermal conductivity value for the entire of the mean dry-out curve for the soil mixed with black ash.

3.4. Quantifying the differences between non-burnt and burnt loam soil

Figure 4 shows the ME and the RMSE for the three different conditions soil in terms of the variability of soil thermal conductivity, and for all soil moisture content scenarios. The mean ME for all conditions was between 0.032 and 0.041 for burnt soil and soil mixed with white ash (Figure 4a), except for soil mixed with black ash (0.087). The maximum differences between conditions were at saturation in burnt soil (about 0.048) and mixed with white ash (0.010), to a lesser extent, near 11 % of water content was in mixed black ash soil (0.066).

All conditions analyzed showed similar patterns of mean RMSE across the six moisture content scenario points (Figure 4b), with values around 0.04 and 0.1 for burnt soil and soil mixed with white ash, respectively. For black ash soil mixed with black ash, the mean RMSE were slightly higher (Figure 4b).

Both ME and RMSE decreased from saturation to the drier water content points over the entire dry-out curves (Figure 4b). Although all the soil conditions exhibited very similar behavior, the maximum thermal conductivity differences were always found when the soil was close to saturation. These were due to differences in the type of ash and the hydrological behavior between fine and coarse particle size, i.e. black and white ash.

4. Conclusion

This study attempts to contribute information on soil thermal properties, especially when the soil has been affected by fire. Also, the study provides some insight into the effect of the ash post-fire on the soil thermal properties. To sum up the highlights of the study, we can conclude as follows;

i) For the burnt soil studied, the thermal conductivity values were lower than the soil measures taken before prescribed fire.
ii) Over the entire soil moisture scenarios, the soil thermal behavior was linear especially when the water content was close to saturation.
iii) The analysis of the ash mixed with the burnt soil indicated that white ash, which is poorer in organic carbon content, provided a better heat flow transfer than soil mixed with black ash.
iv) The finer particle size of the white ash increased the conductance of the heat flux into the soil.
v) The improvements of the white ash to soil water retention content, soil bulk density, and soil organic carbon content, never reached the original values of the soil thermal conductivity before the soil was burnt.
vi) Higher thermal conductivity differences, in terms of ME and RMSE, were for the burnt loam soil with black ash incorporated into its matrix.

In conclusion this work allowed observing how a loam soil is burnt, and therefore its thermal conductivity decreased, even if the water content governed the heat transfer.

Acknowledgements

I want to thank the Department of Agri-Food Engineering and Biotechnology of the Polytechnic University of Catalonia meanwhile this research was carried out. We thank the GRAF team in the fieldwork support during the prescribed fire. Also, I thank to Commission for Universities and Research of the Generalitat of Catalonia DIUE.

References

[1] Guénon R, Vennetier M, Dupuy N, Roussos S, Pailler A, Gros R. Trends in recovery of Mediterranean soil chemical properties and microbial activities after infrequent and frequent wildfires. *Land Degradation and Development* 2013;24:115-28.

[2] Martín A, Díaz-Raviña M, Carballas T. Short and medium term evolution of soil properties in Atlantic forest ecosystems affected by wildfires. *Land Degradation and Development* 2012;23:427-39.

[3] Bodí MB, Martin DA, Balfour VN, Santín C, Doerr SH, Pereira P, Cerda A, Mataix-Solera J. Wildland fire ash: production, composition and eco-hydro-geomorphic effects. *Earth-Science Reviews* 2014;130:103-27.

[4] Scott AC. The pre-Quaternary history of fire. *Palaeogeography, Palaeoclimatology, Palaeoecology* 2000;164:281-329.

[5] DeBano LF, Neary DG, Ffolliott PF. *Fire's Effects on Ecosystems*. NewYork: Wiley; 1999. 352 p.

[6] DeBano LF, Neary DG, Ffolliott PF. Soil physical properties. In: Neary DG, Ryan KC, DeBano LF, editors. *Wildland Fire in Ecosystems: Effects of Fire on Soil and Water*. Ogden: USDA Forest Service; 2005. p. 29-51.

[7] Úbeda X, Lorca M, Outeiro L, Bernia S, Castellnou M. The effects of prescribed fire on soil quality (Prades Mountains, North East Spain). *International Journal of Wildland Fire* 2005;14(4):379-84.

[8] Arcenegui V, Mataix-Solera J, Guerrero C, Zornoza R, Mataix-Beneyto J, García-Orenes F. Immediate effects

of wildfires on water repellency and aggregate stability in Mediterranean calcareous soils. *Catena* 2008;74(3):219-26.

[9] Mataix-Solera J, Doerr SH. Hydrophobicity and aggregate stability in calcareous topsoils from fire-affected pine forests in southeastern Spain. *Geoderma* 2004;118:77-88.

[10] Keeley JE. Fire intensity, Fire severity and burn severity: a brief review and suggested usage. *International Journal of Wildland Fire* 2009;18:116-26.

[11] Huffman EL, MacDonald LH, Stednick JD. Strength and persistence of fire-induced soil hydrophobicity under ponderosa and lodgepole pine, Colorado Front Range. *Hydrological Processes* 2001;15:2877-92.

[12] Neary DG, Ryan KC, DeBano LF, Landsberg JD, Brown JK. In: Neary DG, Ryan KC, DeBano LF, editors. *Wildland Fire in Ecosystems: Effects of Fire on Soil and Water*. Ogden: USDA Forest Service; 2005. p. 1-17.

[13] Campbell GS, Jungbauer JD, Bidlake WR, Hungerford RD. Predicting the effect of temperature on soil thermal conductivity. *Soil Science* 1994;158(5):307-13.

[14] Ellet K, Gustin A. *Monitoring near-surface thermal properties in conjunction with energy and moisture budgets to facilitate the optimization of ground-source heat pumps*. Indianapolis: University of Indiana; 2000. 160 p.

[15] Finn RF. The leaching of some plant nutrients following burning of a forest litter. *Black Rock Forest Papers* 1934;1:128-34.

[16] Burns PY. *Effects of fires on forest soils in the Pine Barren region of New Jersey*. New Haven: Yale University; 1952. 50 p.

[17] Austin RC, Baisinger DH. Some effects of burning on forest soils of western Oregon and Washington. *Journal of Forest* 1965;53:275-80.

[18] DeBell DS, Ralston CW. Release of nitrogen by burning light forest fuels. *Soil Science Society of America Journal* 1970;34:936-38.

[19] Isaac LA, Hopkins HG. The forest soil of the Douglas-fir region and changes wrought upon it by logging and slash burning. *Ecology* 1937;18:264-79.

[20] Block RMA, Van Rees KCJ. Characterization of aspen ash, sand and log-yard waste mixtures from an aspen-based oriented strand board mill for use as an intermediate landfill cover. *Water Air and Soil Pollution* 2004;158: 223-66.

[21] Demeyer A, Vuondi Nkana JC, Verloo MG. Characteristics of wood ash and influence on soil properties and nutrient uptake: an overview. *Bioresource Technology* 2001;77:253-66.

[22] Zhou H. Reducing, reusing and recycling solid wastes from wood fibre processing. In: Burton PJ, Messier C, Smith DW, Adamowicz WL, editors. *Towards Sustainable Management of the Boreal Forest*. Ottawa: NRC Research Press; 2003. p. 759-798.

[23] Pereira P. *Effects of fire intensity in the physico-chemical characteristics of the ashes of plant species Mediterraneas and their impact on water quality*. Barcelona: Universitat de Barcelona; 2010. 163 p.

[24] Saarsalmi A, Mälkönen E, Kukkola M. Effect of wood ash fertilization on soil chemical properties and stand nutrient status and growth of some coniferous stands in Finland. *Scandinavian Journal of Forest Research* 2004;19:217-33.

[25] Karltun E, Saarsalmi A, Ingerslev M, Mandre M, Anderson S, Gaitnieks T, Ozolincius R, Varnagiryte-Kabasinskine I. Wood ash recycling – Possibilities and Risks. In: Röser D, Asikainen A, Raulund-Rasmussen K, Stupak I, editors. Sustainable use of forest biomass for energy: A synthesis with focus on the Baltic and Nordic Region. *Managing Forest Ecosystems Series*, Vol. 12. New York: Springer; 2008.

[26] Ulery AL, Graham RC, Amrhein C. Wood ash composition and soil pH following intense burning. *Soil Science* 1993;156:358-64.

[27] Goforth BR, Graham RC, Hubbert KR, Zanner CW, Minnich RA. Spatial distribution and properties of ash and thermally altered soils after high-severity forest fire, southern California. *International Journal of Wildland Fire* 2005;14:343-54.

[28] Smith AMS, Hudak AT. Estimating combustion of large downed woody debris from residual white ash. *International Journal of Wildland Fire* 2005;14:245-48.

[29] Úbeda X, Pereira P, Outeiro L, Martin DA. Effects of fire temperature on the physical and chemical characteristics of the ash from two plots of cork oak (Quercus suber). *Land Degradation and Development* 2009;20:589-608.

[30] Cerdà A. Postfire dynamics of erosional processes under mediterranean climatic conditions. *Zeitschrift für Geomorphologie* 1998;42(3):373-98.

[31] Kinner DA, Moody JA. *Infiltration and runoff measurements on steep burned hillslope using a rainfall simulator with variable rain intensities*. Washington: U.S. Geological Survey; 2007, 122 p.

[32] Larsen IJ, MacDonald LH, Brown E, Rough M, Welsh MJ, Pietraszek JH, Libohova Z, Benavides-Sorio JD, Shaffrath K. Causes of post-fire runoff and erosion: water repellency, cover, or soil sealing. *Soil Science Society American Journal* 2009;73:1393-1407.

[33] Woods SW, Balfour VN. The effect of ash on runoff and erosion after a severe forest wildfire, Montana, USA. *International Journal of Wildland Fire* 2008;17:535-48.

[34] Mallik AU, Gimingham CH, Rahman AA, Ecological effects of heather burning. I. Water infiltration, moisture retention and porosity of surface soil. *Journal of Ecology* 1984;72:767-76.

[35] Gabet EJ, Sternberg P. The effects of vegetative ash on infiltration capacity, sediment transport, and the generation of progressively bulked debris flows. *Geomorphology* 2008;101:666-73.

[36] Bodí MB, Mataix-Solera J, Doerr SH, Cerdà A. *Effects of ash type and degree of combustion on soil water repellency*. Marmaris: IMFESP; 2009. 44 p.

[37] Farouki OT. Thermal properties of soils. Clausthal-Zellerfeld: Trans. Tech. Publications; 111986 88 p.

[38] Campbell GS, Norman JM. An Introduction to Environmental Biophysics. 2nd ed. New York: Springer; 1998. 286 p.

[39] DeVries DA. Thermal properties of soils In: van Wijk WR, editor. *Physics of Plant Environment*. New York: Wiley; 1963, p. 210235.

[40] Blake GR, Hartge KH. Bulk density. In: Klute AK, editor. *Methods of soil analysis. Part I: Physical and mineralogical methods*. Madison: American Society of Agronomy; 1986. p. 363-75.

[41] Skinner SIM, Halstead RL, Brydon JE. Quantitative manometric determination of calcite and dolomite in soils and limestones. *Canadian Journal of Soil Science* 1959;39:197-204.

[42] Department of Agriculture of Spanish Government. *Methods of Soils Analysis*. Madrid: M.A.P.A; 1986. 532. P.

[43] Walkley A, Black IA. An examination of the Degtjareff method for determining soil organic matter and a proposed modification of the chromic acid titration method. *Soil Science* 1934;3729-38.

[44] Rubio CM, Josa R, Ferrer F. Influence of the hysteretic behaviour on silt loam soil thermal properties. *Open Journal of Soil Science* 2011;3:77-85.

[45] Rubio CM, Úbeda X, Ferrer F. Response of the thermal conductivity as a function of water content of a burnt Mediterranean Loam Soil. *Open Journal of Soil Science* 2012;2:1-6.

[46] Rubio CM. An Approach to make more technical thermal properties measure in porous media. *Applied Ecology and Environmental Sciences* 2014;2(2):60-65.

[47] Pereira P, Úbeda X, Martin DA. Fire severity effects on ash chemical composition and water-extracted elements. *Geoderma* 2012;19:1105-14.

[48] Pereira P, Cerdà A, Úbeda X, Mataix-Solera J, Arcenegui V, Zavala L. Modelling the impacts of ash thickness in a short-term period. *Land Degradation Development* 2013. DOI:10.1002/ldr.2195

[49] IBM Corp. *IBM SPSS Statistics for Windows*. Armonk: IBM; 2013. 96 p.

[50] Soil Survey Staff. *Keys to Soil Taxonomy*. 8th ed. Washington: US Government Printing Office; 1998. 541p.

[51] Nobre RCM, Thomson NR. The effects of transient temperature gradients on soil moisture dynamics. *Journal of Hydrology* 1993;152:57-101.

[52] Rahman MM, Mamun AA, Azim MA, Alim MA. Effects of temperature dependent thermal conductivity on magnetohydrodynamic (MHD) free convection flow along a vertical flat plate with heat conduction. *Nonlinear Analysis Modelling and Control* 2008;13(4):513-524.

[53] Massman WJ, Frank JM, Reisch NB. Long-term impacts of prescribed burns on soil thermal conductivity and soil heating at a Colorado Rocky mountain site: a data/model fusion study. *International Journal of Wildland Fire* 2008;17:131-46.

[54] Pereira P, Cerdà A, Úbeda X, Mataix-Solera J, Jordán A, Burguet M. Spatial models for monitoring the spatio-temporal evolution of ashes after fire – a case study of a burnt grassland in Lithuania. *Solid Earth* 2013;4:153-65.

[55] Certini G. Effect of fire on properties of soil - A review. *Oecologia* 2005;143:1-10.

[56] Badía D, Martí C. Plant ash and heat intensity effects on chemical and physical properties of two contrasting soils. *Arid Land Research and Management* 2003;17(1): 23-41.

[57] Durgin PB. *Organic matter content of soil after logging of fir and redwood forest*. Berkeley: United States Department of Agriculture; 1980. 163 p.

[58] Durgin PB, Vogelsang PJ. Dispersion of kaolinite by water extracts of Duglas-fir ash. *Canadian Journal of Soil Sciences* 1984;64:439-43.

[59] Botelho H. Vegetation coontrol and management In: Eftichidis G, Balbamis P, Ghazi A, editors. *Wildfire Management*. Brussels: European Commission; 1999. p. 93-102.

[60] Pereira P,Úbeda X, Martin D, Mataix-Solera J, Cerdà A, Burguet M. Wildfire effects on extractable elements in ash from a Pinus pinaster forest in Portugal. *Hydrological Processes* 2014;28:3681-90.

[61] Abu-Hamdeh NH, Reeder RC. Soil thermal conductivity: Effects of density, moisture, salt concentration and organic matter. *Soil Science Society of America Journal* 2000;64:1285-90.

[62] Noborio K, McInnes KJ. Thermal conductivity of salt affected soils. *Soil Science Society of America Journal* 1993;57:329-34.

[63] Iverson LR, Hutchinson TF. Soil temperature and moisture fluctuations during and after prescribed fire in mixed-oak forest, USA. *Natural Areas Journal* 2002;22:296-304.

European Journal of Environmental and Safety Sciences 2014 2(2): 37-47
ISSN 1339-472X European Science and Research Institute (Original Research Paper)

Results of forest opening-up analysis for ground mobile fire-fighting equipment deployment in LS Maluzina territory – Case study

Jaroslav Kapusniak[a] · Andrea Majlingová[b]

[a]*VSB – Technical University of Ostrava, Faculty of Safety Engineering, Lumirova 13, 700 30 Ostrava, Czech Republic*
[b]*Fire Research Institute, Ministry of Interior of the Slovak Republic, Rožňavská 11, 83104 Bratislava, Slovakia*

ABSTRACT

The timely and effective intervention of fire brigades to fight the forest fire depends not only on the time of fire sighting and announcing and the time of fire brigades attendance to the intervention place, but also on knowledge on the terrain, existence of forest roads to deploy the ground mobile fire-fighting equipment or even aerial fire-fighting equipment. To have the information on terrain, road network parameters is required to perform a field survey and to process the data of the field survey in the geographic information systems (GIS) environment, where they can be applied in area opening-up analysis. Here we present an approach to opening-up analysis processing in ArcGIS environment. It was performed for the territory of Maluzina Forest Management Unit to deploy the shuttle water relay fire-fighting equipment and for direct fire extinguishing using special forest fire-fighting equipment. The results showed that the territory is opened-up to 23.7 % (2,617.1 ha) for the shuttle water relay fire-fighting equipment and fire extinguishing purposes deploying the ground mobile fire-fighting equipment using only reinforced roads. When deploying the forest special fire-fighting equipment which uses also unpaved roads except the reinforced ones, the opened-up area increased by the 39.3 % to 2,617.1 ha during the dry season and by 14.7 % (5,329.3 ha) during the wet one. Except the ground mobile fire-fighting equipment we also analysed the opening-up level of the territory in case of the "lake system" deployment for forest fire extinguishing. In that case, the index of territory opening-up increased to 85.3 % (8738.2 ha).

Keywords: Fire-fighting equipment • Forest fire • GIS • Opening-up analysis

1. Introduction

In Forest fires belong among the most harmful factors in forestry, representing the highest risk for fulfilling the objectives of forest management planning.

Effective forest fire prevention is a pre-requisite for good forest management in fire prone areas. To have sufficiently developed and quality road network that can be used for efficient fire-fighting is a sign of well-done fire prevention that can lead to reduction of fire vulnerability in that territory.

In period 2000 – 2013, there occurred 5392 forest fires in Slovakia and the damage reached the value of 23,879,900 EUR [1]. That is a reason to incorporate the effective fire protection system into a system of multi-resource forest management. The most effective fire protection is effective prevention, however if a fire occurs is necessary to start with its localization and suppression as soon as possible.

The functional and efficient network of forest roads is a basic pre-requisite as for sustainable multi-resource forest management as well as for fire protection.

In particular the planning of forest roads is commonly oriented to assigning the fundamental management activities in the forest and to reduce the costs and environmental impacts of timber logging. Nowadays, the analyses of forest opening-up are performed mainly as a part of timber logging process optimization. For this purpose the computer aided or GIS approaches are used. These problems have concerned more authors for many years.

The origins of problem addressing are associated with the effort of experts on devolution description processes, documentation of terrain features and mechanization used in to the computing environment. Technological tools - database systems, GIS and data structures have been used in different way and extent for this purpose. Recently, it

Jaroslav Kapusniak (corresponding author)
VSB – Technical University of Ostrava, Faculty of Safety Engineering
Lumirova 13, 700 30 Ostrava, Czech Republic, e-mail: jaroslav.kapusniak@vsb.cz

resulted in efforts to create specific resources to support the (spatial) decision making process. This trend requires not only manage those resources and tools as well, but also adopt new approaches to structuring the data or formal description of knowledge and decision rules.

In general, from historical point of view, there can be recognized solutions realized for “model” (not specific, real) conditions, so conditions that are generally applicable for typical, selected of often occurring, representative conditions. Those are based on deductive or so called theoretical models. The procedures are trying to establish a model of general application that is dependent on the observed actual conditions of any area. The models are characterized by simplification of actual conditions and are only applicable for simplified assumptions such a flat terrain, regular shape of harvesting units area, linear course of cost function, two-sided timber skidding to road, resp. two-sided fire suppression from road in this case, etc. Systemization of those models, typically even without computer support of solution is introduced in work [2]. An example of the newer procedures using abstract models in computer environment are works [3-5].

The next, newer and more suitable group of more practical solutions is represented by solutions which are based on actual conditions in which the activity is carried out or intends to be carried out. Development of this approach is evident from the works of Sever and Knezevic [6]. Development of hardware and software resources, improvement of database management systems (DBMS), the onset of commercial geographic information systems (GIS) and the introduction of digital terrain models (DTM), has a top preference for these methods.

Hereinafter introduced distribution of methods and practices primarily reflects the development of software tools and the ability to structure and store data of the third or vertical dimension of space (the establishment of digital terrain models - DTM). At the beginning of development, there prevailed access through "file processing", which required building a custom user interface, data structures, data modeling and analytical modules. One of the first attempts to use a raster DTM as a source of information for analysis and planning have been described in the following works [7-10].

Comprehensive and effective approach to issues of forest roads locating, planning the deployment of various technologies and the development of strategic projects for the extraction and transport of timber required building a "specific complex environment", which oversaw large percentage of program modules analyzing sub-problems. A typical approach presents a system PLANS - Preliminary Logging Analysis System [11], established to support the creation of strategic plans for timber logging; TERDAS - Terra-data base system [12-13] and PLANEX [14], integrating DTM in the process of planning the project of forest road network.

The application of GIS for forest road network planning purposes is the logical culmination of the previous development. GIS as a technology enables efficient sourcing, storing, editing, analyzing, and displaying all forms of geographic information. Standard GIS modules, however, fail to address the specific problems associated with opening-up of forest and planning of timber logging process. On the other hand, environment and structure of GIS allows the integration of new modules developed in common programming languages and used to solve specific problems. Quantity of authors points to the possibility of linking GIS with custom modules, e.g. [11, 15-20].

Development and improvement of their custom programming languages within GIS (Arc Macro Language - AML), support for statistical and analytical methods of modeling and interactive visualization of the results leads to the formation of the present full spatial decision support system (SDSS) described in the works [21-23], or to the creation of expert systems [24-25]. Those systems find a solution of the problem within a certain set of arguments or the clusters of knowledge that have been formulated by experts for the specified area.

If we take into account the models and techniques in terms of methods and decision-making procedures, the first large group of applications is addressed by methods of mathematical programming. This group of methods includes methods for linear programming and mixed integer programming, which were used in the works [26-27], nonlinear programming methods in [28] and dynamic programming methods in [29]. These methods always lead to the optimal solution, but at the expense of time to process the outcome, respectively they consider only the small number of alternative solutions.

The second group of models is addressed by combination of methods of mathematical programming and network programming. Timber logging model developed for the USDA Forest Service [30] is an example of combining of mixed linear programming method with network programming.

The third large group of models is based on a combination of network programming methods and a variety of heuristic rules. Heuristics used in these models divides [31] into two broad groups:

a) Calculation (network) heuristics and

b) Combinative heuristics, the use of which has branches in different directions:

- Monte Carlo stochastic search techniques such as annealing simulated, threshold acceptance, and the great deluge;

- Non-stochastic search techniques such as tabu search, and
- Evolutionary algorithms including genetic algorithms.

These approaches are used in the works [7, 9-10, 24, 32-36] and using them can be optimized addressing the roads location issues.

Systems based on cartographic modeling fully utilize GIS, GNSS (Global Navigation Satellite Systems, previous GPS) and remote sensing technology. The role of cartographic modeling techniques is primarily analysis and synthesis of spatially linked information, and not just creating maps. In [37] are described two basic approaches to the modeling: the descriptive modeling, which was at the beginning, and which tried to show the geographic shape of "what exists" or "what could be" in space. On the other hand, prescriptive modeling shows the geographic shape of "what should be" in space. Cartographic modeling techniques used to express the problem, derive the results and evaluate the results achieved by cartographic allocation can be divided to the following techniques [37]:

- Atomistic allocation (expressed in relation to individual parts or "atom" of geographic area);
- Holistic allocation (always expressed in relation to "total, groups" of geographic area).

Any of above mentioned approach is also appropriate to be used for fire suppression activities planning and area opening-up analysis to identify the localities where the ground mobile fire-fighting equipment can be used and where aerial attacks must be applied.

In steep mountainous terrain, where it is required to use the ground mobile fire-fighting equipment, the operational capabilities of this equipment (mainly its working range) as well as the access to the fire place, represent the limiting factors [38].

In Slovakia, there are commonly used several types of ground mobile fire-fighting equipment: pumping fire-fighting equipment CAS on TATRA 148 and TATRA 815 chassis and Iveco Trakker, forest specials UNIMOG on Renault and Mercedes chassis and PV3S ARS [39-40].

The pumping fire-fighting equipment is suitable to be used for the fire extinguishing from public roads 1st and 2nd class of quality and from reinforced forest roads (in Slovakia 1L, 2L class forest roads in accordance to STN 73 6108). The UNIMOG and PV3S ARS, due to its technical parameters are suitable to be used for the fire extinguishing from hauling or skidding roads (unpaved roads with the longitudinal slope up to 10-12 %), too.

In the paper we introduce an approach to the assessment of opening up of Maluzina Forest Management Unit for the purposes of forest fire suppression with the deployment of ground mobile fire-fighting equipment: pumping appliance CAS 32 on Tatra 148 and Tatra 815 chassis, Iveco Trakker and forest specials UNIMOG on Mercedes and Renault chassis and Praga V3S ARS. The choice of fire-fighting equipment was oriented to the available fire-fighting equipment that can be deployed in this territory. This approach was first applied for the area of Hrabusice forest management unit, and published in [41]. Here we present the methodology rebuilt to be used in ArcGIS environment. We enriched the analysis with the assessment of opening-up level of the territory, deploying the "lake system" to be used as a way of fire-fighting (fire tactics).

2. Material and methods

2.1. Experimental area

The experimental area is represented by the area belonging under the management of the Maluzina Forest Management Unit (acronym LS Maluzina).

The territory is mountainous and of rugged nature. It is located between altitudes of 667 – 1,727 m above sea level. Forests cover the area of 93%. The total area of the forests in the LS Maluzina is 10,241.33 ha. In the tree species composition of forests dominates mainly spruce, beech and less abundantly is represented fir, larch, pine, dwarf pine, maple and rowan.

2.2. Ground mobile fire-fighting equipment used

The opening-up analysis was performed as for shuttle water relay fire-fighting equipment (pumping appliance CAS 30 Tatra 148 and CAS 32 Tatra 815, CAS 30 Iveco Trakker) as for forest special fire-fighting equipment (UNIMOG on Mercedes and Renault chassis and Praga V3S ARS), and was completed with analysis related to the deployment of "lake system" of water transport to extinguish the forest fire in mountainous conditions, which is composed of hose piping, interconnected with "lakes" (buckets with flowing pump).

2.3. Methodology of road network survey

The road network survey in the territory of Maluzina Forest Management Unit was performed during August – September 2013. As the background for the field survey the aerial photos of the territory and the data of the vector layer of road sections and forest and field roads taken from the Central Spatial Database of the Slovak Republic were used.

During the field survey, there were recorded the data on forest roads parameters (width of the road, road elevation, etc.), their surface and condition.

2.4. Methodology of road network survey

The analysis of forest opening up was performed in ArcGIS environment using the functions of context operators, map algebra and distance analyses. Owing to the variability of conditions by water relay and the direction of extinguishing (up or down slope), there were taken into the consideration the both directions of fire extinguishing in calculation. Based on calculated maximum range values of the delivery fire hose piping was calculated the roads spacing using the formula published in [42]. The calculated maximum range of delivery fire hose piping determines also the zone where ground mobile fire-fighting equipment can be applied for fire extinguishing.

As the input layers to the opening-up analysis there were used digital terrain model with the spatial resolution of 10 m, vector layer of forest unit borders and vector layer of road network representing the actual situation in spatial distribution of forest roads in the experimental area, obtained by road network mapping during the field survey.

The analysis of forest opening-up and extraction resulting values for individual forest stands is also shown in the development diagram (Fig. 1).

The first step was the data pre-processing. The digital terrain model was used as a source for the slope raster deriving – *ArcToolbox/Spatial Analyst Tools/Reclass/Reclassify*. It was calculated in percentage. For the purposes of next analysis it was consecutively converted to the radians, using *ArcToolbox/Spatial Analyst Tools/Map Algebra/Raster Calculator*, because slope calculated in degrees or percentage is linear with a constant change in steepness. It is necessary to create a new raster, where first the slope is converted from degree units to radian units (slope * π / 180) and then the sine is calculated, on a cell-by-cell basis:

$$Sin\ ("Slope\ raster" * \pi / 180) \quad (1)$$

The values range from -1 to 1, which we should expect as values of sine.

Also the vector representation of forest roads, distributed in the experimental area, was converted to the raster representation (module *Reclassify*) – binary raster (1- roads suitable to be used by the ground mobile fire-fighting equipment, 0 - the other roads).

The next step was to calculate the raster of sloping distances using map algebra tools (*ArcToolbox/Spatial Analyst Tools/Map Algebra/Raster Calculator*). The input raster for this calculation was the raster of slope converted to the radians.

The calculation was performed based on the formula:

$$d\_slope = 10 / \cos\alpha \quad (2)$$

where:
d_slope is sloping distance (m),
10 is resolution of the raster cell (m),
A is angle which contain the hypotenuse with an adjacent legs (or raster of slope in GIS) (°).

The output raster was used as a friction surface raster for the calculation of cost distances, using distance operators – *ArcToolbox/Spatial Analyst Tools/Distance/Cost Distance*. In the calculation it had been considered 2 types of analyses. First was performed for the pumping appliance CAS 32 on chassis of Tatra 148 and Tatra 815 and Iveco Trakker, which use to be deployed to ensure the shuttle water delay and use the reinforced forest roads for movement, and the second for the forest special fire-fighting equipment (UNIMOG and Praga V3S ARS) which uses also skidding roads (unpaved roads) except the reinforced ones.

The next step was to calculate the horizontal lengths of the fire hose piping and road spacing. Providing that the road spacing is considered as the cost distance of its orthographic projections into the horizontal level, it was necessary to recalculate the appropriate diagonal lengths of the fire hose line onto horizontal ones according to the following equation. For that purpose the Map algebra tools (module *Raster Calculator*) were applied.

$$d\_horiz = d\_cost * \cos(arctg(s / 100)) \quad (3)$$

where:
d_horiz is horizontal distance (m),
d_cost is cost distance raster (m),
s is slope (°).

The output raster was consecutively reduced (applying module *Reclassify*) to the zone of extinguishing using the ground mobile fire-fighting equipment – the area opened up for ground fire extinguishing. The maximum range of extinguishing zone was determined to 160 m due to the maximum length of delivery fire hose piping. The maximum range of extinguishing zone determined as the "lake system" range was specified to 320 m, based on the previous experience with fire extinguishing in this territory.

Next, there were extracted the fire hose piping range values (sloping length of fire hose piping) to the particular

forest units, using module *Zonal Statistics as Table* which belongs to the zonal functions of Spatial Analyst Tools.

At the end the area opening-up index (%) was calculated as a ratio between accessible area ha / non accessible area extent (ha) to the whole experimental area.

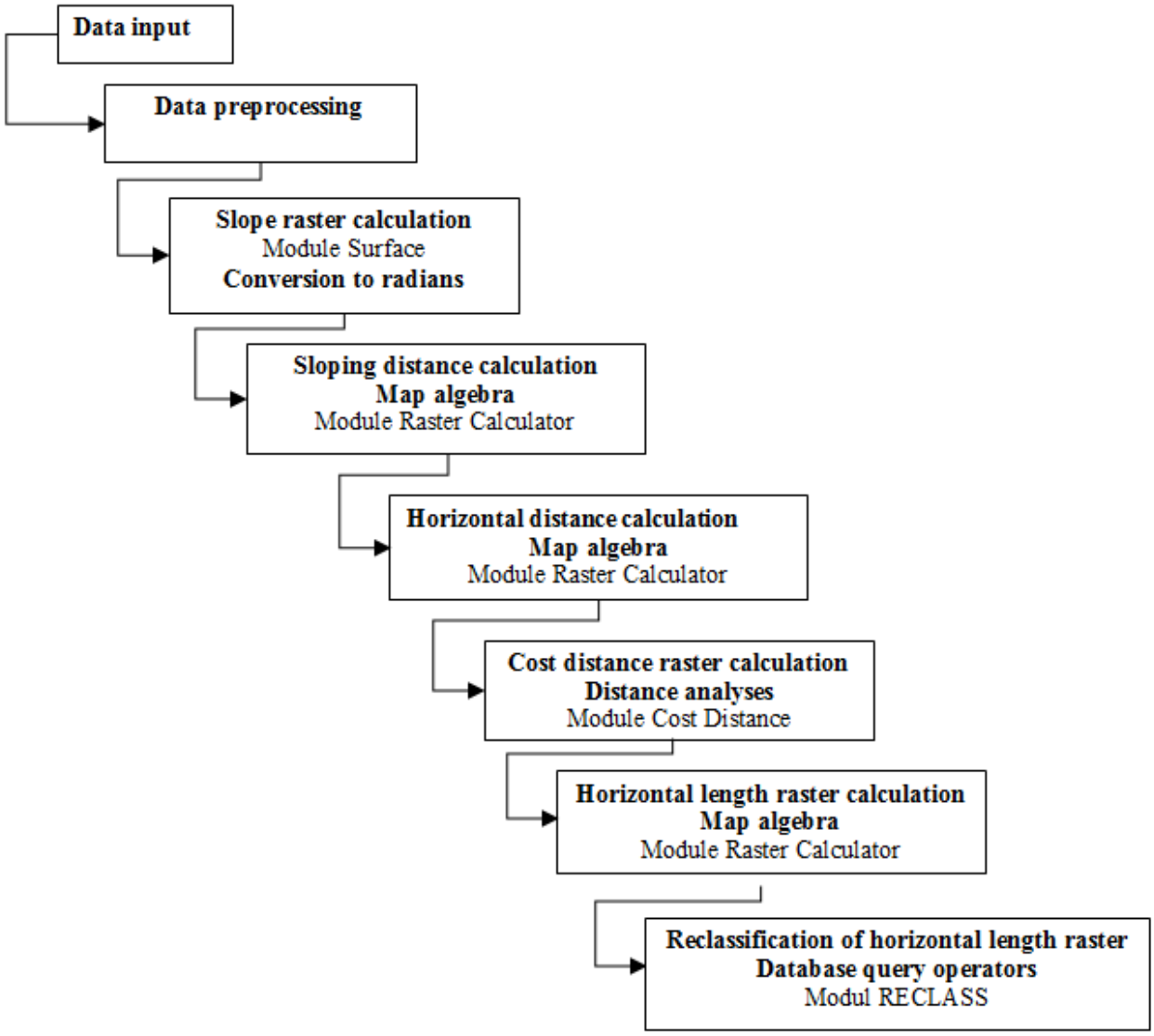

Figure 1 Development diagram of the forest opening up analysis in ArcGIS environment

3. Results and discussion

3.1. Results of road network survey

For the purposes of the road network field survey, there were used the aerial photos of the territory and vector layers of road sections and forest and field roads. The field survey was performed only on the forest road network belonging under the management of the LS Maluzina.

In Fig. 2 we introduce the view of the road in the territory, classified by the road type (state road, forest road).

In Fig. 3 we introduce the view of the road network in the territory, classified by the surface type (type of material which is made from).

Fig. 4 introduces the view of the road network in the territory in view of the particular road sections passability or impassability.

The total length of roads within the territory is 210,593.5 m. Of those, 29,555.5 m of state roads (14 %), 101,191.5 m of reinforced (paved) forest roads (49 %) and 79,846.5 m of unpaved forest roads (37 %).

In terms of paved roads, in the territory, there are 40,027.9 m of forest roads of 1L category (40 %),

40,981.1 m of forest roads of 2L category (40.5 %), 7,218.2 m of forest roads of 3L category (6.5%) and 12,964.3 m of unpaved non-forest roads (13 %).

The unpaved roads are formed by forest slope and skidding roads and earth roads that can be used to fight forest fires with forest special fire-fighting equipment. In the territory, there are totally 70,464.7 m of slope and skidding roads (88 %) and 9,381.8 m of earth roads (12 %).

Forest roads of 1L category are hauling roads that are reinforced (paved) and thus allow year-round operation of vehicles. The minimum lane width is 3 m and free width of road crest is at least of 4 m. The maximum longitudinal gradient of vertical alignment of the road is 10 %, in the mountainous areas in some sections up to 12 % [43].

Forest roads of category 2L are reinforced hauling roads which due to their technical equipment allow at least seasonal operation of vehicles. Like the roads of category 1L, they have the minimum width of the lane of 3 m and free width of road crest is at least of 4 m. The maximum longitudinal gradient of road vertical alignment depends on the terrain morphology, bedrock type, road surface capacity and type of hardening the surface, but the value does not exceed 12 % [43].

Figure 2 Road network in the territory classified by the road type

Figure 3 Road network in the territory classified by the road surface type

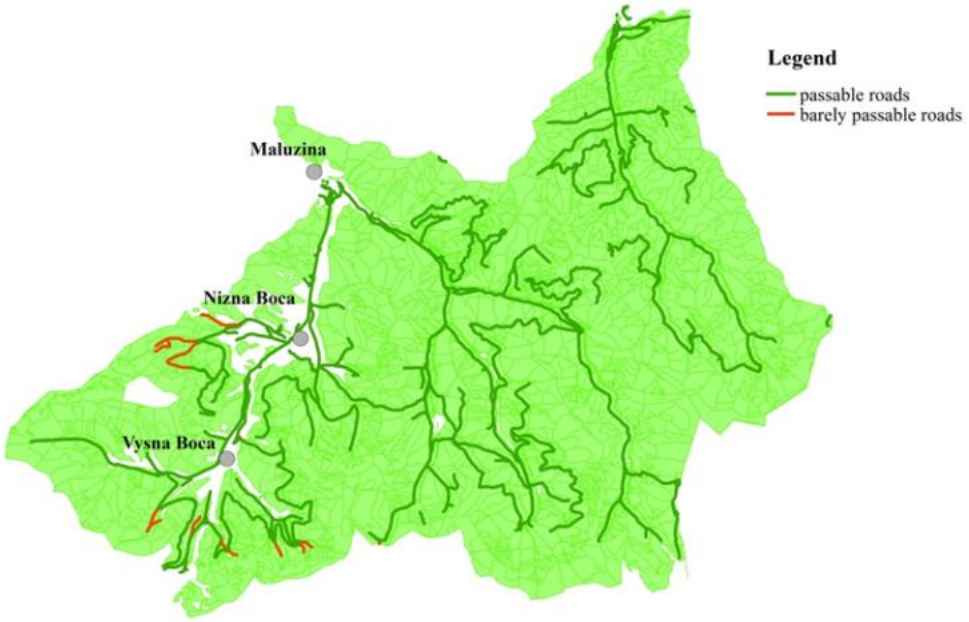

Figure 4 Road network in the territory classified by its passability and impassability

In terms of the surface of the road network (Fig. 3), which exists in the territory, there are 46,951.1 km of roads that surface is made from asphalt, from concrete is made 9.8 km of roads. 83,786.1 km of roads have surface that is made from gravel or rubble. Earth surface have 79,846.5 km of roads.

In terms of passability (Fig. 4), in the territory, there is passable 203,434.6 km of roads and barely passable are 7,158.9 km of roads.

Forest roads of category 3L are the skidding roads passable for tractors, special equipment, such as forest special UNIMOG, and only passable under favourable (dry) conditions. The minimum free width of the road is 4 m. A limiting factor of their use is a longitudinal gradient and soil capacity [43].

Slope roads and earth roads are unpaved, temporarily passable roads. The overall width of the road is at least of 1.5 m. They are passable only under favourable conditions [43].

3.2. Results of territory opening-up analysis to deploy the ground mobile fire-fighting equipment

The results of territory opening-up analysis for the deployment of ground mobile fire-fighting equipment are shown in Fig. 5, 6 and 7.

In consideration of possibilities of the deployment of ground mobile fire-fighting equipment needed for extinguishing the forest fire from the reinforced (paved) roads, as well as to ensure shuttle water relay, we have taken into account as terrain parameters, condition and parameters of the road network, as well as the basic parameters of fire-fighting equipment. In the analysis we considered the following fire-fighting equipment: pumping appliance CAS 30 Tatra 148, CAS 32 Tatra 815 and CAS 30 Iveco Trakker.

Results of the analysis showed (Fig. 5) that the territory is in terms of the possibility of forest fire extinguishing using the aforementioned types of fire-fighting equipment, that allows them to deploy to fight the forest fire only on the reinforced state roads of all classes and forest roads of category 1L and 2L, as well as to ensure the shuttle water relay, is opened-up only to 23.7 % (2,617.1 ha).

In terms of deployment of forest special fire-fighting equipment and identification of area that can be extinguished using this type of fire-fighting equipment (UNIMOG forest specials on Mercedes Benz or Renault chassis, Praga V3S ARS), we considered the two analyses. The first analysis had focused on the conditions, when the surface of unpaved forest roads is dry (or frozen) and therefore passable. The second analysis was carried out for wet, muddy ground of unpaved forest roads.

The results of the first analysis, where the surface of the road network is dry, in particular of the earth roads, are presented in Fig. 6.

In this case, there can be used all road types existing in the territory for fire extinguishing. The opening-up index reached the value of 63 % (6,554.0 ha).

In Figure 7 are presented, in graphical form, the results of territory opening-up analysis for the deployment of ground mobile fire-fighting equipment to extinguish the forest fires - forest special fire-fighting equipment in condi-

tions of saturated, muddy ground of earth roads. These roads are impassable also for forest special vehicles in these conditions, what is confirmed by the fact that the opening-up index of the territory decreased from the previous 63 % in variant with dry ground of earth roads to 48.3 % (5,329.3 ha).

Results of opening-up analysis dealing with deployment of "lake system" of fire extinguishing (Fig. 8) showed that the area is opened-up to 85.3 % (8,738.2 ha), when we consider the optimum variant, in which all roads are involved in the analysis. If only the reinforced roads are taken into consideration than the territory opening-up index decreases to 40.8 % (4,181.7 %).

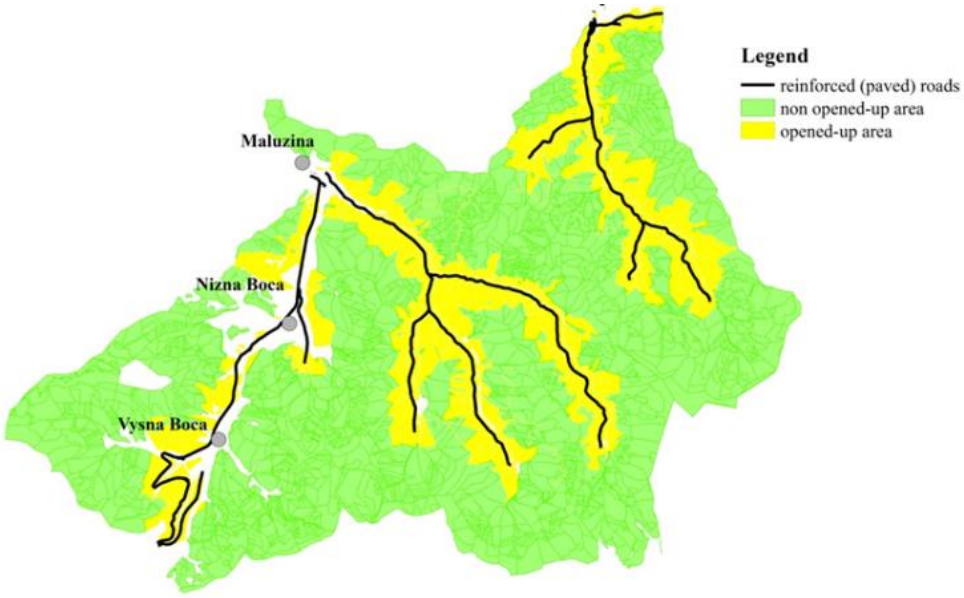

Figure 5 Results of opening-up analysis to deploy the ground mobile fire-fighting equipment to ensure the shuttle water relay during fire extinguishing

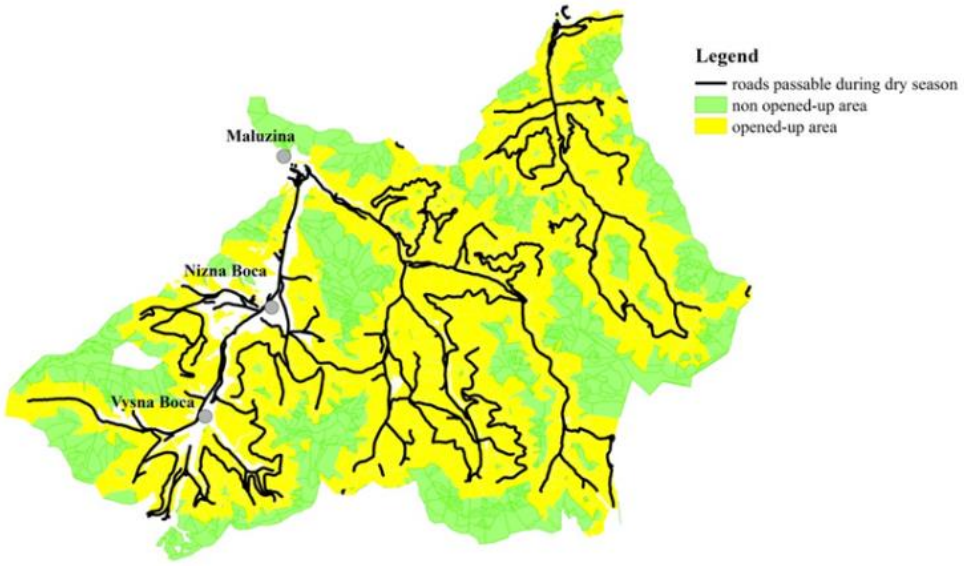

Figure 6 Results of opening-up analysis to deploy the ground mobile fire-fighting equipment – forest special fire-fighting equipment during dry season

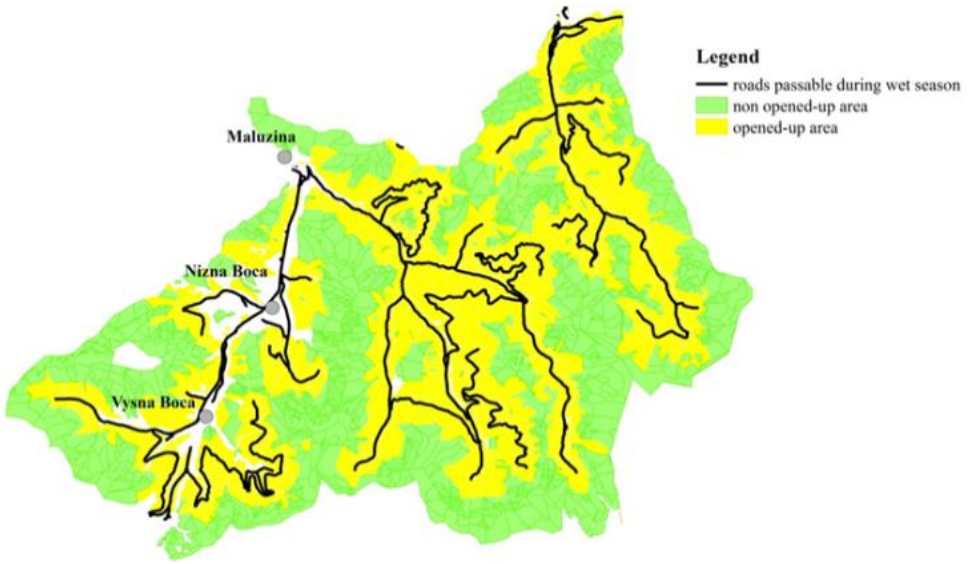

Figure 7 Results of opening-up analysis to deploy the ground mobile fire-fighting equipment – forest special fire-fighting equipment during wet season

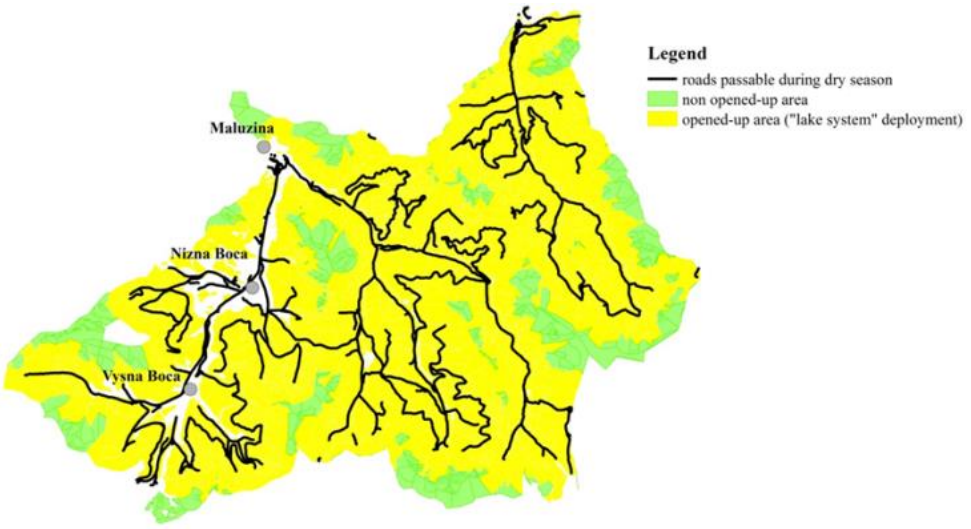

Figure 8 Results of opening-up analysis after deploying the "lake system" of fire extinguishing in the territory

4. Conclusion

The paper presents very current and interesting topic of territory opening-up analysis to deploy the ground mobile fire-fighting equipment to fight the forest fires. Except the introduction of a GIS based approach to analysis, it presents a review of works dealing with the issue of forest road planning, forest opening-up. In the world there is not enough literature sources dealing with the issue of opening-up of forest to deploy the fire-fighting equipment. But there are many sources dealing with planning of forest road network, timber logging technologies optimization from forestry point of view. According to the analogy of those issues – the vehicles and other equipment have often the same parameters, is possible to rationalize the opening-up process focusing the fire-fighting equipment based on the existing results of forestry research. Here we introduced an approach to opening-up analysis that was previously published by Majlingova [41]. That approach we have rebuilt from Idrisi to ArcGIS software environment and applied on LS Maluzina territory.

The results of the analysis showed that the area is opened-up only to 23.7 % if we take into consideration only the reinforced roads to deploy the ground mobile fire-fighting equipment to fight the forest fires. If we consider the entire road network in the territory and dry season the territory opening-up index increases by 39 % to 63 %. In reverse, taking into consideration the wet season the opening-up index decreases to 48.3 %. The best results were achieved when we involved the "lake system" of forest fire

extinguishing into the analysis. In case of involvement of the entire territory road network we reached the opening-up index of 85.3 %.

The results of opening-up analysis can be used as the decision support for planning new sections of road network in any territory, for planning the purchase of new fire-fighting equipment suitable to the natural conditions of territory where it should be located and used.

References

[1] Fire Research Institute of the Ministry of Interior of the Slovak Republic. *Statistical Yearbook 2013*. Bratislava: Fire Research Institute of the Ministry of Interior of the Slovak Republic; 2013. 68 p.

[2] Roško P. *Theoretical principles of timber skidding and opening-up of forests in mountainous terrain*. Bratislava: Veda Publishing House; 1984. 285 p.

[3] Peters PA. Spacing of roads and landings to minimize timber harvest cost. *Journal of Forest Science* 1978;24(2):209-217.

[4] Thompson ID. Habitat needs of furbearers in relation to logging in boreal Ontario. *Forestry Chronicle* 1988;64:251-261.

[5] Imatomi Y, Jinkawa M. *Study on tractor skidding road spacing and density from ergonomic and economic points of view*. Corvallis: Oregon State University; 1994. 74 p.

[6] Sever S, Knezevic I. Computer-aided determination of optimal forest road density in mountainous areas. Feldafing: IUFRO; 1992. 25 p.

[7] Sakai T. Studies on planning method of a forest road in mountainous region, using a simulation model. *Bulletin of the Kyoto University Forests.* 1981;53:162-171.

[8] Sakai T, Suzuki Y. A circular road-network planning by traffic benefit. *Journal of the Japanese Forestry Society* 1993;104:853-854.

[9] Kobayashi H. Planning system for road route locations in mountainous forests. *Journal of the Japanese Forestry Society* 1984;66(8):313-319.

[10] Minamikata Y. *Effective forest road planning for forest operations and the environment*. Fredericton: IUFRO; 1984. 224 p.

[11] McGaughey RJ. *An Overview of PLANS: Preliminary Logging Analysis System*. Feldafing: IUFRO; 1992. 111 p.

[12] Shiba, M. *Optimization of road layout in opening of forest*. Feldafing: IUFRO; 1992. 175 p.

[13] Shiba M. Imagery data processing system using aerial photography for sensitive site investigations in the route selection process. *Journal of Forest Engineering* 1996;7(3):53-65.

[14] Epstein R, Weitraub A, Sapunatr P, Sessions J, Sessions JB. Planex – software for operational planning. In: Sessions J, editor. *International Seminar on Forest Operation under Montainous Conditions*; 1994 July 24-27; Harbin, China. Eugene: Oregon State University; 1994. p. 52-57

[15] Becker G, Jaeger D. *Integrated design, planning and evaluation of forest roads and logging activities using GIS-based interactive CAD-systems*. Thessaloniki: Aristotele University; 1991. 246 p.

[16] Tucek J, Pacola E. Algorithms for skidding distance modelling on a raster digital terrain model. *Journal of Forest Engineering* 1999;10(1):67-79.

[17] Kusan V. Remote sensing and GIS in Croatian forestry. In: Saramaki, editor. *Research Notes 48 from IUFRO XX World Congress*. Joensuu: University of Joensuu; 1995. p. 67-79.

[18] Nieuwenhuis MA. A forest road network location procedure as an integral part of a map-based information system. In: Corcoran TJ, Reams GA, editors. *IUFRO XVII World Congress*. Ljubljana: University of Ljubljana; 1986. p. 111-122.

[19] Musa AKA, Mohamed AN. *Alignment and location forest road network by best-path modeling method*. Kuala Lumpur: Malaysian Center for Remote Sensing; 2002. 128 p.

[20] Tomonori M. *Planning a Forest Road in Consideration for Minimizing Impacts on Streams*. In: *International Seminar on New Roles of Plantation Forestry Requiring Appropriate Trending and Harvesting Operations*; 1999 Sep. 29 – Oct. 5, Tokyo, Japan. Tokyo: University of Tokyo; 1999. p. 294-300.

[21] Heinimann HR. Umweltverträglichkeit forstlicher Erschliessungen. Konzept für die Abwicklung, die Analyse und die Bewertung. *Schweizerische Zeitschrift für Forstwesen* 1994;145(2):139-157.

[22] Tuček J, Suchomel J, Pacola E. Possibilities for SDSS using in Forestry: Focus on Forest Roads and Technologies Planning. In: *International Seminar on New Roles of Plantation Forestry Requiring Appropriate Trending and Harvesting Operations*; 2002 Sep. 29 – Oct. 5, Tokyo, Japan. Tokyo: University of Tokyo; 2002. p. 113-128.

[23] Yoshioka T. Cost, energy and carbon dioxide (CO_2) balance of logging residues as alternative energy sources: System analysis based on the method of a life cycle inventory (LCI) analysis. *Journal of Forest Research* 2002;7(3):157-163.

[24] Yoshimura T. *Development of an expert system planning a forest road based on the risk assessment*. Kyoto: Kyoto University; 1997. p. 82.

[25] Bhattachara SC, Salam PA, Pham HL, Ravindranath NH. Sustainable biomass production for energy in selected

Asian countries. *Biomass and Bioenergy* 2003,25(5):471-482.

[26] Koger JK, Webster DB. Logging Optimization Selection Technique. New Orleans: USDA Forest Service; 1984. 65 p.

[27] Nelson J, Brodie JD. Comparison of a random search algorithm and mixed integer programming for solving area-based forest plans. *Canadian Journal of Forest Research* 1990;20:934-942.

[28] Guangda L, Murphy G. *Steep Terrain Forest Harvest Operations in Asia.* Toronto: IUFRO; 1990, p. 211.

[29] Sakai H. Planning of long-term forest-road networks based on rational logging and transportation systems. *Bulletin of the Tokyo University Forests* 1987;76:1-85.

[30] Sullivan S, Sandford L, Ponce J. Using geometric distance fits for 3D object modeling and recognition. *IEEE Transactions on Pattern Analysis and Machine Intelligence* 1994;16(12):1183-1196.

[31] Sessions J, Chung W, Heinimann HR. New algorithms for solving large transportation planning problems. In: Arzberger U, Grimoldi M, editors. *Workshop on New Trends in Wood Harvesting with Cable Systems for Sustainable Forest Management in the Mountains*; 2001 June 18-24, Ossiach, Austria. Ossiach: IUFRO; 2001. p. 1-5.

[32] Liu K, Sessions J. Preliminary planning of road systems using digital terrain models. *Journal of Forest Engineering* 1993;4:27-32.

[33] Dahlin B, Sallnas O. Designing a forest road network using the simulated annealing algorithm. In: *Computer supported planning of roads and harvesting workshop*. Feldafing: IUFRO; 1992. p. 36-41.

[34] Tan J. Planning a forest road network by a spatial data handling-network routing system. *Acta Forestalia Fennica* 1992;227:1-85.

[35] Chung W, Sessions J. Designing a forest road network using heuristic optimization techniques. In: *24th Meeting of the Council on Forest Engineering*; 2001 July 15-19, Snowshoe, USA. Snowshoe: IUFRO; 2001. p. 35-49.

[36] Sakurai T, Rayamajhi S, Pokharel RK, Otsuka K. Efficiency of Timber Production in Community and Private Forestry in Nepal. *Environment and Development Economics* 2004;9(4):539-561.

[37] Tomlin CD. *Geographic Information Systems and Cartographic Modelling*. New Jersey: Prentice Hall; 1990. 249 p.

[38] Chromek I. *Utilization of aerial technique in forest fire*. Zvolen: Technical University in Zvolen; 2006. 112 p.

[39] Landťák, M., Kapusniak, J. Transport of extinguishing media to the forest fires in relation to the ground transport means. Zilina: Technical University of Zilina; 2010. 178 p.

[40] Landťák M, Monoši M, Kapusniak J. Transport of extinguishing agents to extensive forest fires. Ostrava: VSB TU Ostrava; 2011. 133 p.

[41] Majlingova A. Opening-up of forests for fire extinguishing purposes. *Croatian journal of forest engineering* 2012;33(1):159-168.

[42] Böhmer M, Dvorščák P. Evaluation and optimization of fire control forest accessing for classic fire-fighting attack. In: Marková I, Mračková E, editors. *Fire Engineering. 2nd International Scientific Conference on Fire Engineering*; 2006 October 3-5; Lučenec, Slovakia. Zvolen: Technical University in Zvolen; 2006, p. 35-44.

[43] Slovak Office of Standards, Metrology and Testing. STN 73 6108:2000. *Forest Road Network.* Bratislava: Slovak Office of Standards, Metrology and Testing; 2000.

European Journal of Environmental and Safety Sciences 2014 2(2): 48-52
ISSN 1339-472X European Science and Research Institute (Original Research Paper)

Computational simulation of road tunnel fire protection by sprinklers

Manuel Serban[a] · Silviu Codescu[b] · Ionel-Alin Mocioi[a]

[a]*Police Academy "A.I. Cuza", Fire Officers Faculty, Bucharest, Romania*
[b]*Politehnica University of Bucharest, Romania*

ABSTRACT

This paper proposes a new method of protection of certain areas of the road tunnels, with sprinklers using water as an extinguishing agent. The simulation uses, as input, an architecture as close to that of a real road tunnel as well as information gathered from the literature. The results of the simulation can be implemented as proposal on the protection of users, as a viable alternative when other classes firefighting or spread flames blocking methods can't be used at full scale. The paper focuses on presenting the results of studying the effect of protection and water curtain that can be realized by the sprinkler network water droplets and on the information resulting from the simulation.

Keywords: Road tunnel fire • Sprinklers network • Fire simulation • Water droplets

1. Introduction

Road tunnels are special parts of road traffic infrastructure when it comes to fire safety. These special constructions need to be protected in case of fire. In a road tunnel the main concern is the protection of its users. This is why sprinkler water droplets will be used both to directly extinguish the fire and to create a safer evacuation path. Nowadays, in the world, constructions such as road tunnels are designed, built and used considering the fire safety engineering principles, standards and concepts.

In the specific literature are presented a lot of situations where water or water mist fire sprinklers are used to protect spaces similar to road tunnels, underground tunnels or other confined closed spaces [1-3].

Sprinkler is an active fire protection device discharging water in order to extinguish the fire. In road tunnels electricity is used to power up the auxiliary systems (lighting, video surveillance, traffic control) fact that would disagree with the use of the water sprinklers, taking into account that the water is conducting well the electricity. Anyway, according to the national regulations, in a fire or another emergency situation, the electricity should be automatically disconnected and the auxiliary systems above mentioned should have protection against water infiltration [4].

As stated above, the main concern of fire safety is evacuation of people. In order to protect people in case of evacuation, one need is to protect them from smoke and hot and toxic gases on the evacuation paths.

In order to avoid a fire occurring or to limit its negative consequences, measures including jet fan mounting and active firefighting technical equipment are priority to be taken and followed, in 500 m or long road tunnels, according to specific law.

Taking into account these considerations, the tunnel ventilation may take use of the following measures [5]: fast and safe users evacuation, concentration of different fire effluents as close to the tunnel exhaust as possible, proper use of the extinguishing agents, even if it is water, foam or other substance used in this purpose, maintaining a proper vehicle speed and traffic flow in each tunnel section and compliance of minimum safety distances between vehicles, ventilation system and active firefighting measures [6].

In the present paper, authors use fire simulations as a tool to study the effectiveness of such a protection method. More protection devices will be used in a virtual fire simulation of a fire in a road tunnel (random consider), to protect the evacuation path (both tunnel exists, in this case) from smoke and hot toxic gases, by forming a water droplets barrier.

However, as air currents are quite powerful in such open areas, data are collected from the literature of a real road tunnel fire scenario that served as a model and are implemented into the simulation. Basically, the interactions between smoke and water droplets in the protection curtain, formed by sprinklers, will be studied.

Manuel Serban (corresponding author)
Police Academy "A.I. Cuza", Fire Officers Faculty, Bucharest, Romania
e-mail: manuel.serban@gmail.com

Based on the above mentioned findings, this article aims to analyze some of the circumstances conditions and active measures which can be applied due to a fire taking place in a road tunnel, using Pyrosim (a software program based on FDS platform) in order to simulate a real fire event and estimate its probabilistic evolution in predetermined conditions, with appropriate protection measures.

2. FDS, fire simulation software

FDS (Fire Dynamics Simulator) a software developed by NIST (The National Institute of Standards and Technology – U.S.A.), is a computer program of fluid dynamic simulation, particularly of the heat flow released during a fire; it uses the high definition computer language "Fortran 90" and solves the governing equations of fire dynamics. "Smokeview" program, written in "C/OpenGL" is the pair program that produces images and animation of the results.

Mathematical model adopted by the software is adapted to the fire development in which the fluid dynamics, the heat transfer and combustion occur. FDS computes the temperature, density, pressure, velocity and chemical composition within each numerical grid cell at each discrete time step. In addition, FDS computes on the solid surfaces the temperature, heat flux, mass loss rate and various other quantities [5-7].

Typical output quantities for the gas phase include: gas temperature, gas velocity, gas species concentration (water vapours, CO_2, CO, N_2), smoke flying particles and visibility estimation, space pressure, heat release rate per volume unit, mixture fraction (or air/fuel ratio), gas density, water droplet mass per unit volume contained in the atmospheric moisture, the walls and sprayed particles.

For successfully using the computer modeling, is enough to understand the basic laws of mass, momentum and energy conservation for Newtonian fluids as they are presented below:

- Conservation of mass:

$$\frac{\partial \rho}{\partial t} + \nabla \cdot \rho \mathbf{u} = \dot{m}_b''' \qquad (1)$$

where: ρ is the density (kg m^{-3}); t is the time (s); u is the velocity (m s^{-1}) and m_b'' is the net heat flux from thermal conduction and radiation (W m^{-2}).

- Conservation of momentum (Newton's second law):

$$\frac{\partial}{\partial t}(\rho \mathbf{u}) + \nabla \cdot \rho \mathbf{u}\mathbf{u} + \nabla p = \rho \mathbf{g} + \mathbf{f}_b + \nabla \cdot \tau_{ij} \qquad (2)$$

where p is the pressure (Pa); g is the gravity vector acceleration (m s^{-2}); f_b is the external force in (N m^{-3}) and τ_{ij} is stress tensor in (N m^{-2}).

- Conservation of energy (first law of thermodynamics):

$$\frac{\partial}{\partial t}(\rho h) + \nabla \cdot \rho h \mathbf{u} = \frac{Dp}{Dt} + \dot{q}''' - \dot{q}_b''' - \nabla \cdot \dot{\mathbf{q}}'' + \varepsilon \qquad (3)$$

where h is the enthalpy (J kg^{-1}); q''' is the heat release rate per unit volume (W m^{-3}); q_b'' is the energy transferred to the evaporating droplets (W m^{-3}); q'' is the heat flux vector in (W m^{-2}) and ε is the dissipation rate (W m^{-3}).

The accuracy of this modeling confirmed a high precision of computer modeling and was admitted for its usefulness and its applicability.

3. Input data and results

The geometry of the virtual space is similar to a real road tunnel in Romania, as example. The geometrical data of the road tunnel are presented in the table 1 and different views of the layout in FDS/ Pyrosim are shown in the Fig. 1 and 2.

There were also inserted devices as follow: gas detector, 5 heat detectors, 1 thermocouple and 2 sprinklers with a flow rate of 1 liter minute^{-1} and a droplet mean diameter of 100 μm. All the devices were inserted at approximately equal distances from the burning zone [8].

Fire scenario: it is considered that the fire occurs at one stationary car caught inside the tunnel, at the half of the tunnel length (100 m from each exists) due to an electrical fault at its engine. The car is about 4 m long, 1.5 m high and 1.5 m width, being made of steel, with its predefined physicochemical properties chosen from the program values. There are 30 similar cars in the tunnel, with 1.5 m between them.

The fire burner used in the simulation has a heat release rate of 1.500 kW m^{-2}, with a plane area of 0.72 m^2 [9-10]. The amount of generated smoke is automatically calculated by the program and the user has also the possibility to view it as smoke dissipation along the upper half of the road tunnel, as shown in the Fig. 2.

The smoke dissipation shown in the Fig. 2 reveals that the smoke spread at more than 50 m each side of the burning car, going down to 2.5 m height, which become dangerous for the tunnel users, after 50 seconds from the simulation beginning.

According to the simulation data, the temperature fields develops the gradient on the vertical up to 370 ^{0}C at around 4.5 m height [11]. Also on the ceiling of the tunnel, highest than 5.5 m, the temperature reaches 300 ^{0}C, for an approximately length of 30 cm, around the fire core.

The sprinklers are placed at the ceiling level of the tunnel, measuring 7 m between them, on the O_x axis. The diameter of the spreading water droplets area is 4.5 m around the burning zone. According to this, the sprinklers start working after 4.6 seconds, when the trigger temperature of 65 ^{0}C is reached. After 50 seconds of simulation, the fire is completely extinguished, at which point the smoke fill almost entirely the upper half of the road tunnel.

Table 1 Input data in Pyrosim for road tunnel fire and the protection of the tunnel users

Category	Parameters	Value
Computational domain	Simulation volume	Road tunnel, designed in the program, by taking geometrical data from a random real road tunnel
	Dimension of the volume containing subway station	(200 x 9 x 6) m (in order on 0x, 0y and 0z axis)
Numerical data	Cells per mesh, uniform division	(240 x 60 x 48) cells
	Dimension of one cell	(0.5 x 0.5 x 0.5) m
	The total number of cells	98.688
	Boundary conditions for the simulation volume	The boundary of the domain was considered closed, except for the limit maximum x0y, which was considered open. The whole structure of the road tunnel was considered of concrete
Other data	The fire burner	Imported from the FDS library, HRR (heat release rate) of 1.500 kW m^{-2}, square shape fire source, dimensions (0.9 x 0.8) m
	Environment values	20 °C, relative humidity 40 %, atmospheric pressure 101.325 kPa, ground level at 1.500 m about sea level
	Simulation time	200 seconds
	Sprinklers	Imported from FDS, flow 1 l min^{-1}, k factor = 1, droplet median diameter 100 μm
	Fan - wind current generator	Both tunnel exists, measuring (9 x 6) m

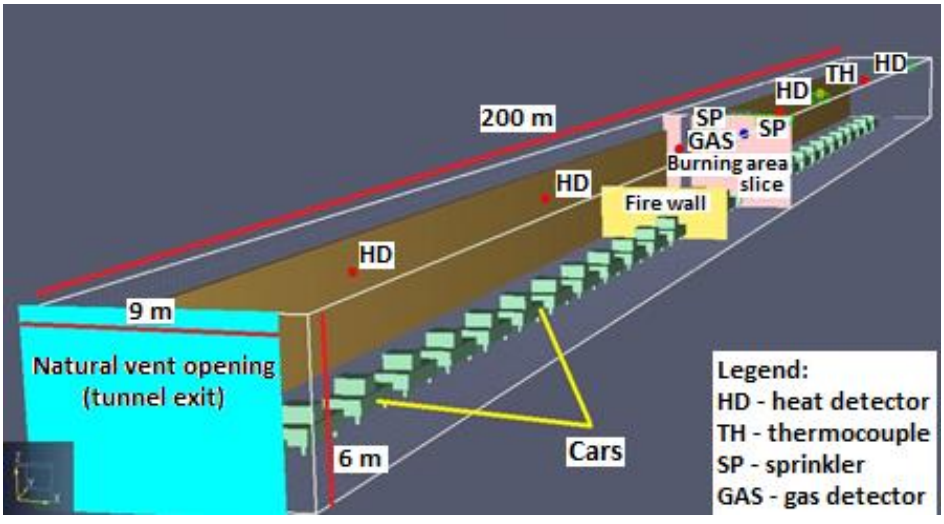

Figure 1 General architecture of the road tunnel, with cars and protection devices, imported in FDS

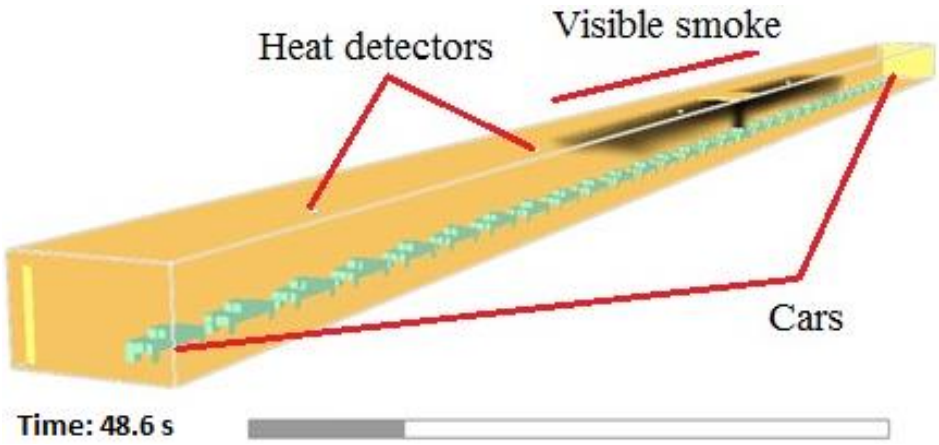

Figure 2 Visible smoke, filling the upper half of the tunnel after almost 50 seconds of simulation

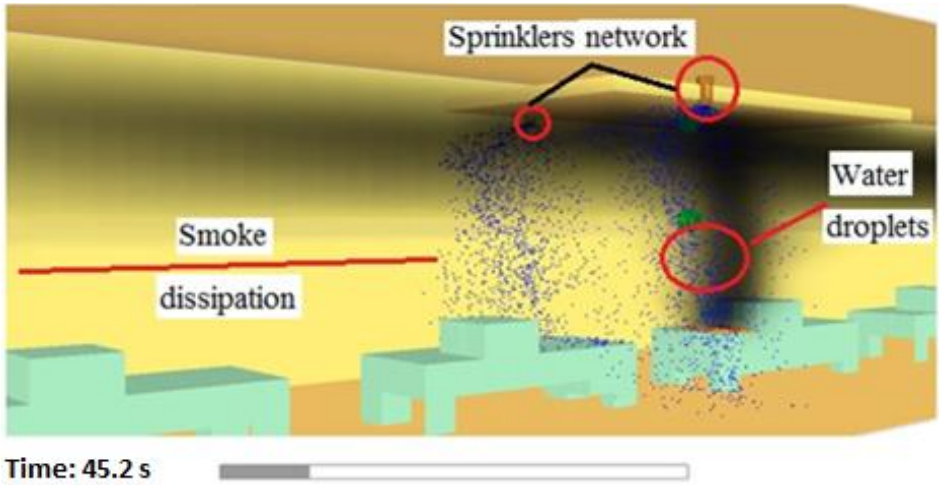

Figure 3 Smoke and water visible as particles

As it can be seen in the Fig. 3, the water droplets generated by the sprinklers network successfully dissipate the smoke around them, thus maintaining better visibility and decreasing the chance of backfiring, by decreasing the O_2 level and giving a lower temperature around them.

As it can be seen in the Fig. 4, the highest temperature reached around the sprinklers network is, in the first 10 seconds of simulation, about 83 °C, this decreasing to almost 65 ^{0}C during the fire action and also decreasing to almost 20 ^{0}C by the end of the simulation.

Sprinklers used in fire simulation are placed as seen in the Fig. 2, in order to produce a protection water curtain. The curtain is intended to protect people and evacuation route, from smoke but also from heat. Throughout the space, mainly on evacuation routes are placed virtual temperature thermocouples and smoke detectors, virtual devices that give information concerning the simulated values of temperature or smoke density in a specific point, as a function of time.

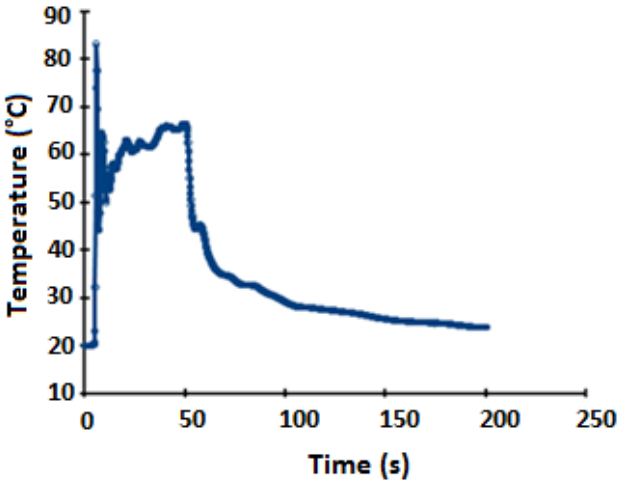

Figure 4 Temperature reaches at the sprinklers level

4. Conclusion

Authors used fire simulations in order to come up with conclusions concerning the effectiveness of water sprinkler curtain protection against fires, in road tunnel fire simulations. The total fire time is about 45 seconds after it was extinguished by the sprinklers. This range of values allows checking the air circulation in the studied tunnel aiming to avoid the disagreeable values for traffic and life protection in road tunnels construction. Also, it has been shown that the smoke spread very fast at long distances, which may affect the users before they can be evacuated.

Although, there were used only 2 sprinklers placed at a relatively small distance between them and it can be revealed that the water droplets generated by the sprinklers network successfully dissipate the smoke around them, thus maintaining better visibility and decreasing the chance of backfiring, by decreasing the O_2 level and lowering temperature around them. Most important, the water droplets are successfully extinguishing the fire. All information above mentioned combined together prove that, at a real scale, with a more complex sprinkler network placed on the entirely tunnel length, the extinguishing action save users, by maintaining a lower temperature and a better visibility.

The article reveal the importance of using sprinklers, without the effects of a fire event occurring in a road tunnel would be more severe for users, material and environment.

References

[1] Kumn M, Nehrenheim E, Odlar M. Innovative measures for environmental technologies at tunnel fires. In: Minkevica S, editor. *Research of Technogenic Envionment Protection, 49th International Scientific Conference on Research of Technogenic Envionment Protection*; 2008 Oct 9-10; Riga, Latvia. Riga: Riga Technical University; 2008. p. 152-159.

[2] Cheong MK, Spearpoint MJ. Fleischmann CM, Calibrating a FDS simulation of goods vehicle fire growth in a tunnel using the Runehemar fire experiment. *J Fire Prot Eng* 2009;19(3):177-196.

[3] Grant GB, Jagger SF, Lea CJ. Computational study of longitudinal ventilation control during an enclosure fire within a tunnel. *J Fire Prot Eng* 2006;16:159-181.

[4] Both C. Tunnel fire safety. *Heron* 2003;48(1):3-16.

[5] Codescu S, Chisacof A, Anghel I, Panaitescu V, *Environmental consequences and risk factors after a fire in a road tunnel*. Paris: CNAM. 2014. 25 p.

[6] Beard A, Carvel R. *The handbook of tunnel fire safety*. London: Thomas Telford Publishing. 2005. 514 p.

[7] Anghel I, Zoicaş C, Popa C, Netcu C. Using 3D dynamic modeling for planning the response to CBRN events in underground public buildings. *J Emerg Med Emerg Situations* 2011;1:15-17.

[8] Netcu C, Panaitescu V, Popa C, Anghel I. *3D simulation of a subway station fire*. Bucharest: Police Academy. 2011. 277 p.

[9] Susan O, Tuleanu C, Panaitescu V. *Computational fluid dynamics (CFD) for fire dynamics simulator (FDS)*. Chisinau: Technical University of Chisinau. 2008. 257 p.

[10] Migoya E. A simplified model of fires in road tunnels: comparison with three-dimensional models and full-scale measurements. *Open Thermodyn J* 2010;4:156-166.

[11] Hua GY, Wang W, Zhao YH, Li L. A study of an optimal smoke control strategy for an Urban Traffic Link Tunnel fire. *Tunn Undergr Space Technol* 2011;26(2):336-344.

European Journal of Environmental and Safety Sciences 2014 2(2): 53-58
ISSN 1339-472X European Science and Research Institute (Original Research Paper)

Water pollution along the Mahim Creek of Mumbai, India - Study of physico-chemical properties

P. U. Singare[a] · S. E. L. Ferns[a] · E. R. Agharia[b]

[a]*Department of Chemistry, Bhavan's College, Munshi Nagar, Andheri (West), Mumbai 400058, India*
[b]*Department of Chemistry, SVKM's Mithibai College, Vile-Parle (West), Mumbai 400056, India*

ABSTRACT

The present study was performed for the period of one year from June 2012 to May 2013 in order to understand the physico-chemical properties of water samples collected along the Mahim Creek of Mumbai. The annual average Total Dissolved Solid (TDS*)* content of the Creek water was found to be 14614 ppm which was very much above the limit of 2100 ppm set by the Central Pollution Control Board (CPCB) for inland surface water. The annual average conductivity was found to be 24023 μS cm^{-1} which was very much above the conductivity limit for inland surface water of 1000 μS cm^{-1} set by CPCB for propagation of fisheries. The annual average hardness level of the creek water was recorded as 1696 ppm, based on the recorded value the creek water can be considered as very hard water. The hardness of creek water was supported from the high annual average concentration levels of calcium (545 ppm) and magnesium (209 ppm) in the creek water. The average annual alkalinity level was recorded as 334.7 ppm, which according to the UN Department of Technical Cooperation for Development can be considered as medium to strongly alkaline. The annual average chloride concentration level was found to be 4770 ppm which was above the US Environment Protection Agency (US EPA) standards of 250 ppm set for chloride in surface water. The overall annual average concentration of sulphate was found to be 605.5 ppm, which was very much above the limit of 400 ppm set by CPCB for inland surface water. It is feared that such high amount of sulphates may lead to pollution problems resulting in the formation of hydrogen sulfide gas. The average concentration level of reactive silica as SiO_2 in the creek water was recorded as 495.3 ppm. Based on the previous study it is feared that such high level of Si at a pH greater than 5 may affect significantly in removal of the As (III) and also reduce the adsorption capacity of ferric hydroxide for As (V) and As (III) at a pH of approximately 6.8. From the results it appears that as India moves towards stricter regulation of industrial effluents to control water pollution, greater efforts are required to control the discharge of pollutants into the aquatic ecosystems.

Keywords: Physico-chemical properties • Creek water • TOC • Conductivity • Mahim Creek • Bandra ki Khadi Mumbai

1. Introduction

In India due to rapid industrialization, urbanization and development of slum areas with improper environmental planning have resulted in heavy discharge of domestic sewage and industrial effluents into the water bodies. Most of the industries in India are situated along the river banks for easy availability of water and also disposal of the wastes. It is found that one-third of the total water pollution in India comes in the form of industrial effluent discharge, solid wastes and other hazardous wastes **[**1-16**]**. Out of this, a large portion can be traced to the processing of industrial chemicals and to the food products industry. The surface water is the main source of industries for waste disposal. Untreated or allegedly treated effluents have increase the level of surface water pollution up to 20 times the safe level in 22 critically polluted areas of the country. It is found that almost all rivers are polluted in most of the stretches by some industry or the other. The industrial wastes often contain a wide range of contaminants such as petroleum hydrocarbons, chlorinated hydrocarbons and heavy metals, various acids, alkalis, dyes and other chemicals which greatly change the pH of water. The waste also includes detergents that create a mass of white foam in the river waters. All these chemicals are quite harmful or even fatally toxic to fish and other aquatic populations **[**17-21**]**. These

Pravin U. Singare (corresponding author)
Department of Chemistry, Bhavan's College, Munshi Nagar, Andheri (West), Mumbai 400058, India
e-mail: pravinsingare@gmail.com

wastes also include various toxic chemicals, acids, alkalis, dyes, detergents, pesticides and agrochemicals which greatly affect the physico-chemical properties of water bodies. Therefore, a better understanding of physico-chemical properties like pH, conductivity, alkalinity, salinity, hardness, Chemical Oxygen Demand (C.O.D) etc. in the water bodies seem to be particularly important issues of present day research on pollution assessments **[**22-32**]**. According to one study it was estimated that Mumbai city of India itself discharges around 2200 MLD of waste to the coastal waters [33].

In view of present day by day increasing pollution level along most of the creeks and rivers in Mumbai, in the present study attempt was made to conduct the systematic study of physico-chemical properties of water samples collected along the Mahim creek of Mumbai. It is expected that the results of our study will help greatly in understanding the water pollution status along the Mahim creek which receives heavy pollution load from the adjoining Mithi River and from the surrounding slum areas discharging domestic effluents.

2. Material and methods

2.1. Study area

The Mahim Creek (locally known as Bandra ki Khadi) is a creek in Mumbai, India. The famous Mithi River which is one of the most polluted river of Mumbai [34-39] drains into the creek which further drains into the Mahim Bay. It is the only Creek which balances the water level of Mumbai during heavy rainfall and during Mumbai monsoon time. The creek is the biggest sink for most of the waste generated by residential complexes and small scale industries. The waters of the creek are foul smelling due to the dumping of untreated industrial effluents further upstream. The creek is swamped by mangroves and has a mini-ecosystem within it. It is a less known fact that the Mahim bay area, where Mahim creek meets Arabian Sea, is a nominated bird sanctuary called "Salim Ali Bird Sanctuary" where migratory birds come for nesting. The Creek is located along western Arabian cost of India from 19^{o}2'52.84'' north and from 72^{o}50'17.56'' east. The depth of the creek is 4.6 m. The area experiences tropical savanna climate. It receives heavy south west monsoon rainfall, measuring 2166 mm on an average every year. The temperature ranges from 16 ^{o}C to 39 ^{o}C with marginal changes between summer and winter months. The relative humidity ranges between 54.5 to 85.5 % [40].

2.2. Requirements

All the glassware, casserole and other pipettes were first cleaned with tape water thoroughly and finally with deionised distilled water. The pipettes and standard flasks were rinsed with solution before final use. The chemicals and reagent were used for analysis were of analytical reagent (A.R.) grade. The procedure for calculating the different parameters were conducted in the laboratory.

2.3. Sampling

The study on pollution status along the Mahim creek of Mumbai was performed for the period of one year from June 2012 to May 2013. The grab samples were collected in polythene bottles of 2.5 l along different locations of the creek. The bottles were thoroughly cleaned with hydrochloric acid, washed with distilled water to render free of acid, rinsed with the water sample to be collected and then filled with the sample leaving only a small air gap at the top. The sample bottles were stoppard and sealed with paraffin wax. The grab samples thus collected were mixed to give gross sample. Such samples were drawn and analysed monthly for the entire year. The samples were analyzed for their physico-chemical parameters so as to get the seasonal variation in pollution level along the Mahim Creek.

2.4. Quality control

The glassware used were soaked in appropriate dilute acids overnight and washed with teepol and rinsed with deionised water before use. All instruments used were calibrated before use. Tools and work surfaces were carefully cleaned for each sample to avoid cross contamination. Triplicate samples were analysed to check precision of the analytical method and instrument.

2.5. Physico-chemical parameters studied

The water samples collected were analyzed for pH, electrical conductivity, Total Dissolved Solid (TDS), alkalinity, hardness, chloride, calcium, magnesium, sulphates and reactive silica. The techniques and methods followed for analysis and interpretation were according to the standard procedures [41-45].

3. Results and discussion

The experimental data on physico-chemical properties of the water samples collected along the Mahim Creek of Mumbai is presented in Table 1. The annual average values of various physico-chemical properties of the water samples are graphically represented in Fig. 1 and 2.

The pH value of creek water was minimum of 7.10 in the month of October to maximum of 7.80 in the month of December with an annual average value of 7.46. The TDS content of water was low of 496 ppm in the month of September to 32300 ppm in the month of May. The annual average TDS content of the Creek water was found to be 14614 ppm which was very much above the limit of 2100 ppm set by CPCB for inland surface water [46]. On the basis of *TDS* values, waters can be classified as, desirable for drinking (up to 500 mg l^{-1}), permissible for drinking (up to 1,000 mg l^{-1}), useful for irrigation (up to 2,000 mg l^{-1}), not useful for drinking and irrigation (above 3,000 mg l^{-1}) [47]. Therefore the creek water can be considered unfit for drinking and irrigation purpose. The electrical conductivity of creek water was in the range of 760 to 51300 µS cm^{-1}. The annual average conductivity was found to be 24023 µS cm^{-1} which was very much above the conductivity limit for inland surface water of 1000 µS cm^{-1} set by CPCB for propagation of fisheries [46]. The total hardness of the creek water was minimum of 145 ppm in the month of September and maximum of 7530 ppm in the month of March, having annual average hardness level of 1696 ppm. Kannan [48] has classified water on the basis of hardness values in the following manner: 0–60 mg l^{-1}, soft, 61–120 mg l^{-1}, moderately hard, 121–160 mg l^{-1}, hard and greater than as 180 mg l^{-1} very hard. Using these criteria, the creek water can be considered as very hard. The overall total hardness values were very much above the limit of 300 mg l^{-1} set by ISI [49]. The observed higher values of hardness indicate the presence of basic salts – sodium and potassium in addition to those of calcium and magnesium [50]. This was supported from the high annual average concentration levels of calcium (545 ppm) and magnesium (209 ppm) in the creek water. The total alkalinity content was found to vary in the range of 153.5 ppm to 653.6 ppm with the average annual alkalinity level of 334.7 ppm. According to the UN Department of Technical Cooperation for Development [51], water having alkalinity up to 50 mg l^{-1} is considered to be weak alkaline, up to 100 mg l^{-1} is considered to be medium alkaline, while if the alkalinity is above 200 mg l^{-1} it is considered as strongly alkaline. Hence based on results of the present investigation, the creek water was found to be medium to strongly alkaline. Chloride occurs in all natural waters in widely varying concentrations. The criteria set for excessive chloride in potable water are based primarily on palatability and its potentially high corrosiveness. Plants do not thrive as well on chlorinated as on unchlorinated water; wild animals develop atherosclerosis by consumption of chlorinated water [52]. From the results of present investigation it was observed that chloride content was minimum (126.5 ppm) during the month of June and maximum (22305.8 ppm) in the month of March. The annual average chloride concentration level was found to be 4770 ppm which was above the US EPA standards of 250 ppm set for chloride in surface water [53]. Sulphates can interfere with the disinfection efficiency by scavenging residual chlorine in the distribution system [54]. Sulphate reducing bacteria produce hydrogen sulfide and lower the aesthetic quality of the water by imparting an unpleasant taste and odour and increases corrosion of metal and concrete pipes [55]. Sulphates can affect industrial water supplies due to formation of hard scales in boilers and heat exchangers. High amount of sulphates in wastewater may lead to problems due to the formation of hydrogen sulfide gas [56]. In the present investigation, the concentration of sulphate was in the range of 12.8 to 2916.7 ppm. The overall annual average concentration of sulphate was found to be 605.5 ppm, which was very much above the limit of 400 ppm set by CPCB for inland surface water [46]. The concentration level of reactive silica as SiO_2 in the creek water was found to vary in the range of 9.0 to 1412.2 ppm, with an average concentration of 495.3 ppm. Based on the previous study [57] it was observed that the As (III) removal was decreased significantly at a pH greater than 5 when Si concentration was higher than 1 ppm. The study also revealed that at a pH of approximately 6.8 and in the presence of 10 ppm Si, the adsorption capacity of ferric hydroxide for As (V) and As (III) was reduced considerably.

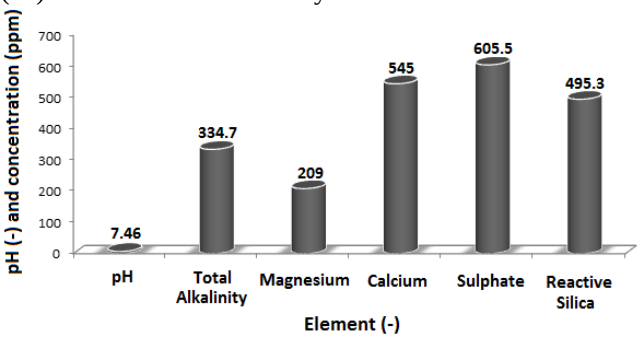

Figure 1 Annual average pH, total alkalinity, magnesium, calcium, sulphate and reactive silica content in Mahim Creek water

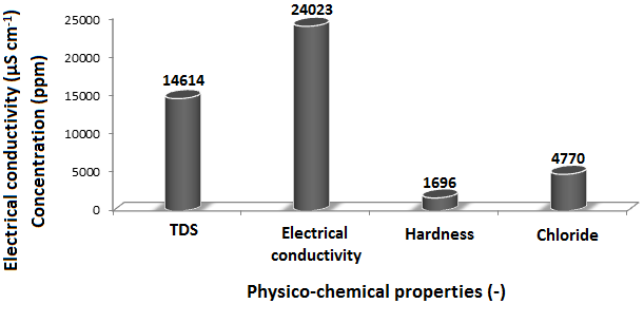

Figure 2 Annual average total dissolved solids (TDS), electrical conductivity, hardness and chloride content in Mahim Creek water

Table 1 Physico-chemical properties of water samples collected along the Mahim Creek

Physico-chemical Properties	pH	Electrical Conductivity ($\mu S.\ cm^{-1}$)	TDS* (ppm)	Alkalinity (ppm)	Hardness (ppm)	Chlorides (ppm)	Ca^{2+} (ppm)	Mg^{2+} (ppm)	SO_4^{2-} (ppm)	Reactive Silica as SiO_2 (ppm)
Months & Year										
June 2012	7.20	21500	15700	320.5	198	126.5	29.5	5	12.8	9.0
July 2012	7.60	11600	6350	207.6	185	149.9	31.3	11	63.5	12.5
August 2012	7.70	3520	1050	198.3	160	128.9	38.9	19	52.8	19.8
September 2012	7.30	760	496	153.5	145	138.6	40.1	11	53.8	15.5
October 2012	7.10	3500	790	165.8	235	356.7	53.9	212	238.5	145.9
November 2012	7.40	7900	1850	173.1	339	983.4	601.3	315	316.9	437.9
December 2012	7.80	15000	9750	205.6	1215	2356.7	951.3	635	750.3	982.7
January 2013	7.30	32000	17560	430.2	3490	6362.8	1312.5	512	1215.9	1125.9
February 2013	7.40	45400	29510	537.5	6435	18802.7	1803.6	487	2916.7	1412.2
March 2013	7.50	46300	28510	653.6	7530	22305.8	1503.5	215	1211.3	1110.3
April 2013	7.60	49500	31500	555.3	250	5352.1	125.9	75	354.8	651.4
May 2013	7.60	51300	32300	415.5	168	175.5	48.5	13	78.5	19.9

* Total dissolved solids

4. Conclusion

With the rapid industrialization in the country, environment pollution by industrial waste has increased tremendously. The discharge of waste water from industries such as oil and surfactants industries, tanneries, pulp and paper, textile, petroleum, chemical industries etc. pollute water bodies. Nature has an amazing ability to cope up with small amount of waste water and pollution, but it would be hazardous or harmful if billions of gallons of waste water produced everyday are not treated before releasing them back to the environment. The quantities and characteristics of discharged effluent vary from industry to industry depending on the water consumption and average daily product. Characterization of raw effluent from oil and surfactants industries revealed a wide variation in the effluent quality and quantity over time, characteristic of the different processing stages employed in product manufacturing. Thus, physico-chemical treatment of these effluents is required to bring them into the biodegradable zone and ensure local sewer standards are meeting.

References

[1] Singare PU, Lokhande RS, Jagtap AG. *International Journal of Global Environmental Issues* 2011;11(1):28-36.

[2] Singare PU, Lokhande RS, Jagtap AG. *Interdisciplinary Environmental Review* 2010;11(4):263-273.

[3] Lokhande RS, Singare PU, Pimple DS. *World Environment* 2011;1(1):6-13.

[4] Lokhande RS, Singare PU, Pimple DS. *Resources and Environment* 2011;1(1):13-19.

[5] Lokhande RS, Singare PU, Pimple DS. *International Journal of Ecosystem* 2011;1(1):1-9.

[6] Sasamal SK, Rao KH, Suryavansi UM. *International Journal of Remote Sensing* 2007;18(19):4391-4395.

[7] Nagaraju A, Suresh S, Killham K, Hudson-Edward K. *Turkish Journal of Engineering and Environmental Sciences* 2006;30(4):203-219.

[8] Rajaram T, Das T. *Futures* 2008;40(1):56-69.

[9] Zingade MD, Sabnis MM, Mandalia AV, Desai BN. *Mahasagar Bulletin of the National Institute of Oceanography* 1980;99(13):27-34.

[10] Singare PU, Dhabarde SS. *International Letters of Chemistry, Physics and Astronomy* 2014;3:56-63.

[11] Singare PU, Dhabarde SS. *International Letters of Chemistry, Physics and Astronomy* 2014;3:48-55.
[12] Singare PU, Dhabarde SS. *International Letters of Chemistry, Physics and Astronomy* 2014;3:40-47.
[13] Singare PU, Dhabarde SS. *International Letters of Chemistry, Physics and Astronomy* 2014;3:32-39.
[14] Singare PU, Dhabarde SS. *International Letters of Chemistry, Physics and Astronomy* 2014;3:8-15.
[15] Singare PU, Dhabarde SS. *International Letters of Chemistry, Physics and Astronomy* 2014;3:16-23.
[16] Singare PU, Dhabarde SS. *International Letters of Chemistry, Physics and Astronomy* 2014;3:24-31.
[17] Aghor A. *Daily DNA* 2007;8(14):24-25.
[18] Patil D. *Daily Times of India* 2009;3(17):10-11.
[19] Kumar A. *Polskie Archiwum Hydrobiologii* 1996;18:469-511.
[20] Singare PU, Talpade MS. *Interdisciplinary Environmental Review* 2013;14(1):59-68.
[21] Chakravarty RD, Ray P, Singh SB. *Indian Journal of Fisheries* 1959;6:36-49.
[22] Singare PU, Mishra RM, Trivedi MP. *Resources and Environment* 2011;1(1):32-41.
[23] Singare PU, Trivedi MP, Mishra RM, Dagli DV. *Interdisciplinary Environmental Review* 2012;13(2/3):220-243.
[24] Singare PU, Trivedi MP, Mishra RM. *Marine Science* 2011;1(1):22-29.
[25] Singare PU, Trivedi MP, Mishra RM. *Interdisciplinary Environmental Review* 2012;13(4):245-268.
[26] Singare PU, Lokhande RS, Bhattacharjee SS. *Interdisciplinary Environmental Review* 2011;12(2):95-107.
[27] Singare PU, Lokhande RS, Naik KU. *Interdisciplinary Environmental Review* 2011;12(3):215-230.
[28] Singare PU, Lokhande RS, Naik KU. *Interdisciplinary Environmental Review* 2010;11(1):90-107.
[29] Singare PU, Lokhande RS, Bhanage SV. *Interdisciplinary Environmental Review* 2011;12(1):1-11.
[30] Singare PU, Lokhande RS, Pathak PP. *Interdisciplinary Environmental Review* 2010;11(1):38-56.
[31] Singare PU, Talpade MS, Dagli DV, Bhawe VG. *Water Resources and Rural Development* 2012;2(3):79-84.
[32] Singare PU, Talpade MS, Bhawe VG, Dagli DV. *Research Journal of Pharmaceutical, Biological and Chemical Sciences* 2012;3(4):545-551.
[33] Zingde MD, Govindan K. Health status of coastal waters of Mumbai and regions around. In: Sharma VK, editor. *Environmental Problems of Coastal Areas in India*. New Delhi: Bookwell Publishers; 2001. p. 119-132.
[34] Singare PU. *Asian Journal of Environment and Disaster Management* 2012;4(3):323-332.
[35] Singare PU, Mishra RM, Trivedi MP. *Advances in Analytical Chemistry* 2012;2(3):14-24.
[36] Singare PU, Mishra RM, Trivedi MP. *Frontiers in Science* 2012;2(3):28-36.
[37] Singare PU, Mishra RM, Trivedi MP. *Interdisciplinary Environmental Review* 2012;13(4):245-268.
[38] Singare PU, Mishra RM, Trivedi MP. *Resources and Environment* 2011;1(1):32-41.
[39] Klean EC. *Survey Report on Mithi River Water Pollution and Recommendations for its Control*. Mumbai: Klean Environmental Consultants; 2004. 285 p.
[40] Singare PU. *Marine Science* 2012;2(1):1-5.
[41] Rainwater FH, Thatchar LL. *Methods for Collection and Analysis of Water Samples*. Reston: U.S. Geological Survey; 1960. 301 p.
[42] Brown E, Skougstad MW, Fishman MJ. *Methods for Collection and Analysis of Water Samples for Dissolved Minerals and Gases*. Reston: U.S. Geological Survey; 1970. 160 p.
[43] ICMR. *Manual of Standards of Quality for Drinking Water Supplies*. New Delhi: Indian Council of Medical Research; 1975. 112 p.
[44] Hem JD. *Study and Interpretation of Chemical Characteristics of Natural Water*. Washington: U.S. Geological Survey; 1985. 97 p.
[45] APHA. *Standard Methods for Estimation of Water and Wastewater*. Washington: American Water Works Association; 1995. 57 p.
[46] CPCB. *Standards for classification of inland surface water for propagation of wild life*. New Delhi: CPCB; 2012. 77 p.
[47] Wilcox LV. *Classification and Use of Irrigation Waters.* Boston: U.S. Department of Agricultural Sciecnes; 1955. 966 p.
[48] Kannan K. *Fundamentals of Environmental Pollution*. New Delhi: S. Chand and Company; 1991. 361 p.
[49] Indian Standard Institute. *Drinking Water Specification*. New Delhi: Indian Standard Institute; 1991.
[50] Moundiotiya C, Sisodia R, Kulshreshtha M, Bhatia *Jounral of Environmental Hydrology* 2004;12:1-7.
[51] DTCD. *The use of non-conventional water resources in developing countries*. New York: U.S. Department of Technical Cooperation for Development; 1985. 97 p.
[52] Hattersley JG. *The Journal of Orthomolecular Medicine* 2000;15(2):89-95.
[53] US EPA. *Surface water quality standards*. Washington: US EPA; 2013. 86 p.
[54] Faust SD, Osman A. *Chemistry of water treatment*. Woburn: Butterworth Publishers; 1983. 167 p.
[55] Singh G, Bhatnagar M. *International Journal of Mine Water* 1989;13(7):80-86.

[56] Hammarstrom JM, Seal RR, Meier AL, Kornfeld JM. *Chemical Geology* 2005;215:407-412.

[57] Meng X, Bang S, Korfiatism GP. *Water Resources* 200;34(4):1255-1261.

European Journal of Environmental and Safety Sciences 2014 2(2): 59-64
ISSN 1339-472X European Science and Research Institute (Original Research Paper)

Assessment of phytoremediation potentials of legumes in spent engine oil contaminated soil

H. Y. Ismail[a] · U. J. J. Ijah[b] · M. L. Riskuwa[c] · I. A. Allamin[a] · M. A. Isah[a]

[a]*Department of Microbiology Faculty of Science, University of Maiduguri, Nigeria*
[b]*Department of Microbiology, Faculty of Science, Federal University of Technology, Minna, Nigeria*
[c]*Department of Microbiology, Faculty of Science, Usmanu Danfodiyo University, Sokoto, Nigeria*

ABSTRACT

This study was conducted to evaluate the growth and phytoremediation potential of Pigeon pea (*Cajanus cajan*) and Hyacinth bean (*Lablab purpureus*) in spent engine oil (SEO) contaminated soil. The study involved a field experiment conducted in a botanical garden under irrigation. The two plant species were grown on (0.0, 2.5, 5.0 and 10.0) % (v/v) spent engine oil contaminated soil. Percentage emergence of *C. cajan* was between (14.81 and 29.63) %, while that of *L. purpureus* was between (14.84 and 44.44) %. The plants were able to grow on all the contaminated soil except for *Lablab purpureus* at 10.0 % SEO contamination. Longest shoots of both plants were observed in 2.5 % SEO contaminated soil after 3 months. Similar observations were made for other parameters except in the leaf length (LL) of *Lablab purpureus* where plant grown on (2.5 and 5.0) % had longer LL than the control plants ($p \leq 0.05$). Microbial analyses revealed higher counts of oil utilizing bacteria in rhizosphere ($36.0 \pm 6.7\times10^8$ cfu g^{-1}) than non rhizosphere ($14.0 \pm 5.3\times10^7$ cfu g^{-1}) soil and in uncontaminated ($29.0 \pm 5.5\times10^8$ cfu g^{-1}) than contaminated ($14.0 \pm 5.3\times10^7$ cfu g^{-1}) soil. Rhizosphere effect (RE) values were positive (≥ 1) in all treatments with the exception of *Lablab purpureus*, which recorded RE value of 0.6 (negative RE) for total fungal counts. The plants therefore, have potentials for phytoremediation and could be important tools in reclaiming soil with low levels of SEO contamination.

Keywords: Legumes • Phytoremediation • Spent engine oil • Rhizosphere • Contamination

1. Introduction

In Soil, for a long time, has been a reservoir of various environmental and industrial wastes. With emergence of petroleum industry, soil contamination due to petroleum and its derived products has been a problem. However, the global emphasis on soil health and sustainable food security is persuading scientists to consider rehabilitation of degraded lands, especially where oil contamination limits the use of such soils [1]. Bioremediation is identified as the most promising means of soil reclamation and attempts to integrate plant and microbial activities in the process are fascinating. Plants especially legumes and grasses have been identified to play important role in remediating oil polluted soil in both laboratory and field scales [2-3]. Nigeria being an oil-producing country and experiencing contamination due to oil exploration and indiscriminate disposal of spent engine oil, is in dare need of effective and environment friendly remediation measures. Therefore, research in phytoremediation is being intensified [1, 4].

Various plants have been identified for their potential to facilitate the phytoremediation of sites contaminated with petroleum hydrocarbons and the majority of studies singled out grasses and legumes for higher potentialities [5]. Legumes are known to have an advantage over non-leguminous plants in phytoremediation because of their ability to fix nitrogen and thus, do not have to compete with microorganisms and other plants for limited supplies of available soil nitrogen at oil-contaminated sites [6].

Cajanus cajan L. (Pigeon pea, also known as Red gram, Congo pea, Gungo pea, No Eye pea) and *Lablab purpureus* L. (lablab bean, dolichos or hyacinth bean) are important leguminous plants and they occur in many parts of the world [7-8]. Both of the plants are members of the family Fabaceae and their cultivation as green manure has been

H. Y. Ismail (corresponding author)
Department of Microbiology Faculty of Science, University of Maiduguri, Nigeria
e-mail: yismailh@gmail.com

reported [9-10]. Pigeon pea is found useful in many areas as growth enhancer, alley crop, and protein and trace nutrient supplement, control of weeds and nematodes as well as medication [11]. Similarly, hyacinth bean is being used in addition to increasing soil fertility, as food supplement for live stocks (forage) and humans (pulse) [8]. Common desirable characteristics of these plants are ability to fix nitrogen (a major limiting factor for effective degradation of pollutants) and drought tolerance [10, 12].

The present study was designed to assess the growth and phytoremediation abilities of the plants to low SEO contamination levels through effective growth and enhancement of microbial populations. This is with a view to harnessing its nitrogen fixing ability and drought tolerance for reclaiming SEO damaged soils in semi-arid regions.

2. Material and methods

2.1. Study area

The experiments were carried out at the Botanical Garden of Usmanu Danfodiyo University between November, 2012 and January, 2013. The University is located in Sokoto, the capital of Sokoto State (between longitudes 4º 8'E and 6º54'E and latitudes 12ºN and 13º 58'N.), north western Nigeria (Sokoto State, 2000). The seeds of *C. cajan* and *L. purpureus* were obtained from National Animal Production and Research Institute (NAPRI), Ahmadu Bello University, Zaria, Nigeria while the spent engine oil (SEO) used in this study was obtained from a filling station (Total Plc.), along Bello Way, Sokoto, Nigeria.

2.2. Experiment description

The experimental site was cleared of all grasses and unwanted materials prior to treatment. The soil was ploughed to an approximate depth of 10 cm and plots of (20 × 20) cm were made. Four plots were made for each of the two plants.

Aliquot (100 ml) of SEO was spread on 400 cm^2 soil to obtain 2.5% (v/v) concentration. The soil was properly agitated and thoroughly mixed to ensure uniform soil contamination. Similar procedure was employed to prepare (5 and 10) % (v/v) contamination for which (200 and 400) ml were added respectively. The concentration used in this experiment acknowledged previous investigations that reported contamination beyond 3 % concentration has been increasingly deleterious to soil biota and crop growth [13]. Out of the four plots constructed for each of the plants, three were contaminated (contaminated rhizosphere plots) to yield (2.5, 5.0 and 10.0) % v/v respectively. The remaining plot was left uncontaminated to serve as control (uncontaminated rhizosphere plot) for each of the plants. A set of two more plots were constructed (comprising of each one contaminated and one uncontaminated) in order to obtain non rhizosphere plots (negative controls). The plots were allowed to remain undisturbed for one week. After the one week period, seeds of *C. cajan* and *L. purpureus* were planted accordingly as described by [14].

2.3. Planting of seeds

The viability of the seeds was tested by floatation method [3], whereas the dormancy was broken by softening or weakening the seed coat (scarification) using warm water overnight [15], due to the fact that both seeds were dormant due to coat [16]. The seeds were then surface sterilized with 10% hydrogen peroxide solution before planting.

The seeds of both plants were sown to a depth of (2.5 to 5) cm, a depth recommended for *Lablab purpureus* [17]. For better establishment of the plants, three seeds were planted in a hole. Each plot was harboring three holes replicated three times. After sowing, the soil was irrigated every day and emergence was observed subsequently.

Parameters such as days of emergence, percentage emergence, shoot length, leaf length and numbers of leaves were determined at the interval of one month for three months. Percent (%) germination was calculated using this formula. Number of seedlings that sprouted over/Number of seeds planted multiplied by 100. Days to germination were calculated by counting from the day of sowing to the day of unequivocal emergence of ridicules. Length of shoots and leaves were determined using meter rule.

2.4. Enumeration of microorganisms

Microbial population of the soil samples were enumerated by making tenfold dilution of the samples collected from rhizosphere of the plants. Using a dropper pipette, 0.025 ml of each dilution was inoculated on Nutrient agar (for bacteria), Sabuoraud Dextrose agar (for fungi) and oil agar [18] (containing 0.1 % v/v SEO) (oil utilizing bacteria and fungi). The plates were incubated at 30 ^{0}C for 24h, 5days, and 48h to 5 days respectively. The number of viable bacteria, fungi and hydrocarbon utilizing organisms in the samples were estimated from the number of colonies formed. The result was determined from the number of counts and dilution used and expressed as colony forming units per gram of soil (cfu g^{-1}) [19].

Data generated form the experiments were subjected to analysis of variance (ANOVA) with the aid of GraPhpad InStat 3a statistical package. Significant treatment means were separated using Duncan's multiple range tests.

3. Results

The results of the emergence of plants after germination indicated that the emergence started four and six days after sowing for *C. cajan* and *L. purpureus* respectively. The number of plants that emerged was considerably low when compared with the number of seeds planted (Table 1). The percentage emergence ranged between (14.81 and 29.63) % for *C. cajan* (Table 1) and between (14.81 and 44.44) % for *L. purpureus* (Table 1). Statistical analysis indicated no significant difference ($p \leq 0.05$) between the two plants in terms of emergence. There was no significant statistical difference ($p \leq 0.05$) in plants' percentage emergence with regards to SEO concentration in *C. cajan*. For the *L. purpureus* however, there was significant difference between the control and other treatments at 95 % level of significance.

The growth parameters of the plants were also monitored. Shoot length, leaf length, number of leaves and number of flowers were determined and presented in Tables 2 and 3. Longest and shortest shoots leaves were both observed in (2.5 and 10) % respectively in both of the plants after the three month experiment. The growth was generally less pronounced in 10 % plots especially in the case of *L. purpureus* were very poor growth and eventual stagnancy was observed. Statistical analyses showed that there is variation between the various treatments at 95 % level of significance (Table 2 and 3).

Tables 4 and 5 showed the average microbial counts of the rhizosphere and non rhizosphere soils for *C. cajan and L. purpureus* respectively. The rhizosphere soil generally showed high bacterial counts, ranging from (3.410^9 to 6.8×10^9) cfu g^{-1} (aerobic heterotrophic bacteria), (4.0×10^9 to 7.0×10^9) cfu g^{-1} (oil utilizing bacteria), (5.0×10^4 to 2.4×10^5) cfu g^{-1} (fungi) and (1.0×10^4 to 6.0×10^4) cfu g^{-1} (Oil utilizing fungi) for *C. cajan.* On the other hand, the counts of microorganisms associated with the rhizosphere of *L. purpureus* ranged from (5.8×10^9 to 1.4×10^{10}) cfu g^{-1} (aerobic heterotrophic bacteria), (1.4×10^9 to 9.6×10^9) cfu g^{-1} (oil utilizing bacteria), (0.0×10^4 to 1.0×10^5) cfu g^{-1} (fungi) and (0.0×10^4 to 8.0×10^4) cfu g^{-1} (oil utilizing fungi). The rhizosphere effect values were much more pronounced in uncontaminated rhizosphere of *C. cajan* than the contaminated rhizosphere in all of the four microbial groups. This was in contrast to *L. purpureus* rhizosphere where considerable variations occurred.

Table 1 Emergence of *C. cajan and L. purpureus* in SEO contaminated soil

SEO concentration (%)	*Cajuns cajan*					*Lablab purpureus*				
	No. of seeds		Mean	Standard error	% Emergence	No. of seeds		Mean	Standard error	% Emergence
	planted	Emerged				Planted	Emerged			
0	27	8	2.6	0.02	29.6	27	4	0.4	0.2	14.8
2.5	27	4	1.3	0.03	14.8	27	12	1.3	0.20	44.4
5	27	6	2.0	0.29	22.2	27	9	1.0	0.2	33.3
10	27	4	1.3	0.18	14.8	27	8	0.9	0.3	26.6

Table 2 Growth parameters of *C. cajan*

Treatment SEO (%)	Monthly means ± standard error* Shoot length (cm)			No. of leaves			Leaf length (cm)	No. of flowers
	1st	2nd	3rd	1st	2nd	3rd		
Control (0)	22.5 ±1.4	41.7 ±1.7[a]	110.0 ± 0.0	35.7±4.7[a]	107.0 14.1[a]	180.0 ±6.9[ab]	6.8 ± 0.7	20.3 ±3.3
2.5	24.2 ±3.6	76.7 ±4.4[a]	139.2 ±8.5[a]	62.0 ±3.0[b]	84.7 ±6.4	169.0 ± 9.5[c]	8.5 ±0.6	19.3 ±2.0
5.0	22.5 ±2.5	74.2 ±7.4[a]	124.2 ± 6.0	56.0 ±3.5[a]	72.7 ±5.3	135.0 ±3.5[ac]	8.0 ±0.2	23.3 ± 2.4
10.0	18.3 ±0.8	57.5 ±7.6	105.8 ±7.9[a]	37.0 ±7.8[b]	68.3 ±1.2[a]	106.0 ±5.3[bc]	7.9 ±0.4	12.3 ±1.8

* Values with the same superscript in a column are statistically significant

Table 3 Growth parameters of *L. purpureus*

Treatment SEO (%)	Monthly means ± standard error							
	Shoot length (cm)			No. of leaves			Leaf length (cm)	No. of flowers
	1st	2nd	3rd	1st	2nd	3rd		
Control (0)	24.4 ±2.0[a]	57.2 ±3.8[a]	76.7 ±8.2[a]	26.0 ±6.1	70.0 ± 5.6	172.0±17[a]	8.9 ±0.4[a]	19.0 ± 4.6[a]
2.5	21.6 ±1.4[b]	56.4 ± 4.0[b]	181.7±29.2[ab]	28.0 ±3.6	109.0±15[a]	129.0±19[b]	10.2±0.7[b]	16.0 ± 4.0[b]
5.0	21.1 ±1.3[c]	54.6 ± 5.2[c]	136.7 ±34.7[c]	24.0 ±5.2	85.7±12.6[b]	138.0±6.2[c]	10.2±0.6[c]	16.0 ± 3.1[c]
10.0	6.4 ±0.4[abc]	12.5±0.0[abc]	12.5 ±0.0[bc]	11.0±1.0	33.0±0.0[ab]	0.0 ±0.0[abc]	5.7±0.1[abc]	0.0 ±0.0[abc]

* Values with the same superscript in a column are statistically significant

Table 4 Microbial counts of rhizosphere and non rhizosphere soil of *C. cajan*

Microbial group	Counts ($\times10^8$ cfu g^{-1})		RE value	Counts ($\times10^8$ cfu g^{-1})		RE value
	CR	CN	CR/CN	CU	UN	CU/CN
AHB	56.6	4.73	12	51.7	16.9	3.1
OUB	36.0	1.4	26	29.0	9.1	3.2
THF[a]	12.0	1.0	12	12.0	2.0	6.0
OUF[a]	5.0	1.7	2.9	5.0	1.3	3.8

CFU: Colony Forming Unit, RE: Rhizosphere Effect, CR: Contaminated Rhizosphere; CN: Contaminated Non rhizosphere; CU: Uncontaminated Rhizosphere; UN: Uncontaminated Non rhizosphere; AHB: Aerobic Heterotrophic Bacteria; THF: Total Heterotrophic Fungi, OUB: Oil Utilizing Bacteria; OUF: Oil Utilizing Fungi; a: Expressed as $\times10^4$ cfu g^{-1}.

Table 5 Microbial counts of rhizosphere and non rhizosphere soil of *L. purpureus*

Microbial group	Counts ($\times10^8$cfu g^{-1})		RE value	Counts ($\times10^8$cfu g^{-1})		RE value
	LR	CN	LR/CN	LU	UN	LU/CN
THB	108.0	47.3	2.3	65.3	16.9	3.9
OUB	73.0	14.0	5.2	20.0	9.1	2.2
THF[a]	6.0	10.0	0.6	7.3	2.0	3.7
OUF[a]	5.3	1.7	3.1	1.6	1.3	1.2

CFU: Colony Forming Unit, RE: Rhizosphere Effect, CR: Contaminated Rhizosphere; CN: Contaminated Non rhizosphere; CU: Uncontaminated Rhizosphere; UN: Uncontaminated Non rhizosphere; AHB: Aerobic Heterotrophic Bacteria; THF: Total Heterotrophic Fungi, OUB: Oil Utilizing Bacteria; OUF: Oil Utilizing Fungi; a: Expressed as $\times10^4$ cfu g^{-1}.

4. Discussion

Results shows that (Table 1), the emergence of the two plants was generally poor and despite the fact that no variations existed in terms of days of emergence of germinated seeds between control and treated soils, there were decreases in the percentage emergence of *C. cajan* between the control (29.63 %) and contaminated soils (22.2 to 14.8) %. This agreed with previous findings as similar researches have reported decrease in emergence of plants in hydrocarbon contaminated soils [20]. Anoliefo and Vwioko [21] noted poor germination of *Capsicum annum* and *Lycopersicon esculentum* in soil when treated with 4 and 5% of spent engine oil. Agbogidi [22] reported significant decrease in germination of six *Vigna unguiculata* cultivars due to exposure to SEO.

Statistical analyses for plant growth parameters revealed different level of variability between the treatments and the control. Significant difference ($p < 0.05$) was observed in shoot length of *C. cajan* in the second month of the experiment even though no such variation was observed in the first month. Longer shoots were observed in the soil amended with 2.5 % and 5% of SEO (Table 2). This indicated a kind of stimulatory effect that warranted plant

growth at these contamination levels. More effect was noticed in the third month where the longest shoots were recorded at 2.5 % contamination. This might be as a result of ability of the plant to tolerate the contaminant to the level it was exposed to. This agreed with the findings of Radwan *et al.* [23] who reported that some plants in Kuwait (such as *Senecio glaucus*) grew well in areas considered to be weakly to moderately contaminated (i.e., < 10 % by weight of oil). Frick *et al.* [24] also reported that barley was more sensitive than field pea to hydrocarbon content as indicated by reduced root growth with increasing hydrocarbon concentration (i.e., 0.5 %, 2.5 % or 5.5 % w/w); a trend that was not observed with the field pea. The investigators also opined that forage yield, plant height and maturity of plants in the contaminated soil improved in the later stages of the study – when contaminant concentrations may have been reduced. This strongly supports our findings as the plant used in this study was a pea plant.

Conversely, the differences observed in terms of shoot length in *L. purpureus* were more pronounced in plant grown in 10 % SEO (Table 3). The plants were shorter than in all other treatments. Stunted growth was observed since the early stage of the experiment and the plants later died. The same pattern of variation was observed in the remaining parameters evaluated. The inability of the plant to grow at such concentration of the pollutant may be as a result of toxic effect beyond which the plant could tolerate. This is in accordance with the findings of Rogers *et al.* [25] that growth of white clover, tilesy sage, Bering hair grass, and alpine bluegrass was enhanced by exposure to a low concentration (1000 mg kg^{-1}) of a mixture of organic chemicals and was severely limited by exposure to higher concentrations of the same mixture.

The number of leaves on the plants varied with increasing hydrocarbon contamination (Tables 2 and 3). Lower number of leaves was generally observed in higher concentration of (5 and 10) %. No significant difference ($P \leq 0.05$) was observed in the number of leaves in plants grown in 2.5 % oil contamination and control soil. Similarly, leaf length and number of flowers slightly differed although without statistical significance ($P \leq 0.05$). No yellowing or chlorosis of leaves was observed during the experiment except for *L. purpureus* at 10 % SEO concentration. This might enable us suggest that plants could carry out phytoremediation by other means like rhizodegradation but not phytovolatilization as was observed by Stephene and Ijah [4] in a similar study using *Glycine max* and *Sida acuta*. The one observed (*L. purpureus* at 10 % SEO concentration), however, may be as a result of toxicity due to higher concentration of spent engine oil. However, statistical analysis showed no significant difference ($P \leq 0.05$) between *C. cajan* and *L. purpureus* in terms of shoot length, number of leaves, leaf length and number of flowers after three months except for *L. purpureus* at 10 % SEO.

Higher microbial counts were generally observed in rhizosphere soil of both contaminated and uncontaminated soils (Tables 4 and 5). This is clearly shown by the positive rhizosphere effects (≥ 1) observed in the soils. For example, microbial counts of *C. cajan* rhizosphere were about 1.2 to 6 times greater than the non rhizosphere soil. Similarly, the microbial counts were much more pronounced in uncontaminated than contaminated sites (Table 4). This contradicts the findings of Narino *et al.* [26] who reported positive rhizosphere effects of maize and oat on microorganisms of contaminated soil in comparison with uncontaminated planted soil. Similar pattern was also observed in the rhizosphere of *L. purpureus* especially for fungi counts and oil utilizers. The rhizosphere effects of total and oil utilizing fungi in the contaminated sites were 6.0 and 3.8 respectively (Table 5). These values are higher than those obtained in the contaminated non rhizosphere soil. This may be due to the inability of some of the fungi species to withstand the toxicity of the hydrocarbon contaminants and as a result, they were eliminated from the environment. It was also observed that in most cases, the total counts of heterotrophic bacteria and fungi were higher than the oil utilizers. The work of Ikhajiagbe and Anoliefo [27] supports findings of the present study.

5. Conclusion

Conclusively, results this study showed that the leguminous plants involved could perform effectively in spent engine oil contaminated soil especially below 10 % contamination level. The ability of the plants to grow up to flowering stage was a clear indication that both could be cultivated in farm lands damaged by low levels of hydrocarbons. Enhancement of microbial population by the plants was an important attribute that could encourage their use in large scale phytoremediation processes. Hence *C. cajan* and *L. purpureus* have good potentials for phytoremediation of spent engine oil impacted soil.

References

[1] Udom BE, Nuga BO. Characterization of soil health using microbial community and maize germination as bioindicators in oil-contaminated Soil. *Journal of Advances in Developmental Research* 2011; 2(2):191-197.

[2] Philips AL. *The Relationship Between Plants and their Root-associated Microbial Communities in Hydrocarbon Phytoremediation Systems*. Saskatoon: University of Saskatchewan; 2008. 144 p.

[3] Diab E. Phytoremediation of oil contaminated desert soil using the rhizosphere effects. *Global Journal of Environmental Research* 2008; 2 (2): 66-73.

[4] Stephen E, Ijah UJJ. Comparison of glycine max and sida acuta in the phytoremediation of waste lubricating oil polluted soil. *Nature and Science* 2011; 9(8):190-193.

[5] Gunther T, Dornberger U, Fritsche W. Effects of ryegrasss on biodegradation of hydrocarbons in soil. *Chemosphere* 1996; 33:203-215.

[6] Aprill W, Sims RC. Evaluation of the use of prairie grasses for stimulating polycyclic aromatic hydrocarbon treatment in soil. *Chemosphere* 1990; 20:253-265.

[7] Van der Maesen LJG. Pigeonpea: origin, history, evolution, and taxonomy. In: Nene YL, Hill SH, Sheila VK, editors. *The Pigeon Pea.* Wellingford, UK: CAB International; 1990. p. 15-46.

[8] Cameron AG. *Lab Agnote No. C38*. New York: Lab Agnote; 2003. 77 p.

[9] Bodner G, Loiskandl W, Kaul HP. Cover crop evapotranspiration under semi-arid conditions using FAO dual crop coefficient method with water stress compensation. *Agricultural Water Management* 2007; 6(3):23-51.

[10] ILRI. *Lablab for livestock feed on small-scale farms*. Addis Ababa: International Livestock Research Institute; 2010. 44 p.

[11] Odeny DA. The potential of Pigeonpea (Cajanus cajan (L.) Millsp.) in Africa. *Natural Resources Forum* 2007;31:297–305.

[12] Troedson RJ, Wallis ES, Singh L. Pigeon pea: adaptation. In: Nene Y, Hall SD, Sheila VK, editors. *The Pigeon pea*. Wallingford: CAB International; 1990. p. 159-177.

[13] Akpovuta OV, Egharvba F, Medjor O. W, Osaro KI, Enyemike ED. Microbial degradation and its kinetics on crude oil polluted soil. *Research Journal of Chemical Sciences* 2011;1(16):8-14.

[14] Mullen CL, Holland JF, Heuke L. Cowpea, *Lablab and Pigeon Pea*. Paris: AGFACT; 2003. p. 421.

[15] Verma SK, Verma M. *A Text Book of Plant Physiology*. New Delhi: S. Chanda and Company; 1995. 176 p.

[16] Taiz L, and Zeiger E. *Plant Physiology*. Sunderland: MA; 2002. 57 p.

[17] Nasir M. *Production of Lablab in Nigeria.* Zaria: National Agricultural Extension and Research Liaison Services; 2001. 98 p.

[18] Ismail HY, Ijah UJJ, Riskuwa ML, Ibrahim AA. Biodegradation of spent engine oil by bacteria isolated from the rhizosphere of legumes grown in contaminated soil. *International Journal of Environment* 2014;l3 (2):85-97.

[19] Udeani TK, Obroh CAA, Okwuosa, CN, Achukwu, PU, Azubike, N. Isolation of bacteria from mechanic workshops' soil environment contaminated with used engine oil. *African Journal of Biotechnology* 2009;8(22): 6301-6303.

[20] Kathi S, Khan AB. Toxicity of spent oil contaminants on dolichos lablab l. and abelmoschus esculentus l. *The Ecoscan* 2011;4(1):133-136.

[21] Anoliofo GO, Vwioko DE. Effects of spent lubricating oil on the growth of capsicum annum and lycopersicon esculentum. *Pollution* 1995;88:361-314.

[22] Agbogidi OM. Response of six cultivars of cowpea (vigna unguiculata(L.) walp) to spent engine oil. *African Journal of Food Science and Technology* 2010;1(6):139-142.

[23] Radwan S, Sorkhoh N, El-Nemr I. Oil Biodegradation around roots. *Nature.* 1995;376:302.

[24] Frick CM, Farrell RE, Germida JJ. *Assessment of phytoremediation as an in-situ technique for cleaning oil-contaminated sites.* Calgary: Petroleum Technology Alliance; 1999. 133 p.

[25] Rogers HB, Beyrouty CA, Nichols TD, Wolf DC, Reynolds CM. Selection of cold-tolerant plants for growth in soils contaminated with organics. *Journal of Soil Contamination* 1996;5(2):171-186.

[26] Norino E, Norino O, Zaripore S, Breus IP. *Influrence of Cerial Plant on Microorganism of Leached Chernozem Polluted by Hydrocarbons*. Orlando: Bioremediation Association; 2004. 162 p.

[27] Ikhajiagbe B, Anoliefo GO. Substrate bioaugmentation of waste engine oil polluted soil. *Research Journal of Environmental and Earth Sciences* 2012;4(1):60-67.

European Journal of Environmental and Safety Sciences 2014 2(2): 65-70
ISSN 1339-472X European Science and Research Institute (Original Research Paper)

The synergistic approach of plants and rhizobacteria in crude oil contaminated soil remediation

K. M. Ukaegbu-Obi[a] · C. C. Mbakwem-Aniebo[b]

[a]*Department of Microbiology, College of Natural Sciences, Michael Okpara University of Agriculture, Umudike, P.M.B 7267, Abia State, Nigeria*
[b]*Department Department of Microbiology, Faculty of Science, University of Port Harcourt, Choba, Rivers State, Nigeria*

ABSTRACT

The synergistic approach of plants and rhizobacteria in crude oil contaminated soil in three different locations were carried out. The presence of heterotrophic bacteria and hydrocarbon-utilizing bacteria isolated from the polluted and pristine rhizosphere and non-rhizosphere soils of the plants were compared. The polluted rhizosphere of total culturable heterotrophic bacterial count gave a range of (0.98×10^6 to 1.37×10^6) cfu g^{-1}. The pristine rhizosphere count ranged from (4.11×10^5 cfu g^{-1} to 7.55×10^5) cfu g^{-1}. The polluted non-rhizosphere gave ranged from (2.39×10^5 to 3.28×10^5) cfu g^{-1}. The pristine non-rhizosphere had a range of (2.90×10^5 to 3.97×10^5) cfu g^{-1}. The polluted rhizosphere counts for hydrocarbon-utilizing bacteria ranged from (1.60×10^5 to 6.91×10^5) cfu g^{-1}. The pristine rhizosphere gave a range of (1.85×10^5 to 3.38×10^5) cfu g^{-1}. In the polluted non-rhizosphere, the range was from (1.02×10^5 to 1.42×10^5) cfu g^{-1}. A range of (6.05×10^4 to 9.75×10^4) cfu g^{-1} was obtained from the pristine non-rhizosphere. There was no significant difference ($P > 0.05$) between the rhizosphere and non-rhizosphere of total heterotrophic and hydrocarbon-utilizing bacterial counts in both polluted and pristine soils. All the plants exhibited positive rhizosphere effects on the rhizobacteria. Hydrocarbon-utilizers were identified as *Acinetobacter, Arthrobacter, Alcaligenes, Bacillus, Corynebacterium, Flavobacterium, Micrococcus, Serratia and Pseudomonas* spp. All the isolates grew on petroleum hydrocarbon at different growth rates. Based on these results, the organisms isolated can serve as seeds for bioaugmentation during remediation of crude oil polluted soil environment. The plants may be employed in rhizoremediation of oil polluted soil.

Keywords: Plants • Synergistic approach • Crude oil • Phytoremediation • Soil • Rhizoremediation

1. Introduction

The usage of petroleum hydrocarbon products has increased soil contamination. This is one of the major environmental problems in Nigeria and globally. Research efforts have been devoted to develop new, low-cost, low-technology, eco-friendly treatments capable of reducing and even eliminating pollution in the atmosphere, the hydrosphere and soil environments [1]. To investigate the countermeasure to remediate soils contaminated with oils, bioremediation provide such an effective and efficient strategy to speed up the clean-up processes.

Bioremediation of contaminated soil is low cost, causes less interference with the soil structure and has a higher public acceptance than other approaches including soil thermal desorption and soil leaching treatment [2].

Remediation of soils containing organic pollutants can be enhanced by plants by various processes [3]. *In-situ* phytoremediation strategy exploits natural or genetically engineered plant species to accumulate toxic substances (heavy metals, radioactive compounds, organic pollutants) directly from the soil [4]. Partial or complete degradation of organic substances have been demonstrated in some cases [5]. The use of plants to extract, sequester or detoxify pollutants is therefore known as phytoremediation [6]. Plants frequently do not possess complete metabolic degradation pathway for pollutants, and even more toxic by-products may be produced.

Most plants have symbiotic relationships with soil microorganisms. For example, root nodule bacteria that have

K. M. Ukaegbu-Obi (corresponding author)
Department of Microbiology, College of Natural Sciences, Michael Okpara University of Agriculture
Umudike, P.M.B 7267, Abia State, Nigeria
e-mail: kelechi.ukaegbuobi@yahoo.com

symbiotic relationships with legumes are involved in Nitrogen fixation. The area around plant roots, known as the rhizosphere contains higher populations, greater diversities and activities of microorganisms than soil with no plants [7].

This synergistic approach of using plants and their rhizobacteria in remediation of oil polluted soil is known as rhizoremediation [8]. Application of the synergistic action of plants and their rhizobacteria in crude oil contaminated soil remediation have been demonstrated as an appropriate and more practical alternative to clean-up of petroleum hydrocarbon in the contaminated environments.

A plant can be considered to be a solar-driven biological pump and treatment system, attracting water with its root system, accumulating water-soluble pollutant in the rhizosphere and concluding with the degradation or translocation of pollutants [9]. In some cases, rhizosphere microbes are even the main contributors to the degradation process. Plants release exudates into the soil ecosystem that increases the microbial activity and aid the degradation of xenobiobiotic substances. The soluble root exudates include enzymes, amino acids, sugars and low molecular weight carbohydrates [10].

The objective of this study therefore was to isolate rhizosphere-inhabiting indigenous oil-degrading bacteria in plants growing in crude oil-polluted areas.

2. Material and methods

2.1. Study area

Polluted rhizosphere and non-rhizosphere soil samples were collected from the three different crude oil polluted sites in Imo and Rivers States, Nigeria. These sites could be described as recovering ecosystems with few plants growing at these locations. Unpolluted rhizosphere and non-rhizosphere soil samples were collected from the same areas where there has been no known crude oil pollution which served as the control.

2.2. Collection of soil samples

Plants of the same species were collected from the crude oil polluted and unpolluted sites in separately in marked sterile plastic bags. The plants were pulled out slowly to avoid breaking their roots. Non-rhizosphere (bulk) soil samples of crude oil polluted and unpolluted sites were collected at a distance of thirty centimeters (30 cm) from the plants' roots as described by Ukaegbu-Obi and Mbakwem-Aniebo [11] in marked sterile plastic bags and transported in an ice chest to the laboratory for analyses. The plants were taken to a Plant taxonomist for identification.

2.3. Bacterial counts and isolation

The total culturable heterotrophic bacterial (TCHB) count was determined using the spread plate method on nutrient agar (Oxoid) according to Chikere et al. [12]. Soil suspensions were prepared by 10 fold serial dilutions with 1 g of soil and then 10-3 to 10-6 dilutions were spread on the plates in duplicates. The colony forming units of heterotrophs were counted after incubation at 28 °C for 18 h. Hydrocarbon utilizing bacteria (HUB) were enumerated as adopted from Hamamura et al. [13] using mineral salts medium with crude oil supplied by the vapour phase transfer. Isolated colonies were further purified by subculturing and identified using biochemical tests and microscopy.

2.4. Identification of bacterial isolates

The bacterial isolates were examined for colonial morphology, cell micro-morphology and biochemical characteristics. Tests employed included: Gram staining, Motility test, Catalase test, Citrate Utilization test, Indole test, Hydrogen Sulphide Production test, Methyl Red-Voges Proskauer test, Oxidase test, Sugar Fermentation test. Confirmatory identities of the bacteria were made using the *Bergey's Manual of Determinative Bacteriology* [14].

2.5. Screen test for hydrocarbon-utilization by bacterial isolates

The bacterial isolates were tested for their ability to utilize crude oil using the turbidity method as described by Ukaegbu-Obi and Mbakwem-Aniebo [11]. The bacterial isolates were cultured in nutrient broth and incubated at 28 + 2 ^{0}C for 24 hours. Aliquot (0.1 ml) of the young culture in nutrient broth grown was inoculated into each test tube containing 9.9 ml of sterile mineral salt broth and 0.1 ml of crude oil. A control test tube containing 9.9 ml of sterile mineral salt broth plus 0.1 ml of crude oil remained uninoculated. The tubes were incubated at room temperature for 7 days. The growth of the inocula was determined by visual observation of the mineral salt broth turbidity, as compared with the uninoculated control tube.

2.6. Statistical analysis

The statistical tools – One-way Analysis of Variance (ANOVA) was used to analyze the data obtained from the plants while Independent Student's t-test was used to analyze the polluted and unpolluted soil sample of each plant.

3. Results and discussion

Plant-assisted bioremediation (rhizoremediation) stands out as a potential tool to inactivate or completely remove xenobiotics from the polluted environment. Therefore, it is of key importance to find an adequate combination of plant species and microorganisms that together enhance the clean-up process.

Field trials have shown that remediation of petroleum contaminated sites can be enhanced by cultivation of plants. To date, a great variety of grasses, legumes and fast growing trees with high transpiration rates such as poplars, alder or willow have been applied for phytoremediation. These plants provide large surface area for root soil contact due to their expansive root system. Roots also provide ideal attachment sites for microbes and food supply/exudates consisting of amino acid, organic acids, sugars, enzymes and complex carbohydrate [15].

The results of the enumeration of the total culturable heterotrophic bacterial counts of the polluted and pristine rhizosphere and bulk soil are shown in Fig. 1-6. The total culturable heterotrophic bacteria counts for polluted rhizosphere ranged from (0.98×10^6 to 1.37×10^6) cfu g^{-1}; the pristine rhizosphere (control), ranged from (4.20×10^5 to 7.55×10^5) cfu g^{-1}; the polluted non-rhizosphere, ranged from (2.56×10^5 to 3.12×10^5) cfu g^{-1} while the pristine non-rhizosphere, ranged from (3.10×10^5 to 4.12×10^5) cfu g^{-1}.

The polluted rhizosphere counts for hydrocarbon-utilizing bacteria ranged from (1.60×10^5 to 6.91×10^5) cfu g^{-1}. The pristine rhizosphere gave a range of (1.85×10^5 to 3.38×10^5) cfu g^{-1}. In the polluted non-rhizosphere, the range was from (1.02×10^5 to 1.42×10^5) cfu g^{-1}. A range of (6.05×10^4 to 9.75×10^4) cfu g^{-1} was obtained for pristine non-rhizosphere.

The bacterial counts of polluted and pristine rhizosphere and non- rhizosphere of different locations are shown in Fig. 1-6. It was observed that the total heterotrophic bacterial counts were higher in the polluted rhizosphere than in the polluted non-rhizosphere of all the plants. This was the same for hydrocarbon-utilizing bacteria; the counts were also higher in the polluted rhizosphere than the polluted non-rhizosphere. Lynch [16] stated that on a per gram basis, rhizosphere soil has 10–100 times more microbes than unvegetated soil. This expresses the rhizosphere effect of the plants on the bacteria.

The low counts of heterotrophic bacteria (Fig. 1, 3 and 5) recorded in this study for most crude oil-contaminated soils compared to that of pristine soils agreed with the previous reports by Umanu *et al.* [17] and Ukaegbu-Obi and Mbakwem-Aniebo, [11] which could be attributed to the toxic effect of petroleum-pollution. Microbial community structure has been recommended as a biological indicator of heavy metal stress.

Unlike the result of total culturable heterotrophic count, in the non-rhizosphere soil, the mean counts of the hydrocarbon-utilizing bacteria were higher in the contaminated non-rhizosphere soil for all the plants (Fig. 2, 4 and 6). This finding was also reported by Leahy and Colwell [18] and Ukaegbu-Obi and Mbakwem-Aniebo [11] who observed that hydrocarbon-utilizing bacteria and fungi were readily isolated from soil and also that the application of oil or oily waste to soil resulted in increased numbers of hydrocarbon-utilizing bacteria and fungi. This phenomenon of selective enrichment causes the numbers of microorganisms that can utilize the compound of interest to increase within the community [18]. The addition of crude oil results in an immediate change in bacterial community structure, increasing abundance of hydrocarbon– degrading microorganisms and a rapid rate of oil degradation, which suggests the presence of a pre-adapted oil-degrading microbial community and sufficient supply of nutrients [13].

The rhizosphere (both polluted and pristine) had higher frequencies of occurrence of bacterial isolates than the non-rhizosphere. This result may indicate the fact that vegetation influences some specific degradative groups of bacteria already present in the polluted sites than the total microbial diversity. Juhason *et al.* [19] reported that in their field experiment phytoremediation increased the number of phenol-degrading bacteria in semi-coke (processed oil shale solid wastes) as well as metabolic diversity of microbial community. Exudates derived from plants can help to stimulate the survival and action of bacteria, which subsequently results in more efficient degradation of pollutants [8].

The bacterial isolates obtained from different rhizosphere and non-rhizosphere of polluted and pristine soils in this study were identified to be of the following genera: *Acinetobacter, Alcaligenes, Arthrobacter, Bacillus, Corynebacterium, Flavobacterium, Micrococcus and Pseudomonas* and *Serratia*. This agrees with the findings of [15] who reported that a broad phylogenetic range of bacteria including species/strains of *Achromobacter, Acidovorax, Alcaligenes, Arthrobacter, Bacillus, Corynebacterium, Flavobacterium, Micrococcus, Mycobacterium, Norcadia, Pseudomonas, Rhodococcus, Sphinogomonas* and *Xanthomonas* have been identified in the breakdown of hydrocarbons.

The bacterial isolates utilized crude oil at different rates with *Pseudomonas* sp. having the highest growth rate followed by *Bacillus* sp., *Acinetobacter* sp., *Alcaligenes* sp., *Micrococcus* sp., and *Corynebacterium* sp., that had moderate growth rate and *Arthrobacter sp., Flavobacterium sp., Micrococcus* sp., *Serratia sp.* having scanty growth rates (Table 1). Some isolates may withstand toxic components

of the oil and thrive, others may be inhibited. Other investigators [20] have made similar observations. The result also showed that some bacteria isolated from uncontaminated sites had the potential to utilize crude oil but these potentials were not as high as their counterparts isolated from contaminated sites.

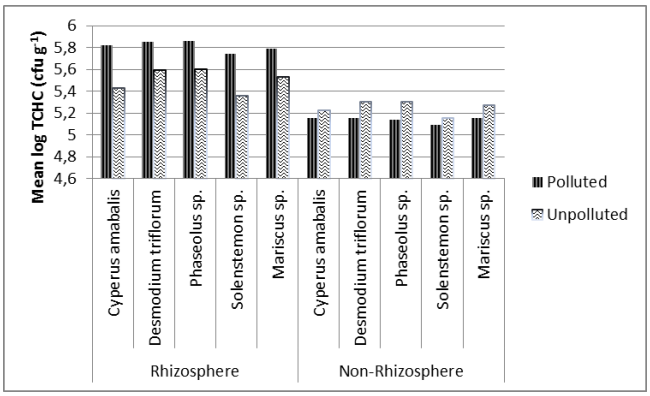

Figure 1 Total heterotrophic bacterial counts (TCHC) of polluted and pristine rhizosphere and non-rhizosphere soils at location 1

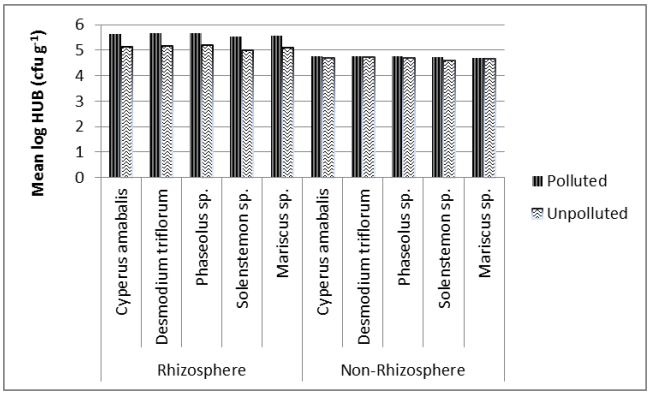

Figure 2 Hydrocarbon utilizing bacterial (HUB) counts of polluted and pristine rhizosphere and non-rhizosphere soils at location 1

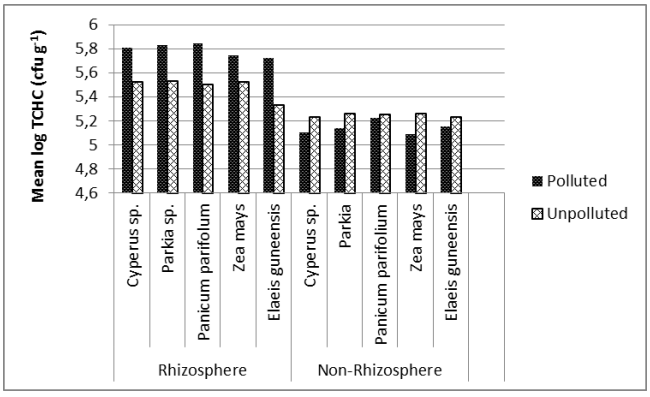

Figure 3 Total heterotrophic bacterial counts (TCHC) of polluted and pristine rhizosphere and non-rhizosphere soils at location 2

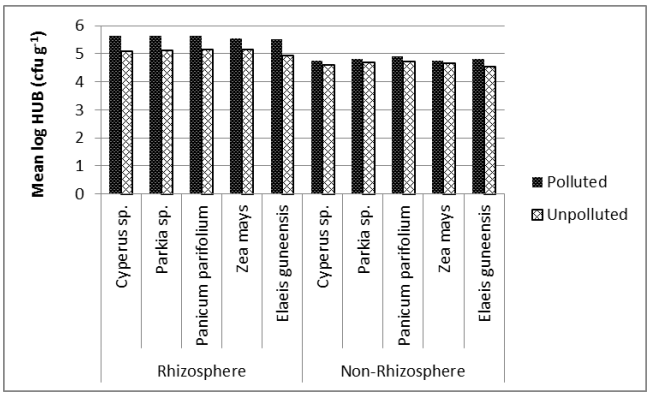

Figure 4 Hydrocarbon utilizing bacterial (HUB) counts of polluted and pristine rhizosphere and non-rhizosphere soils at location 2

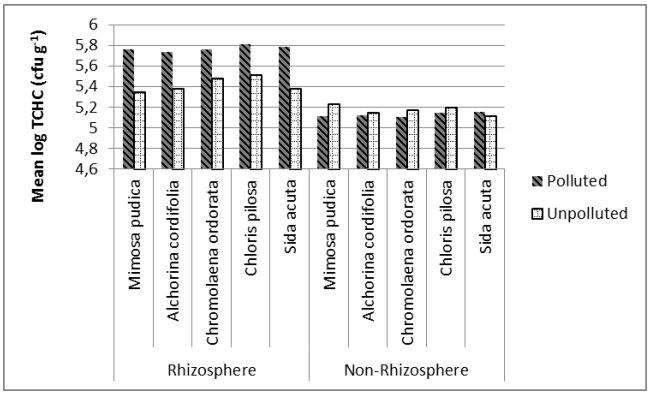

Figure 5 Total heterotrophic bacterial counts (TCHC) of polluted and pristine rhizosphere and non-rhizosphere soils at location 3

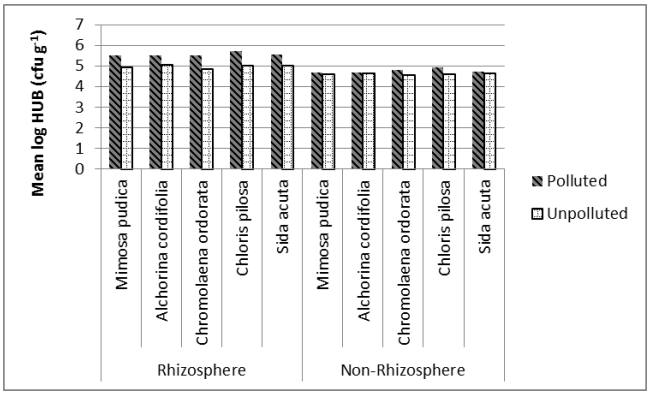

Figure 6 Hydrocarbon utilizing bacterial (HUB) counts of polluted and pristine rhizosphere and non-rhizosphere soils at location 3

Table 1 Screen test for the utilization of petroleum hydrocarbon by the bacterial isolates

Isolate code	Growth in crude oil medium	Bacterial isolate
PRO 1A	++	*Arthrobacter* sp.
PSO 2B	++	*Corynebacterium* sp.
PSO 3A	++	*Alcaligenes* sp.
PRO 5A	++	*Acinetobacter* sp.
NSO 1B	++	*Pseudomonas* sp.
NSO 2A	+	*Flavobacterium* sp.
NRO 3A	+	*Arthrobacter* sp.
NRO 3A	+	*Serratia* sp.
NRO 4B	++	*Pseudomonas* sp.
NRO 5B	+	*Corynebacterium* sp.
PRU 1A	++	*Flavobacterium* sp.
PSU 2B	++	*Micrococcus* sp.
PRU 3A	++	*Alcaligenes* sp.
PSU 3A	++	*Bacillus* sp.
PRU 3B	+++	*Pseudomonas* sp.
PRU 1B	+	*Arthrobacter* sp.
NSU 4B	+	*Arthrobacter* sp.
NRU 5B	++	*Acinetobacter* sp.
PSA 1A	++	*Bacillus* sp.
PRA 4B	++	*Bacillus* sp.
PRA 5A	+++	*Pseudomonas* sp.
NSA 3A	+	*Acinetobacter* sp.
NRA 2B	+	*Micrococcus* sp.

Note: +++ denote highest growth rate, ++ denote moderate growth rate and + denote scanty growth rate.

4. Conclusion

The use of plants for rehabilitation of crude oil contaminated environments is an emerging area of interest because it provides an ecologically sound and safe method for restoration and remediation. A clever solution is to combine the advantages of microbe-plant symbiosis within the plant rhizosphere into an effective cleanup technology as this may be a promising strategy to remediate more contaminated sites.

References

[1] Rao MA, Scelza R, Scotti R, Gianfreda L. Role of enzymes in the remediation of polluted environments. *J Soil Sci Plant Nutr* 2010;10(3):333-353.

[2] Tang JC, Wang RG, Niu XW, Wang M, Chu HR, Zhou QX. Characterisation of the rhizoremediation of petroleum-contaminated soil: effect of different influencing factors. *Biogeosciences* 2010;7:3961-3969.

[3] Cunningham SD, Anderson TA,Schwab V, Hsu FC. Phytoremediation of soils contaminated with organic pollutants. *Adv Agron* 1996;56:55-114.

[4] Zhou Q, Cai Z, Zhang Z, Liu W. Ecological remediation of hydrocarbon contaminated soils with weed plant. *J Resour Ecol* 2011;2(2):97-105.

[5] White P. Phytoremediation assisted by microorganisms. *Trends Plant Sci* 2001;6:502-512.
[6] Gurska J, Wang WX, Gerhardt KE, Khalid AM, Isherwood DM, Huang XD, Glick BR, Greenberg BM. Three year field test of a plant growth promoting rhizobacteria enhanced phytoremediation system at a land farm for treatment of hydrocarbon waste. *Environ Sci Technol* 2009;43(12):4472-4479.
[7] Nicholas TD,Wolf DC, Rogers HB, Beyrouty CA, Reynolds CM. Rhizosphere microbial population in contaminated soil. *Water Air Soil Pollut* 1997;95:165-178.
[8] Kuiper IEL, Lagendijk GV, Bloemberg BJ. Lugtenberg J. Rhizoremediation: a beneficial plant-microbe interaction. *Mol Plant-Microbe Interact* 2004;17(1):6-15.
[9] Liste HH, Alexander M. Plant promoted pyrene degradation in Soil. *Chemosphere* 2000;40:7-10.
[10] Burken JG. Schnoor JDL. Phytoremedation: plant uptake of atrazine and role of root exudates. *J Environ Eng* 1996;122:958-963.
[11] Ukaegbu-Obi KM, Mbakwem-Aniebo CC. Bioremediation potentials of bacteria isolated from rhizosphere of some plants of oil contaminated soil of Niger Delta. *J Appl Environ Microbiology* 2014;2(4):194-197.
[12] Chikere CB, Okpokwasili GC, Chikere BO. Bacterial diversity in a tropical crude oil-polluted soil undergoing bioremediation. *African J Biotech*. 2009;8(11);2535-2540.
[13] Hamamura N, Olson SH, Ward DM, Inskeep WP. Microbial population dynamics associated with crude-oil biodegradation in diverse soils. *J Appl Environ Microbiology* 2008;72:6316-6324.
[14] Holt JG. *Bergey's Manual of Determinative Bacteriology*. Baltimore: Williams and Wilkins Pub; 1994. 787 p.
[15] Tesar M, Reichenauer TG, Sessitsch A. Bacterial rhizosphere populations of blank poplar and herbal plants to be used for phytoremediation. *J Soil Biol Biochem* 2002;34:1883-1892.
[16] Lynch JM. The Rhizosphere. New York: Wiley; 1990. 324 p.
[17] Umanu G, Akpe AR, Omoikhudu AR. Oil degradation assessment of bacteria isolated from used motor oil contaminated soils in Ota, Nigeria. *Int J Adv Biol Res* 2013;3(4): 506-513.
[18] Leahy JG, Colwell RR. Microbial degradation of hydrocarbons in the environment. *Microbial Rev* 1990;54: 305-315.
[19] Juhanson J, Truu J, Heinaru E, Heinaru A. Temporal dynamics of microbial community in soil during phytoremediation field experiment. *J Env Eng Lands Manag* 2007;15(4): 213-220.
[20] Ibrahim MLU, Ijah JJ, Manga SB, Rabah AB. Occurrence of hydrocarbon utilizing bacteria in the rhizosphere of eucalyptus camaldulensis, lablab purpureus and moringa oleifera. *Int J Pure Appl Sci* 2008;2(3):21-26.

European Journal of Environmental and Safety Sciences 2014 2(2): 71-78
ISSN 1339-472X European Science and Research Institute (Original Research Paper)

Research and analysis of noise emitted by vehicles according to the type of surface roads and driving speed

Marek Rybakowski[a] · Grzegorz Dudarski[a] · Edward Kowal[a]

[a]*University of Zielona Góra, Faculty of Mechanical Engineering, Institute of Safety Engineering and Work Sciences, prof. Z. Szafrana 4, 65-516 Zielona Góra, Poland*

ABSTRACT

This study deals with examine and assess the noise emitted by the vehicles, depending on the type of road surface and driving speed. Studies have shown that the noise reduction can be achieved by the reduction of the speed of movement of vehicles. The changes to the noise level emitted by passenger car, a commercial vehicle and a truck were also measured. The results give an answer to the question of whether the type of road surface has a significant impact on the noise level of a moving car or it is rather caused by other factors related to the movement of the car at a certain speed. Noise measurements were carried out using a controlled pass-by method (CPB). The results of measurement show significant influence of the type of road surface and driving speed on the noise level.

Keywords: Survey • Noise • Motor vehicles • Road surface • Work and life safety

1. Introduction

Traffic noise is today one of the most common hazards of life and work of humans. It is a social problem for many people and their environment. It is a source of discomfort and stress at work [1], after work and during leisure time. Exposure to traffic noise in cities is so common that it is difficult to find a place and time in which we would be outside the emissions of that type of noise.

In the vast majority of vehicles, we can distinguish the following sources of noise: engine, powertrain, tires cooperating with the road surface, the aerodynamic phenomena while driving, the flow of liquids and gases in systems and installations of the vehicle, vibration of other components of the vehicle [2-4]. It is estimated that the most intense source of noise and vibration is not a motor but the cooperation of the wheels with the road surface and the airflow around the vehicle. There are many sources of noise in vehicles and their elimination is quite effective in the design phase of the vehicle. Unfortunately, neither the vehicle manufacturer nor its user has the influence on the type and quality of the road surface.

With the increase in traffic volume there is a problem with noise emission while cars ride on old road surfaces of stone paving. These types of surfaces, often in a very good condition can be found in both urban and rural areas. These are usually historic sections of the road surface that, due to its historical value are not exchanged for less noisy ones.

The aim of this study is to evaluate the noise emitted by motor vehicles, depending on the type of road surface and driving speed. The results give an answer if the type of road surface has a significant impact on the volume of a moving car or rather it is caused by other factors that are directly related to the movement of the car at a given speed.

One way to eliminate traffic noise is to reduce the speed of traffic. This method is mainly used in urban areas, where other methods of reducing the noise propagation are not feasible.

Two questions were the aims of the study. The question of what effects of noise reduction will be achieved by reducing the speed of movement of vehicles and by how much will the noise level change if it is emitted by the passenger car, van and truck depending on the type of road surface.

2. Material and methods

To evaluate the noise conditions, the application has three methods of measurement. The first is the CPX method (called Close Proximity Method), also known as the method

Marek Rybakowski (corresponding author)
University of Zielona Góra, Faculty of Mechanical Engineering, Institute of Safety Engineering and Work Sciences, prof. Z. Szafrana 4, 65-516 Zielona Góra, Poland, e-mail: mrybakow@uz.zgora.pl

of attachment that takes into account only the noise of rolling tires [5]. Other sound sources of moving vehicle are ignored in this method. All other noise sources are taken into account in SPB method (called Statistical Pass-By Method), in Poland called statistical method of travel or the method of road traffic [6]. Both methods are standardized and widely used around the world. The third is a method of the controlled passage CPB (called Controlled Pass-By method) [7].

The studies used the CPB method, which is called controlled pass-by passage in Poland. It measures the level of sound coming from the tested vehicle that is travelling, fitted with tires of known characteristics. The noise measurement is carried out using a microphone placed on the side of the road at a distance of 7.5 m from the middle of the traffic lane where vehicles are driving. The microphone is mounted on a stand at a height of 1.2 m in relation to a level road surface.

Measurements were performed on selected sections of roads with surfaces:

1. asphalt: bitumen – (Fig. 1);
2. concrete – (Fig. 2);
3. paving stones – (Fig. 3).

For the study, the road sections were selected in such a way that there were no other objects in their environment, which could cause an additional source of noise or screen causing the reflection of the acoustic wave. Weather conditions: air temperature 9 – 10˚C, no wind, no rain, and dry road surface. The air humidity was not measured. In the first part of the examination procedure there was used a car: OPEL Vectra Combi. The study was conducted at two different speeds: 50 and 80 km h^{-1} on each of the surfaces:

- travel at a constant speed (50 km h^{-1} - riding on 4th gear, RPM 1600 r min^{-1}; 80 km h^{-1} – riding in 5th gear, RPM 2000 r min^{-1});
- drive at neutral gear the vehicle was speeded up earlier to provide the required speed on the measurement section). On the measurement section the car was moving at neutral gear with the uniformly retarded motion. It was set by repeated attempts that the speed of the vehicle could be required at the measuring point, when at the beginning of the measuring section it moves at 50 km h^{-1} (at 53 km h^{-1} exactly), while for the 80 km h^{-1} (84 km h^{-1} exactly).

Figure 1 Asphalt - bitumen road

Figure 2 The road of the concrete slabs on the terrain of the old airport

Figure 3 The road of paving stones

Research on the influence driving speed on noise emission was carried out using three types of vehicles: the car OPEL Vectra Combi – a factory vehicle without any modification; van – type 'BUS' by RENAULT MASTER brand – a factory vehicle without any modification; heavy goods vehicle by SCANIA brand without trailers - vehicle factory without any modifications. All vehicles selected for the study were fitted with tyres fitted at the factory and in a good condition. The diagram of a research is shown in Figure 4. Portable sound and vibration analyzer SVAN 912 was used for noise measurements. During the measurements there was made the registration of the time charts of noise with A correction and step buffer 0.125 s. This feature allowed the graphical representation of changes in the level of noise while zooming in and out of the vehicle from the point of measurement. At the same time it was measured the frequency analysis of noise in one-third octave frequency bands with a linear correction.

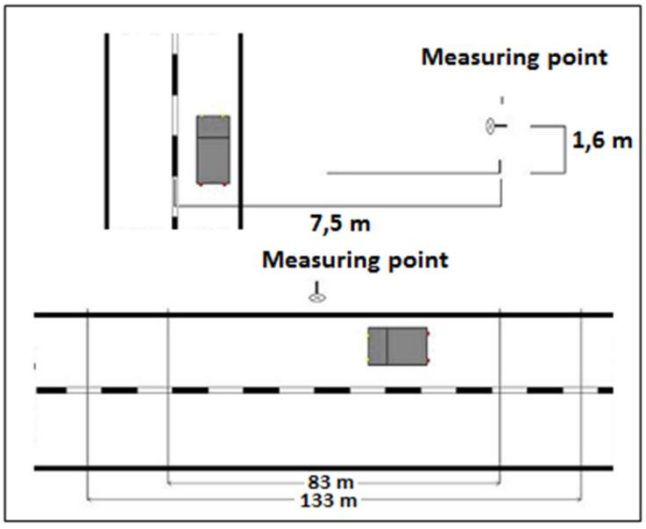

Figure 4 The outline of research

3. Results and discussion

Analysing changes at the level of noise emitted by the vehicle during the passing of the measuring point, there was used the recording of the time course of individual research events. The results of analyzes are shown in Fig. 5 to 8.

The waveforms recorded during the measurement illustrate the variations in noise level at the measuring point. For further analysis there was taken into account the maximum noise level that occurred at the time when the vehicle was passing the measuring point.

The overall level of noise emitted by the vehicle on the tested road surfaces are shown in Table 1.

Noise emitted by the passenger vehicle during the passage was of a low frequency. Changes in the level of noise occurred in the entire frequency band and in particular in the range from 100 Hz to 1600 Hz.

The emission of noise when driving on roads with paving stone is by far the biggest and reaches an average of 82 dB (A) at a speed of 50 km h^{-1} and 90 dB (A) at a speed of 80 km h^{-1} When driving on an asphalt surface it was recorded the lowest level of noise – 75 dB (A) at a speed of 50 km h^{-1} and 82 dB (A) at a speed of 80 km h^{-1}.

Changing speeds (from 50 km h^{-1} to 80 km h^{-1}) causes an increase in the noise level at the measuring point. When driving on an asphalt surface it increases by about 7 dB, while on the surface of the paving stones by about 9 dB. No significant difference was observed in the emission of noise when driving in 4^{th} gear and neutral gear. Changing the engine speed does not have a significant impact on the level of noise.

In the next stage it was measured the influence of speeds of cars, vans and trucks on the noise level. The study was performed on the asphalt surface. The obtained measurement results are presented on Fig. 9 – 11.

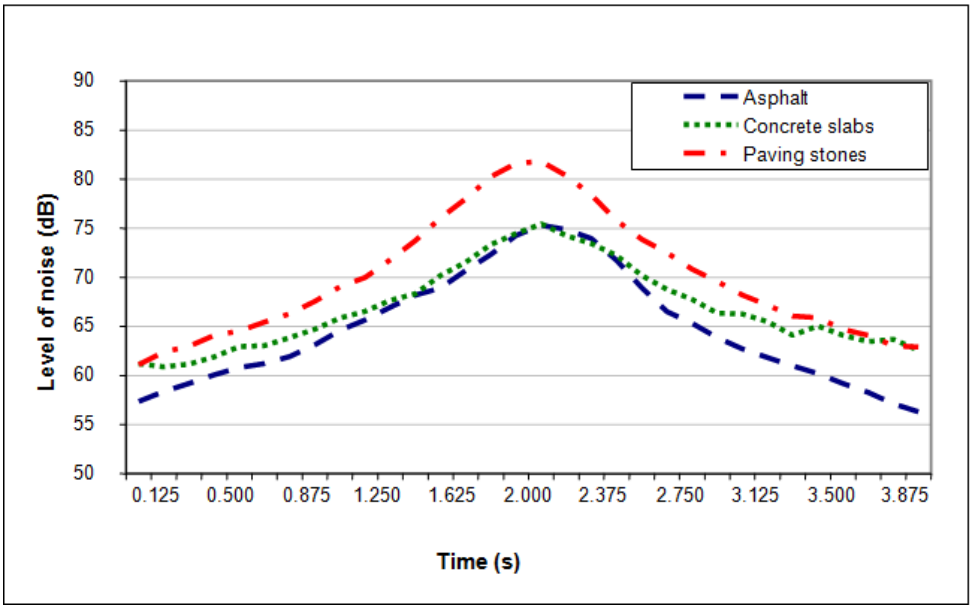

Figure 5 Noise emitted by passenger vehicle at 50 km h^{-1} – riding on 4th gear

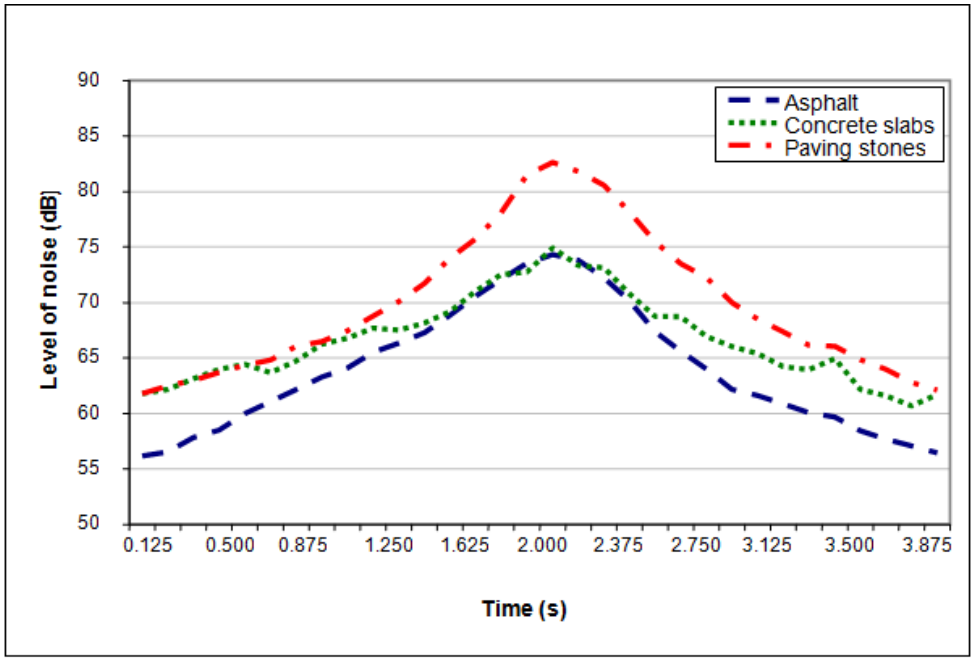

Figure 6 Noise emitted by passenger vehicle at 50 km h^{-1} – riding on neutral gear

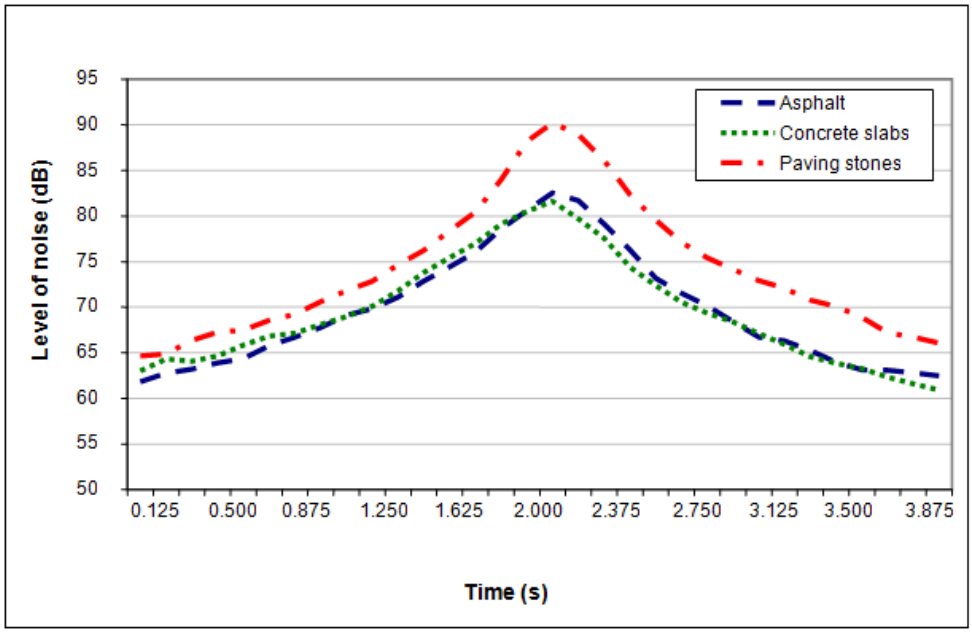

Figure 7 Noise emitted by passenger vehicle at 80 km h^{-1} – riding on 5th gear

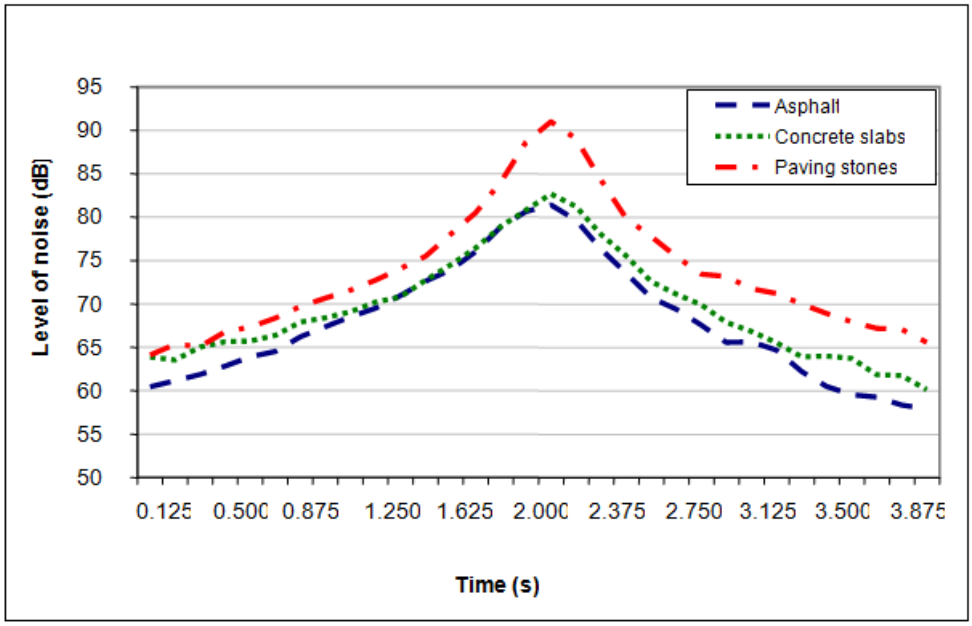

Figure 8 Noise emitted by passenger vehicle at 80 km h^{-1} – riding on neutral gear

Table 1 Noise emitted by the passenger vehicle under investigated conditions

	Noise level L_{max} (dB(A))			
Type of the surface	50 km h^{-1}		80 km h^{-1}	
	Gear	Neutral gear	Gear	Neutral gear
Asphalt	75.3	74.3	82.5	81.4
Concrete	75.4	74.9	81.6	82.7
Paving stone	81.8	82.6	90.2	91.0

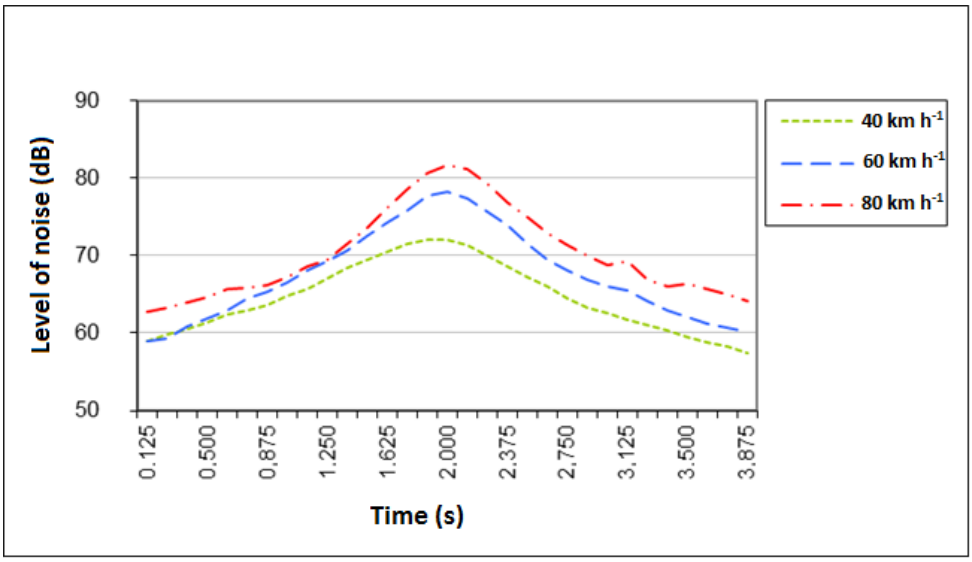

Figure 9 Comparison of noise emitted by passenger vehicle at 3 different speeds (asphalt surface)

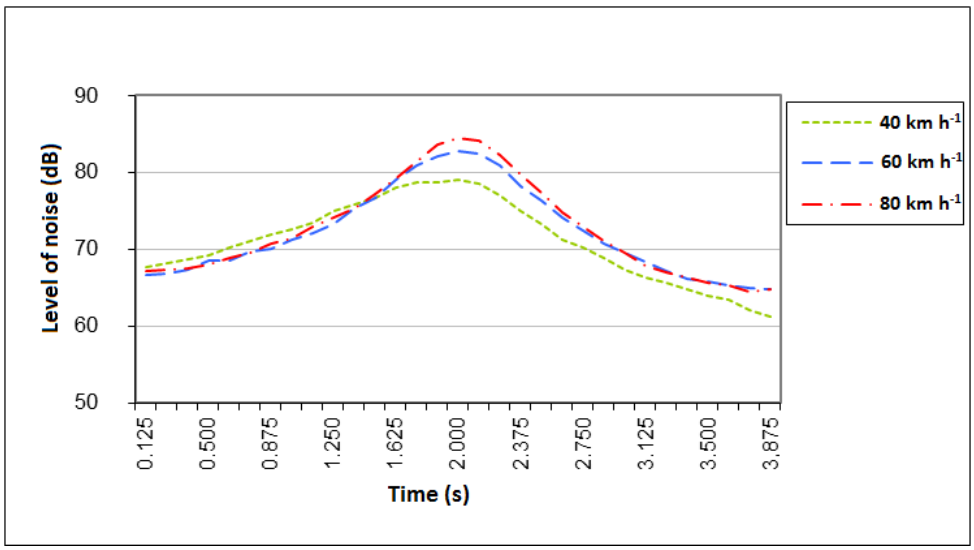

Figure 10 Comparison of noise emitted by the vehicle van at 3 different speeds (asphalt surface)

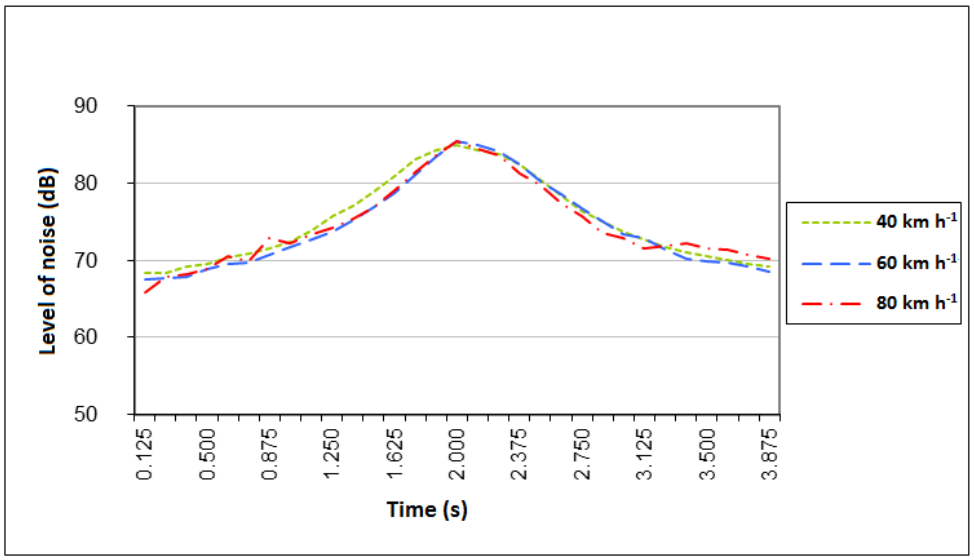

Figure 11 Comparison of noise emitted by heavy goods vehicle at 3 different speeds (asphalt surface)

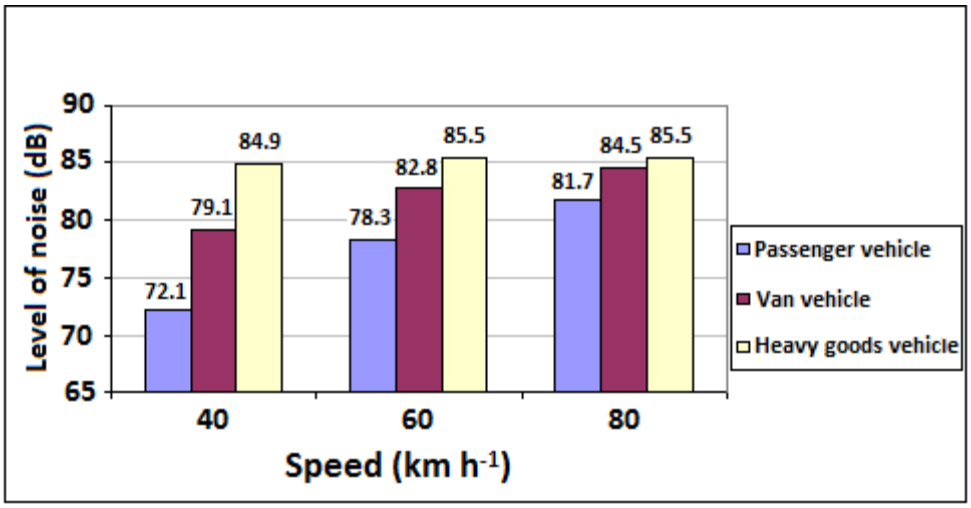

Figure 12 The maximum noise level at 3 speeds, by type of vehicle

The overall level of noise emitted by the tested types of vehicles while driving at different speeds is shown in Fig. 12.

Noise emissions when driving a car increases strongly with increasing speed. At a speed of 40 km h^{-1} is about 72 dB (A), while at 80 km h^{-1} almost 82 dB (A). The noise tests of road vehicles using the method of CPB indicate that limiting the speed of the passenger vehicle from 80 km h^{-1} to 40 km h^{-1} can reduce noise emissions by approximately 10 dB.

Definitely less impact of speed on noise reduction was observed for the type of delivery vehicles and trucks. A speed limit of vehicles in the same speed range reduces the noise level by about 5 dB, while for the truck by about 0.6 dB.

4. Conclusion

The problem of noise emission by moving vehicles on public roads with different types of surfaces in the literature was undertaken on several occasions. It is obvious that the noise levels of vehicles depend largely on the size and construction of vehicles (cars, trucks, special), traffic volume, speed of vehicle, type and characteristics of the road surface with which tires of different types and manufacturers cooperate [8-10].

An important result of the study is data that allow predicting changes in the level of noise emission by motor vehicles in the case of e.g. changing the surface of the paving stone to asphalt - bitumen surface. The applied research method and the results obtained allow assessing whether a change to a quieter road surface will bring the expected results of noise reduction, or whether restrictions should be imposed at the same time speed.

Reducing the speed can always reduce the level of noise emitted by road vehicles. An alternative method is to change the road surface. Such a treatment will increase the speed of movement of vehicles in areas with high traffic without increasing noise.

The results also allow to determine for what type of vehicles, the introduction of speed limits will bring the best results, while maintaining the required bandwidth for a specific (for appointed research) road surface.

References

[1] Kowal E, Rybakowski M, Dudarski G. Subjective assessment of the ergonomics of a professional driver's workstation. *Bezp Pracy Nauka Praktyka* 2013;5:15-18.

[2] Dudarski G, Rybakowski M. Assessment of the driver's safety in road transport in the context of noise hazards. In: Bartlova I, editor. *Occupational Safety and Health. 12th International Conference on Occupational Safety and Health*; 2012 May 16-17; Ostrava, Czech Republic. Ostrava: VSB TU Ostrava; 2012. p. 7-14.

[3] Harangozo J, Turekova I, Szabova Z. Truck drivers occupational health. In: Bartlova I, editor. *Occupational Safety and Health. 13th International Conference on Occupational Safety and Health*; 2013 May 15-16; Ostrava, Czech Republic. Ostrava: VSB TU Ostrava; 2012. p. 32-36.

[4] Czestochowski CZ, Dudarski G, Rybakowski M. *Exposure to noise and vibrations in machines and construction vehicles.* In: Culik M, Danihelova A, Nemec M, editors. *New trends of acoustic spectrum*. Zvolen: Technical University in Zvolen; 2013. p. 21-25.

[5] International Organization for Standardization. ISO 11819-2:1997. *Acoustics-Method for measuring the*

influence of road surfaces of traffic noise. Part 2: The Close-Proximity method. Geneva: ISO; 1997.

[6] International Organization for Standardization. ISO 11819-1:1997. *Acoustics - Measurement of the influence of road surfaces on traffic noise - Part 1: Statistical Pass-By method*. Geneva: ISO; 1997.

[7] Ejsmont A. The noise of cars tires - selected problems. *Zeszyty Naukowe Politechniki Gdanskiej* 1992;68:44-48.

[8] Burdzik R. The research on influence of tire air pressure on noise generated by vehicles tires. *Zeszyty Naukowe Politechniki Slaskiej* 2013;78:13-18.

[9] Lemaitre G, Susini P, Winsberg S, McAdam S. The sound quality of car horns: designing new representative sounds. *Acta Acust united Ac* 2009;95:356-372.

[10] Parizet E, Brocard J, Piquet B, Cedex V, Loing S. Influence of noise and vibration to comfort in diesel engine cars running at idle. *Acta Acust united Ac* 2004;90:987-993.

European Journal of Environmental and Safety Sciences 2014 2(2): 79-83
ISSN 1339-472X European Science and Research Institute (Original Research Paper)

Probabilistic-deterministic modelling of fire spread

Vladimir Mozer[a] · Peter Wilkinson[b] · Miroslav Smolka[a] · Piotr Tofilo[c]

[a]*Department of Fire Engineering, Faculty of Security Engineering, University of Zilina, Univerzitna 8215/1, 010 26 Zilina, Slovakia*
[b]*School of Building and Civil Engineering, Loughborough University, Ashby Road, Loughborough, United Kingdom*
[c]*The Main School of Fire Service, ul. Slowackiego 52/54, 01-677, Warsaw, Poland*

ABSTRACT

This paper deals with the topic of fire spread from the first item ignited onto items that are in its proximity. This potential is very important from the fire-growth point of view, since statistically only a certain proportion of fires spread beyond the first item ignited in compartment fire scenarios. A number of parameters that affect the potential of fire spread, such as fire load density, room geometry and fuel, size of compartment and ignition source are investigated. The fire load density and fuel geometry are selected such that they represent real-world occupancy examples. To evaluate the above parameters computer modelling is used, namely BRISK from BRANZ. Each of the variables is assigned interval boundaries and statistical distribution and a number of iterations are run, each varying one of the parameters randomly within the prescribed boundaries. The results are then analysed and probabilities of fire spread are derived for the specified configurations. The main outcomes of this work are the probabilities of fire spread beyond the first item ignited and to the entire compartment.

Keywords: Probabilistic • Deterministic fire model • BRISK • Fire spread • Fire load density

1. Introduction

The potential for fire spread from the first item ignited is of critical importance in the overall fire growth. Naturally, not all fires spread from the first item ignited and grow to the fully developed stage. However, the greater the probability of fire being transferred from one fuel item to another, the greater the probability of sustained fire growth and potentially flashover, due to increasing amount of heat being released in the compartment.

Despite being such an important parameter, fire spread potential is rather difficult to quantify due to an extremely high level of variability, even in two similarly sized spaces of the identical type of use, e.g. offices or shops. A common way of quantifying the potential for fire spread from the first item ignited is the determination of its probability, i.e. in what number of cases of all ignitions does the fire spread onto a second fuel item, which is a probabilistic approach.

If the particular room and fuel configuration is known, it is possible to determine the potential by employing the principles of fire dynamics. By specifying, or calculating, the heat output of the first item ignited it is possible to determine the heat flux to which the surrounding items are exposed. Should its intensity exceed critical levels, the item exposed to such a heat flux would ignite as a result of its temperature rising above the ignition temperature.

2. Approaches to establishing potential for fire spread

As described above, the potential of fire spread can be expressed in two ways – probabilistically as a probability of fire spreading from the first item ignited and deterministically as a value of critical heat flux. The following sections discuss these approaches.

2.1. Probabilistic approach

If the number of all fires that started in a monitored group of buildings during a given period is known, it is possible to establish what proportion of grew beyond the item of fire origin. If the conditions are not expected to change significantly in the future, the probability of a fire spread from the first item ignited can be mathematically expressed as:

Vladimir Mozer (corresponding author)
Department of Fire Engineering, Faculty of Security Engineering, University of Zilina
Univerzitna 8215/1, 010 26 Zilina, Slovakia, e-mail: vladimir.mozer@fbi.uniza.sk

$$p_s = \frac{n_{f,t}}{n_{f,2nd}} \quad (1)$$

where: p_s is probability of fire spread beyond first item ignited (-); $n_{f,t}$ is total number of fires recorded in selected group of buildings and given period of time (-) and $n_{f,2nd}$ is number of fires in selected group of buildings and given period of time that spread beyond the first item ignited (-).

Literature offers limited experimentally derived data on the probabilities of interest, and when it does there is a high level of variability. For example a general approach described by Mowrer [1] suggests that only 10 % of the fires will spread beyond the first item ignited without further specification of the building use type. On the other hand, Hasofer [2] states percentages of 36 % and 41 % for apartment and commercial buildings, respectively. PD 7974-7 [3] states a percentage of 51 % which spread from the first item ignited, in this case, however, the value is specific for the textile industry. As stated previously, if occupancies are sufficiently similar, the above percentages may be translated into probabilities for future fire spread prediction.

2.2. Deterministic approach

In cases when the compartment(s) of interest are well described and fire scenarios formulated, it is possible utilize direct deterministic fire calculations or modelling. Three mechanisms of fire spread may be considered in general [4]: piloted ignition, direct flame impingement, and spontaneous ignition under sufficient heat flux. Each of the mechanisms has a specific set of principles and conditions governing them and their description is beyond the scope of this paper.

Three variables are of primary interest when using a direct mathematical description of fire spread:

1. Intensity of fire source (geometry may be disregarded if point source radiation model is employed).
2. Material properties of other fuel items, particularly their thermal inertia ($k\rho c$) [4].
3. Distance between fire source and other fuel items.

3. Proposed approach description

The basic logic of the proposed approach is to combine the deterministic and probabilistic approaches and derive the theoretical probability of fire spreading beyond the first item ignited.

At first, a set of specifications, or boundary conditions, describing the target building or space use, need to be specified. The purpose of this paper is to introduce the new approach so the set of condition is reduced to the necessary minimum.

Each building or space has a characteristic value of fire load. It represents the mass of wood, the total heat of combustion of which equals to the total heat of combustion of all real fuels usually found in the given type of occupancy. Fire load may be seen as the limiting amount of combustibles present in the particular space.

Further input required is the typical, or representative, set of fuel items. For example, in the office type of occupancy desks, filing cabinets, cupboards, computers and chairs are usually present. It is usually possible to simplify these items to rectangular object of characteristic height, width and depth, thereby creating a set of heat-flux-receiving surfaces. Furthermore their weight is often known or possible to estimate with sufficient precision. The quantities of the individual fuel items may be mathematically determined as:

$$Q = \sum m_i . h_{c,i} . k_i \quad (2)$$

where: Q is total fire load (MJ); m_i is mass of i-th fuel item (kg); $h_{c,i}$ is heat of combustion of i-th fuel item (MJ kg^{-1}) and k_i is heat of combustion equivalence ratio (real fuel to reference wood) (-).

Design standards and guides typically use fire load density instead of total fire load. Fire load density is calculated as:

$$Q'' = Q / S \quad (3)$$

where: Q'' is fire load density (MJ m^{-2}) and S is floor area on which fire load is distributed (m^{-2}).

The next step is the specification of the first item ignited. It is worth noting that the property of interest is the potential, or probability, of fire spreading beyond the first item ignited. This means it is not of interest to simulate or predict the ignition of the first item itself. For most cases it should be sufficient to assume a fixed heat output surface, e.g. a wastebasket may be represented as a rectangular shape of 0.3 m side elevated 0.5 m above floor level with a heat output of 50 kW.

As the final step the compartment geometry is specified. Fire spread is for this phenomenon limited to fuel items located in the close proximity of the item ignited first. Also, for the spread of fire beyond the first item the initial stages of fire growth are relevant, i.e. no significant thermal feedback from the hot layer and/or bounding construction is expected. Therefore, the compartment in question may be specified in a relatively simple way since the only ceiling

height and proximity to the walls have a more pronounced effect early in a fire [5].

The above paragraphs describe the deterministic part of the model. As mentioned previously, no two buildings or even rooms are exactly the same. Therefore, a degree of randomness must be introduced in order to be able to derive a value of probability of fire spread beyond the first item ignited.

What clearly plays the most important role is the distribution of the individual items of fire load within the compartment of interest; particularly the distance between the source – first item ignited – and targets – other fuel items. Hence, the functional (architectural) configuration of target fuel items within the compartment is not of significant importance and may be disregarded. For relevant results, each of the evaluated compartment configurations should be arranged uniquely, yet adhere to the specific fuel load limits. One way of addressing this requirement is to "shuffle" the fuel items each run.

Finally, each of the randomized fuel configurations is calculated and monitored for critical heat flux levels or direct flame impingement on the target fuel items. Should one of these two mechanisms of fire spread be of sufficient intensity and duration, fire spread to the target fuel item occurs.

4. Demonstration of proposed approach

To illustrate this approach a series of computer simulations were carried out.

4.1. Computer model – B-RISK

B-RISK is a fire simulation model and software program comprising a fire risk simulator for generating probability distributions for relevant model outputs, given that statistical distribution to key input parameters are assigned. Central to B-RISK is an underlying deterministic fire zone model previously developed and known as BRANZFIRE. The B-RISK model may be used for both single deterministic runs as well as for multiple iterations of a scenario for the purpose of sensitivity analysis or for producing probabilistic descriptors of fire risk under defined conditions [6].

4.2. Case model description

The occupancy types used in the demonstration were office, shop and library, with their respective fuel load densities of 670MJ m^{-2}, 1100MJ m^{-2}, 2550MJ m^{-2}, all taken from [7]. There was no particular reason for selecting the above occupancies; they represent increasing values with a sufficient level of difference.

Target fuel items were designed and assigned to the individual occupancy types as per Table 1. Their exact number is random in each run, observing the fuel load and item count limits. All of the target fuel items were of cellulosic type.

The fire source, i.e. item first ignited is a rectangular object with dimensions of (0.3x0.3x0.4) m with the heat output levels of 25, 50, 75 and 100 kW. The total combustible mass was 5 kg for each level of heat output. The fire source was therefore able to release heat at the prescribed level during the entire duration of each simulation which was set to 600 seconds.

The ignition criterion for heat-flux driven fire spread is based on the critical heat flux of 9.5 kW and the duration of exposure at or above this threshold. If the exposure is sufficiently long the target fuel item will ignite. Further details on the ignition mechanism may be found in [6]. The ignition of cellulosic fuels exposed to radiant heat flux is discussed in depth in [8-9].

The simulated compartment was represented by a single, undivided, rectangular 5 m by 10 m room with a clear height of 3 m.

To generate the individual random configuration a built-in feature of the B-RISK simulation software was used. A snapshot of the set-up window is shown in Fig. 1. As stated previously, each compartment configuration is original with varying distances to target fuel items. 250 simulations was run for each type of occupancy and heat output level of the first item ignited, yielding a total of 3000 runs.

Table 1 Specification of target fuel items

Fuel item	Dimensions HxWxD (m)	Combustible mass (kg)	Max number of items allowed		
			Office	Shop	Library
Chair	1.5x5.0x0.5	10	5	3	3
Desk	1.0x2.0x1.0	30	5	1	1
Cupboard	2.0x1.0x0.6	70	5	5	5
Goods shelf	2.0x2.0x0.5	100	0	10	0
Book shelf	2.0x2.0x0.5	200	0	0	10

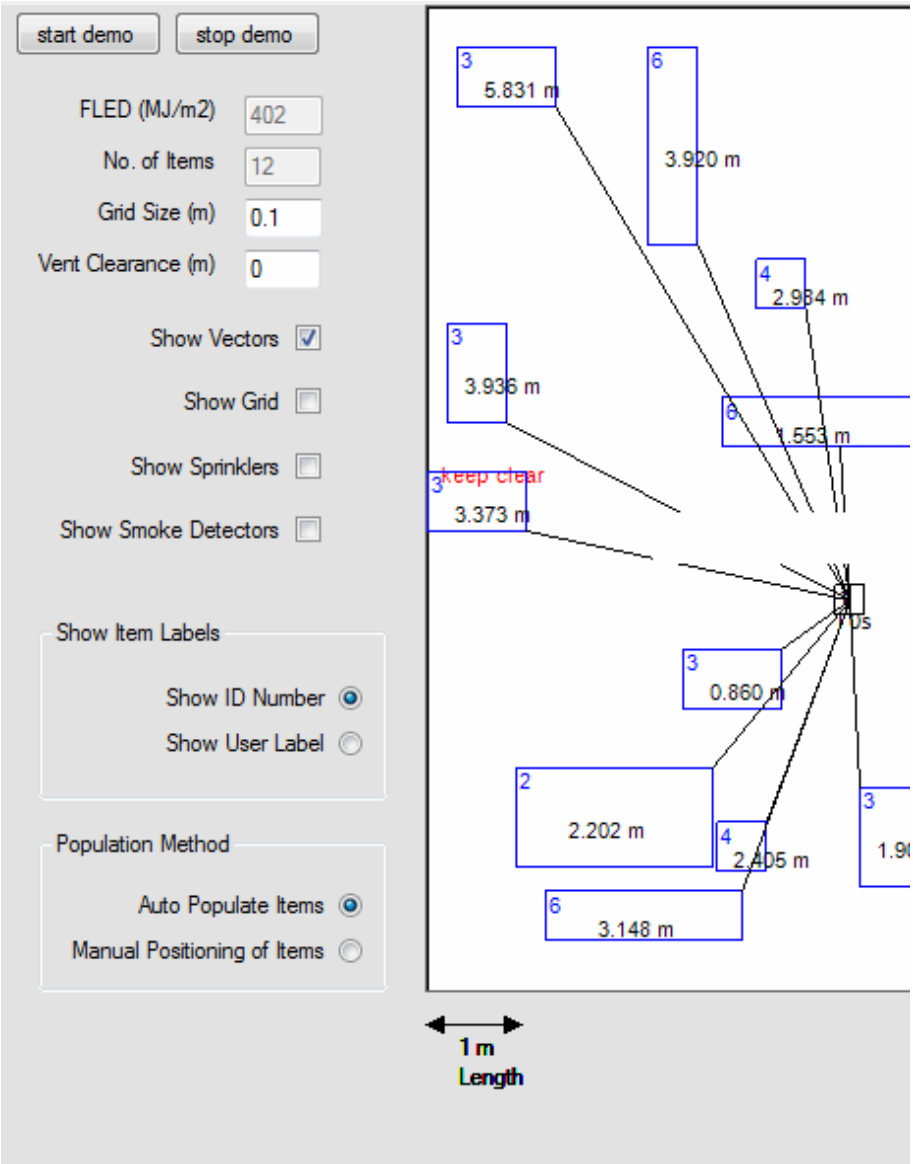

Figure 1 B-RISK random room configuration generator

4.3. Simulation results

After running all the cases, probabilities of fire spreading beyond the first item ignited were derived using Eq (1). The basic set of ignited fires was 250 and represented $n_{f,t}$ and the proportion of fires in which the configuration allowed for fire spread to one or more target fuel items represented $n_{f,2nd}$. The mechanism of fire spread – piloted ignition, flame impingement, autoignition – was not distinguished. The resulting values of probabilities are listed in Table 2.

Table 2 Probabilities of fire spread beyond first item ignited

Source intensity (kW)	Probability of fire spread beyond first item ignited p_s (-)		
	Office $Q'' = 670$ MJ m^{-2}	Shop $Q'' = 1100$ MJ m^{-2}	Library $Q'' = 2550$ MJ m^{-2}
25	0.208	0.192	0.168
50	0.381	0.396	0.232
75	0.560	0.528	0.396
100	0.648	0.660	0.500
Average of above	0.449	0.444	0.324

5. Discussion

Despite the simplifications assumed, the obtained average probability values appear to reasonably match those found in literature [2-3] which were based on actual statistical data. It should be noted that the average values are based on an equal occurrence of each source heat output level.

As expected the probability of fire spread beyond the first item ignited increases with increasing source heat output level. Greater levels of heat flux are achieved therefore reaching further away from the fire source item and causing exposure of target fuel items in a greater area.

What may appear somewhat illogical at first is the negative correlation of fuel load to the probability of fire spread. This must be, however, seen in relation to the properties of the fuel items forming the overall fuel load which relate to the occupancy type. Despite having the highest fuel load density, the library occupancy yielded the lowest probabilities of fire spread beyond the first item ignited.

The main target fuel item in the library – the book shelf – has the lowest weight to surface area ratio; only 0.06 m^2 of surface area per kg of combustible mass. Another set of simulations was run, reducing the dimensions of the bookshelf from (2x2x0.5) m to (2x1x0.5) m as well as the combustible mass from 200 kg to 50 kg. The weight to surface area ratio for this target fuel item increased to 0.14 m^2 of surface area per kg of combustible mass. In addition, the maximum allowed number of the bookshelf target fuel items was increased to meet the fuel load density criterion. These adjustments led to an increase in probability of fire spreading from 0.232 to 0.468 for the 50 kW source; the value represents the highest probability at this level of source heat output.

6. Conclusion

The aim of the paper was to investigate the utilization of a combination of deterministic and probabilistic fire modelling for the purpose of determining the potential of fire spread beyond the first item ignited. The B-RISK computer model was used for this purpose as the computation tool.

The results indicate that three variables are key to the potential for fire spread beyond the first item ignited: heat output of first item ignited (source), weight-to-surface-area ratio of target fuel items and the fuel load density. The latter two variables are closely dependent and the weight-to-surface-area ratio appears to have a greater impact than fire load density; the sensitivity study of this dependency was only limited, however.

The results of this study offer an initial insight at the deterministic-probabilistic fire modelling approach. Since the probability of fire spread beyond the first item ignited has a great importance it could offer a viable alternative to deriving it from fire statistics where data may often be difficult to source or unavailable at the level of detail required.

Acknowledgements

This work was supported by the Slovak Research and Development Agency under the contract No. APVV-0727-12.

References

[1] Mowrer FW, Brannigan V, Pruser DA. A probabilistic approach to tenability criteria. In: Johnson P, editor. *Performance-based codes and fire safety design methods. 4th International Conference on Performance-based codes and fire safety design methods*; 2002 March 20-22; Melbourne, Australia. Lancaster: DEStech Publications; 2002. p. 174-178.

[2] Hasofer AM, Beck VR, Bennetts ID. *Risk analysis in building fire safety engineering*. London: Butterworth-Heinemann; 2007. 208 p.

[3] British Standards Institutions. PD 7974-7:2003. *Probabilistic risk assessment*. London: BSI; 2003.

[4] Drysdale D. *An introduction to fire dynamics*. Chichester: Wiley; 1999. 574 p.

[5] Karlsson B, Quintiere J. *Enclosure fire dynamics*. Boca Raton: CRC Press; 2002. 336 p.

[6] Wade C. *B-RISK user guide and technical manual*. Judgeford: NZ Branz; 2002. 118 p.

[7] Cote AE. *Fire protection handbook*. 20th ed. Quincy: National Fire Protection Association; 2008. 3680 p.

[8] Martinka J, Chrebet T, Kral J, Balog K. An examination of the behaviour of thermally treated spruce wood under fire conditions. In: *Wood Res* 2013;61(1):243-253.

[9] Xu Q, Majlingova A, Zachar M, Jin C, Jiang Y. Correlation analysis of cone calorimetry test data assessment of the procedure. *J Therm Anal Calorim* 2012;110(1):65-70.